IONIAN UNIVERSITY

Faculty of Information Science and Informatics

Department of Informatics

Ph.D. Thesis

Energy Consumption Optimization in Wireless Sensor Networks

Georgios Tsoumanis

10 September 2018

Supervisor

Konstantinos Oikonomou, *Associate Professor*,
Ionian University

Advisory Committee Members

Ioannis Stavrakakis, *Professor*,
National and Kapodistrian University of Athens
Konstantinos Oikonomou, *Associate Professor*,
Ionian University
Dimitrios Tsoumakos, *Associate Professor*,
Ionian University

Reviewing Committee Members

Ioannis Stavrakakis, *Professor*,
National and Kapodistrian University of Athens
Panayiotis Tsanakas, *Professor*,
National Technical University of Athens
Konstantinos Oikonomou, *Associate Professor*,
Ionian University
Dimitrios Tsoumakos, *Associate Professor*,
Ionian University
Dimitrios Vergados, *Associate Professor*,
University of Piraeus
Andreas Floros, *Associate Professor*,
Ionian University
Markos Avlonitis, *Assistant Professor*,
Ionian University

To Despoina,
for her patience, her faith and because she always understood.

Abstract

Prolonging a wireless sensor network's *lifetime* is closely related to energy consumption and particularly to the *energy hole problem*, where sensor nodes close to the *sink node* consume a considerable amount of their energy for relaying purposes. In order to tackle the energy hole problem's effects, this thesis proposes two approaches that counter the problem from two perspectives: (i) the minimization of the energy consumption by approaching the *sink placement problem* as a *k-median problem* and (ii) the prolongation of the network's lifetime by recharging its sensor nodes.

In the first approach, an analytical model for analyzing the available energy in the network is proposed. The next step is to analytically model the overall energy consumption as a k-median facility location problem, its solution corresponding to the location of k sinks in the network. As analytically shown, when k sinks are placed according to the solution of the previous facility location problem, then the overall energy consumption is minimized, resulting in a higher energy-saving system. Thus, the saved energy can be further utilized, e.g., to extend the network's lifetime and support modern replenishing techniques such as energy harvesting and battery recharging. Simulation results validate the analytical model that is the basis of the analysis and confirm the results with respect to the available energy in the network. In particular, significant energy savings are observed when the analytical results are applied, thus resulting in better energy utilization and subsequent network lifetime increment.

The second approach is focused on two proposed recharging policies. The first one is a simple recharging policy that permits a mobile recharger, initially stationed at the sink node, to move around and replenish any node's exhausted battery when a certain recharging threshold is violated. This policy, as well as the second proposed recharging policy (i.e., the enhanced recharging policy), refer to *on-demand* recharging policies which base their operation on local information, allowing the mobile recharger to move – upon request – to a node of reduced energy level and replenish its battery. When under the enhanced recharging policy and after completing the latter replenishment, the mobile recharger continues operating in a hop-by-hop manner to the neighbor nodes of the lowest energy level, thus replenishing their

batteries too. It is shown that the minimization of the recharging distance covered by the mobile recharger is a facility location problem, and particularly an 1-median one. Simulation results, regarding the simple recharging policy, investigate various aspects of it related to the recharging threshold and the level of the energy left in the network nodes' batteries. In addition, it is shown that when the sink's location is set to the solution of the particular facility location problem, then the recharging distance is minimized irrespectively of the recharging threshold. As for the enhanced recharging policy's simulation results, its effectiveness is investigated using simulation results and compared against an existing well-known on-demand recharging policy that exploits global knowledge (i.e., knowledge of both the energy level of all nodes and the network topology). It is shown that the enhanced recharging policy, even though based on local information, maintain the average energy level and termination time higher than that under the existing one that exploits global knowledge. Furthermore, it is observed that the network's lifetime is maximized when the basis of the mobile recharger is located at the solution of the mentioned median problem for all studied policies.

The approaches studied in this thesis establish a relation between facility location problems (particularly the k-median problem) and energy consumption and battery replenishment. This is a significant contribution that is expected to trigger future work in the area and reveal further aspects of the energy consumption issues and how lifetime may be prolonged in wireless sensor networks.

Περίληψη

Η παράταση της *διάρκειας ζωής* ενός δικτύου ασύρματων αισθητήρων σχετίζεται στενά με την κατανάλωση ενέργειας και ειδικότερα με το *πρόβλημα της ενεργειακής τρύπας* (energy hole problem), όπου οι κόμβοι που βρίσκονται κοντά στον *κόμβο-συλλέκτη* (sink node) καταναλώνουν σημαντικό μέρος της ενέργειας τους για λόγους αναμετάδοσης. Για την αντιμετώπιση των επιπτώσεων του προβλήματος της ενεργειακής τρύπας, αυτή η διατριβή προτείνει δύο προσεγγίσεις που αντιμετωπίζουν το πρόβλημα από δύο οπτικές γωνίες: (i) την ελαχιστοποίηση της κατανάλωσης ενέργειας προσεγγίζοντας το *πρόβλημα της τοποθέτησης του συλλέκτη* (sink placement problem) ως *πρόβλημα τοποθέτησης υπηρεσίας* (facility location problem) και (ii) την παράταση της διάρκειας ζωής του δικτύου επαναφορτίζοντας τους κόμβους του.

Στην πρώτη προσέγγιση προτείνεται ένα αναλυτικό μοντέλο για την ανάλυση της διαθέσιμης ενέργειας στο δίκτυο. Το επόμενο βήμα είναι η μοντελοποίηση της συνολικής κατανάλωσης ενέργειας ως πρόβλημα τοποθέτησης υπηρεσίας και πιο συγκεκριμένα ως *πρόβλημα k-διάμεσων* (k-median problem), η λύση του οποίου αντιστοιχεί στη θέση των k συλλεκτών στο δίκτυο. Όπως παρουσιάζεται αναλυτικά, όταν οι k συλλέκτες τοποθετούνται σύμφωνα με τη λύση του προηγούμενου προβλήματος τοποθέτησης υπηρεσίας, τότε ελαχιστοποιείται η συνολική κατανάλωση ενέργειας, με αποτέλεσμα ένα ενεργειακά αποδοτικότερο σύστημα. Η εξοικονόμηση ενέργειας που επιτυγχάνεται μπορεί να χρησιμοποιηθεί περαιτέρω, π.χ., για να επεκταθεί η διάρκεια ζωής του δικτύου και να υποστηριχθούν σύγχρονες τεχνικές ανανέωσης ενέργειας όπως οι εκμετάλλευση ανανεώσιμων πηγών ενέργειας και η επαναφόρτιση των μπαταριών των κόμβων. Τα αποτελέσματα των προσομοιώσεων επικυρώνουν το αναλυτικό μοντέλο που αποτελεί τη βάση της ανάλυσης και επιβεβαιώνουν τα αποτελέσματα σε σχέση με τη διαθέσιμη ενέργεια στο δίκτυο. Συγκεκριμένα, παρατηρείται σημαντική εξοικονόμηση ενέργειας κατά την εφαρμογή των αναλυτικών αποτελεσμάτων, με αποτέλεσμα την καλύτερη αξιοποίηση της ενέργειας και την επακόλουθη αύξηση της διάρκειας ζωής του δικτύου.

Η δεύτερη προσέγγιση εστιάζεται σε δύο προτεινόμενες πολιτικές επαναφόρτισης. Η πρώτη είναι μια απλή πολιτική επαναφόρτισης που επιτρέπει σε ένα *φορητό φορτιστή* (mobile recharger), αρχικά τοποθετημένο στην ίδια θέση με τον κόμβο-συλλέκτη,

να κινείται και να αναπληρώνει την εξαντλημένη μπαταρία ενός κόμβου όταν παραβιάζεται ένα συγκεκριμένο όριο επαναφόρτισης. Η πολιτική αυτή, όπως και δεύτερη πολιτική επαναφόρτισης που μελετάται λειτουργούν *κατόπιν αιτημάτων* (on-demand) και βασίζουν τη λειτουργία τους σε τοπική πληροφόρηση επιτρέποντας στο φορητό φορτιστή να μετακινηθεί – κατόπιν αιτήματος – σε έναν κόμβο με μειωμένο επίπεδο ενέργειας και να ανανεώσει την μπαταρία του. Κατά τη δεύτερη πολιτική και μετά την ολοκλήρωση της τελευταίας διαδικασίας, ο φορητός φορτιστής συνεχίζει να λειτουργεί με πολυ-αλματική λογική στους γειτονικούς κόμβους με το χαμηλότερο επίπεδο ενέργειας, ανανεώνοντας έτσι και τις μπαταρίες αυτών. Όπως δείχνεται, η ελαχιστοποίηση της απόστασης επαναφόρτισης που καλύπτεται από τον φορητό φορτιστή είναι ένα πρόβλημα τοποθέτησης υπηρεσίας και συγκεκριμένα ένα πρόβλημα 1-διάμεσου. Τα αποτελέσματα προσομοίωσης, σχετικά με την πρώτη προτεινόμενη πολιτική, διερευνούν διάφορες πτυχές της πολιτικής επαναφόρτισης - συμπεριλαμβανομένης μιας βελτιωμένης έκδοσής της - που σχετίζονται με το όριο επαναφόρτισης και το επίπεδο ενέργειας που απομένει στις μπαταρίες των κόμβων του δικτύου. Επιπλέον, δείχνεται πως όταν η θέση του συλλέκτη έχει επιλεγεί βάση της λύσης του συγκεκριμένου προβλήματος τοποθέτησης υπηρεσίας, τότε η απόσταση επαναφόρτισης ελαχιστοποιείται ανεξάρτητα από το όριο επαναφόρτισης. Όσον αφορά τα αποτελέσματα προσομοίωσης της δεύτερης προτεινόμενης πολιτικής, η αποτελεσματικότητά της διερευνάται χρησιμοποιώντας αποτελέσματα προσομοίωσης και συγκρίνεται με μια υπάρχουσα γνωστή πολιτική ανανέωσης που λειτουργεί κατόπιν αιτημάτων που εκμεταλλεύεται την γνώση όλου του δικτύου (δηλαδή γνώση τόσο του ενεργειακού επιπέδου όλων των κόμβων όσο και της τοπολογίας του δικτύου). Αποδεικνύεται ότι η προτεινόμενη πολιτική, αν και βασίζεται σε τοπική πληροφόρηση, διατηρεί το μέσο ενεργειακό επίπεδο και τον χρόνο τερματισμού υψηλότερο από εκείνο της υφιστάμενης πολιτικής που εκμεταλλεύεται την γνώση όλου του δικτύου. Επιπλέον, παρατηρείται ότι η διάρκεια ζωής του δικτύου μεγιστοποιείται όταν η βάση του φορητού φορτιστή βρίσκεται στη λύση του αναφερόμενου προβλήματος 1-διάμεσου για όλες τις πολιτικές που μελετούνται.

Οι προσεγγίσεις που μελετούνται σε αυτή τη διατριβή καθιστούν μια συσχέτιση μεταξύ των προβλημάτων τοποθέτησης υπηρεσίας (ιδιαίτερα του προβλήματος k-διάμεσων) με την κατανάλωση ενέργειας και την αναπλήρωση της μπαταρίας. Πρόκειται για μια σημαντική συμβολή που αναμένεται να προκαλέσει μελλοντικές έρευνες στην περιοχή και να αποκαλύψει περαιτέρω πτυχές των ζητημάτων κατανάλωσης ενέργειας και του τρόπου με τον οποίο η διάρκεια ζωής μπορεί να παραταθεί στα ασύρματα δίκτυα αισθητήρων.

Acknowledgments

Firstly, I would like to express my sincere gratitude to my supervisor Dr. Konstantinos Oikonomou. It has been an honor to be a Ph.D. student of him. His guidance helped me in all the time of research and I could not have imagined having a better advisor and mentor for my Ph.D. study. The joy and enthusiasm he has for research were contagious and motivational for me, even during tough times in the Ph.D. pursuit.

Besides my advisor, I would like to thank the Advisory Committee Members, Prof. Ioannis Stavrakakis and Dr. Dimitrios Tsoumakos, for their guidance during my Ph.D. research. I would also like to thank Prof. Panayiotis Tsanakas, Dr. Dimitrios Vergados, Dr. Andreas Floros and Dr. Markos Avlonitis for their participation in the Reviewing Committee.

I thank my fellow labmates at NMSLab, Dr. Vasileios Komianos, Dr. Konstantinos Giannakis, Alexandros Tsompolis, Sofia Fanarioti and Athanasios Tsipis for the sleepless nights we were working together before deadlines, and for all the fun we have had in the last years. All the moments we have shared together, have turned them all into good friends of mine. Special thanks to my colleague and friend George Koufoudakis, for his support and for always giving me the best advice.

I would also like to thank my parents, Athina and Vasileios for their continuously supporting my decisions, without expressing any reservations about them. Additionally, I thank my brother, Dr. Konstantinos Tsoumanis, for always being supportive and for all the meaningful discussions we always have.

Last but not least, I would like to thank my family, for supporting me spiritually throughout my Ph.D. studies and my life in general. I thank my two daughters, for not complaining when we had to skip the playground and for hugging me all the time. Thank you, Despoina, for all...

Parts of this research were supported by project “A Pilot Wireless Sensor Networks System for Synchronized Monitoring of Climate and Soil Parameters in Olive Groves,” (MIS 5007309) which is partially funded by European and National Greek Funds (ESPA) under the Regional Operational Programme “Ionian Islands 2014-2020”.

Contents

List of Figures

List of Tables

Chapter A

Introduction

WIRELESS sensor networks have experienced exceptional growth over the past decades, their success reflecting their continuously increasing areas of application [1], [2]. Recent technological advancements have permitted for the creation of small and low-cost sensor nodes capable of monitoring targeted areas and wirelessly transmitting the corresponding data. This wireless nature allows for applications in places where traditional wiring would be either expensive (e.g., large-scale environments), difficult (e.g., underwater), or even impossible (e.g., space).

Recharging wireless sensor nodes has also attracted significant research attention (see, e.g., [3], [4], [5]) as an alternative way to tackle the difficult problem of prolonging a *network's lifetime*. This is made possible due to recent technological advances in wireless battering charging, e.g., through wireless energy transfer [6], [7].

A.1 Wireless Sensor Networks

Wireless sensor networks consist of autonomous sensors, spatially distributed, able to monitor physical or environmental conditions (e.g., temperature, sound, pressure, etc.) and send their data to a central location (e.g., a server). Like many advanced technologies, wireless sensor networks were firstly introduced for implementing military applications. The first wireless network that was similar to modern wireless sensor networks is the *Sound Surveillance System* (SOSUS), a *battlefield surveillance application* that was developed by the United States Military in the 1950s for detecting and tracking Soviet submarines. This network consisted of submerged acoustic sensors, called *hydrophones* which were distributed both in the Atlantic and Pacific oceans. While their first application was for military purposes, nowadays wireless

sensor networks are widely implemented for a variety of tasks.

Apart from SOSUS and battlefield surveillance, wireless sensor networks are nowadays developed for a wide range of applications which can vary significantly in their requirements, such as the mode of deployment, the sensor types they need and the means of energy supply (e.g., battery, wall socket, etc.).

Wireless sensor networks applications include:

- Environmental/Earth monitoring (e.g., traffic, habitat, air pollution, etc.) [8], [9]
- Industrial monitoring (e.g., machine health monitoring, wine production, etc.) [10], [11]
- Infrastructure protection (e.g., water distribution, etc.) [12], [13]
- Battlefield awareness (e.g., multi-target tracking, etc.) [14], [15]
- Context-aware computing (e.g., intelligent home, etc.) [16], [17]

A.1.1 Architecture

Wireless sensor networks can be seen as a special sub-class of *ad hoc* networks. In ad hoc networks, nodes comprising them can communicate with each other in the absence of a fixed infrastructure. Additionally, communication between them is not always direct and is proceeded in a multi-hop fashion; thus every node also plays the role of a router. While wireless sensor networks operate in the same spirit with their ad hoc predecessors, they are differentiated in many ways from them, such as:

- Applications: Wireless sensor networks focus mainly on sensing data, transferring it to a computational center through the *sink node* (i.e., the node that 'holds' the *sink* and is responsible for collecting all sensed information), while ad hoc networks are based on *peer to peer* applications (e.g., data sharing).
- The number of nodes: Wireless sensor networks usually handle more network nodes than ad hoc ones.
- Communication traffic: Wireless sensor networks' communication traffic usually flows on the direction of the computation center through one or more sink nodes, while in ad hoc networks the communication can be established between any two or more nodes without any central control.

- Communication Technology: Wireless sensor networks can use multiple wireless standards (e.g., IEEE 801.11 and IEEE 801.15 variances) in addition to *Global Positioning System* (GPS) as needed, while ad hoc are based only on one of the variances of IEEE 801.11.

- Mobility: ad hoc nodes are mostly mobile as the nodes are human-driven (e.g., *vehicular ad hoc networks* (VANETs), *smartphone ad hoc networks* (SPANs), etc.), while wireless sensor networks' nodes mobility depends on the application's demands and environment deployed in.

- Energy: Wireless sensor networks' nodes operation is usually based on small batteries, while ad hoc nodes usually operate under larger batteries with AC-DC charger/adapter as well.

- Software: Both are application driven, but ad hoc nodes' applications have higher requirements than the simple ones in wireless sensor networks.

In Figure A.1 a typical multi-hop wireless sensor network architecture is shown, where all nodes consisting it send their sensed data to the sink node. The sink node in turn forwards all data to a server, thus making them available for users (e.g., through applications). In this figure a traditional single - sink wireless sensor network is depicted, but multiple sinks may exist too, placed on multiple nodes in the network. In these cases, all sink nodes cooperatively collect the sensed information and forward them towards a computation center.

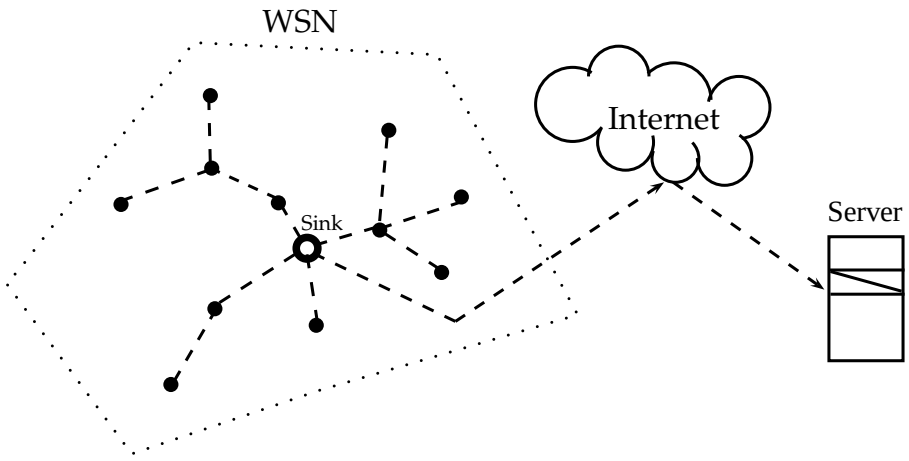

Figure A.1: *Typical multi-hop wireless sensor network architecture.*

Protocol Stack

The protocol stack under which the nodes of a wireless sensor network operate is given in Figure A.2 [1], consisting of the *application layer*, *transport layer*,*network layer*, *data link layer*, *physical layer*, *power management plane*, *mobility management plane*, and *task management plane*. Note that, in many works the data link layer is replaced by the *medium access control* (MAC) layer while, in others, the MAC layer is treated as a sub-layer of the data link layer, the latter being used here. More specifically:

- Application layer: Software developed belongs in the application layer, and it depends on the tasks the sensor nodes are expected to perform.
- Transport layer: The protocols of the transport layer provide host-to-host communication services for applications that require them.
- Network layer: The layer that takes care of routing.
- Data link layer: MAC protocols are applied here, taking into consideration power consumption and collision avoidance
- Physical layer: Modulation, transmission and receiving technologies apply to the physical layer.
- Power management plane: Management of energy.
- Mobility management plane: Management of mobility.
- Task management plane: Management of sensing tasks.

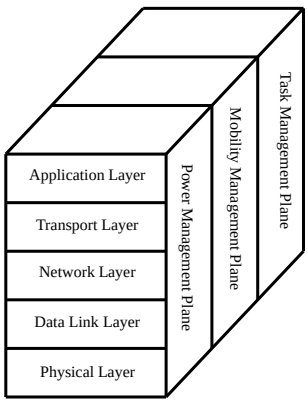

Figure A.2: *The wireless sensor networks protocol stack.*

Note that the management planes apply to all layers, in the sense that their outcome derives from a combination of tasks among them. For example, in the power management plane, the management of energy consumption can be affected by the consumption of the application layer (e.g., how long is the sensor sensing based on the application's demands), the network layer (e.g., knowing the node that is to receive a packet is always the same, less energy is consumed for finding it), data link layer (e.g., an energy efficient MAC protocol that switches off some parts of the node when they are not needed can minimize energy consumption).

A.1.2 Standards and Technologies

Over the past years, many works have provided the wireless sensor networks with wireless communication standards and technologies. While many standards already existed (e.g., *IEEE 802.11* and *IEEE 802.15*), in wireless sensor networks it has been (and it is) of significant importance to develop technologies that take into consideration the minimization of the energy consumption of the sensor devices, as well as the low data rate and cost. *IEEE 802.15.4* is designed to fill this gap, albeit disadvantaged against existing technologies in other aspects, such as data throughput and range. For example, *Wi-Fi* (IEEE 802.11) offers better throughput and range but higher energy consumption, too. Note that most of the technologies operate in the *Industrial, Scientific and Medical radio band* (ISM band). Besides IEEE 802.15.4, other standards (applying to many of the layers of the protocol stack earlier shown) that also promote the energy saving for wireless sensor networks [18] include *ZigBee* [19], *WirelessHART* [20], *ISA100.11a* [21], *Bluetooth Low Energy (BLE)* [22], *IEEE 802.15.6* [23], *6LoWPAN* (RFC 4919) [24] and *RPL* (RFC 6550) [25]. A brief description of them is given in the sequel while their progress over the time is presented in Figure A.5.

IEEE 802.15.4

The IEEE 802.15.4 standard was developed for providing a framework for low cost, low energy consumption networks. It only provides the data link and physical layers, leaving the upper layers to be developed by other technologies, according to the needs. Unlike other standards (e.g., Wi-Fi) that offer more bandwidth and are more energy-consuming, in 802.15.4 the emphasis is on minimization of energy consumption. It provides low cost, short-range, low power, and low data-rate communication for wireless sensor networks and is designed to support applications that require short-range communication, thus maximizing the battery life of the sensor nodes [26].

Regarding the physical layer, IEEE 802.15.4 specifies a total of 27 half-duplex channels across the three frequency bands [27] and is organized as given in Table A.1.

Table A.1: *IEEE 802.15.4 Frequencies and Frequency Bands.*

Frequency band (MHz)	Channels available	Throughput available (kbps)	Regions use allowable
868 - 868.6	1	20	Europe
902 - 928	10	30	USA
2400	16	250	Global

Note that the 868 [MHz] band operates with -92 *dBm* RF *sensitivity* and *ideal transmission* range approximatively equal to 1 *km*, while for the 915 MHz band the same values apply for both the receiver sensitivity and the ideal transmission range respectively. The 2.4 *GHz* ISM band which makes use of sixteen channels with data rate 250 *kbps*, operates under a -85 *dBm* RF sensitivity while its ideal transmission range equals 220 *m*. As for the energy efficiency issue, IEEE 802.15.4 allows the devices to activate their transmitter and receiver during operating periods and deactivate them during non-operating periods, thus saving energy.

The MAC protocol implemented by IEEE 802.15.4 in the data link layer's MAC sub-layer, is based on the *Carrier-sense multiple access with collision avoidance* (CSMA/CA) algorithm, thus listening to the channel is carried out before transmitting, in order to reduce the collisions among transmissions. Additionally, it offers two operational modes, the *beacon-enabled* and the *non beacon-enabled*. When the beacon is enabled, periodic beacons are transmitted by the coordinate (i.e., a full function device with extra functionality that provides coordination) in order to maintain synchronization and exchange network information between the devices [28]. These beacons are part of a 16 slot superframe (the first slot of it) depicted in Figure A.3 and exchanging data takes place during the superframe. During the inactive part of the superframe, nodes are in *sleep mode*, while the active part is divided into two parts: (i) the *Contention Access Period* (CAP) and (ii) the *Contention Free Period* (CFP) that is composed of *Guaranteed Time Slots* (GTS). GTSs are optional slots allocated to specific nodes. Note that the superframe structure given here is the basic proposed, but other versions of it have been proposed too, e.g., in [29].

ZigBee

ZigBee defines the network and application layers while for the other layers it is based on the IEEE 802.15.4 standard. Their cooperation concerning protocol layers'

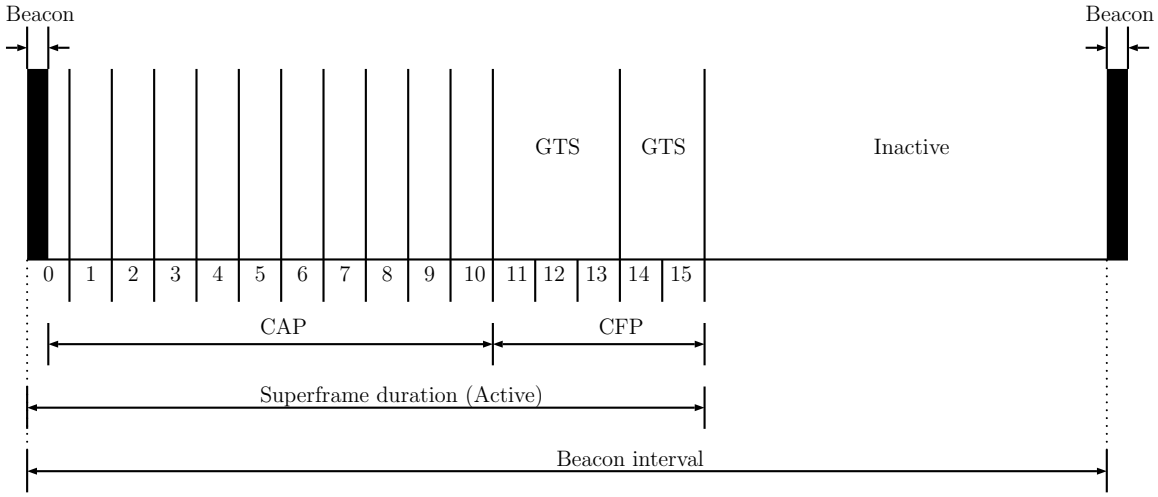

Figure A.3: *IEEE 802.15.4 superframe structure*

assignment is given in Figure A.4, where which layers of the protocol stack are assigned to ZigBee and which are assigned to IEEE 802.15.4 is shown. Note that the ZigBee specification does not define a transport layer [30], while for the network layer, *Ad hoc On-Demand Distance Vector* (AODV) routing is implemented. Under AODV, routes are formed between nodes only under a request. The formed routes are maintained as long as they are required, while sequence numbers are used in order to ensure route 'freshness'.

The application layer in ZigBee consists of *Application Support* (APS) sub-layer and *ZigBee Device Object* (ZDO). Discovery and binding services are under the APS sub-layer's responsibility, while ZDO performs control and management of *application objects*, which consist the *Application Framework* that controls and manages the protocol layers. The latter can contain up to 240 Application Objects.

WirelessHART

WirelessHART (Wireless Highway Addressable Remote Transducer Protocol) is mostly implemented for monitoring plant equipment or processes. Considering the physical layer, it operates under the IEEE 802.15.4 specification, in the sense of transmitting on the frequency bands defined there, with the same channel designations. Besides that, similar to ZigBee characteristic, it is differentiated from it in a lot of significant characteristics. One such characteristic is WirelessHART's relying on a fixed length *Time Division Multiple Access* (TDMA) scheme when dealing with the data link layer's MAC sub-layer, allowing nodes to go to sleep when it is not their slot time. As for the network layer, configuration under WirelessHART is based

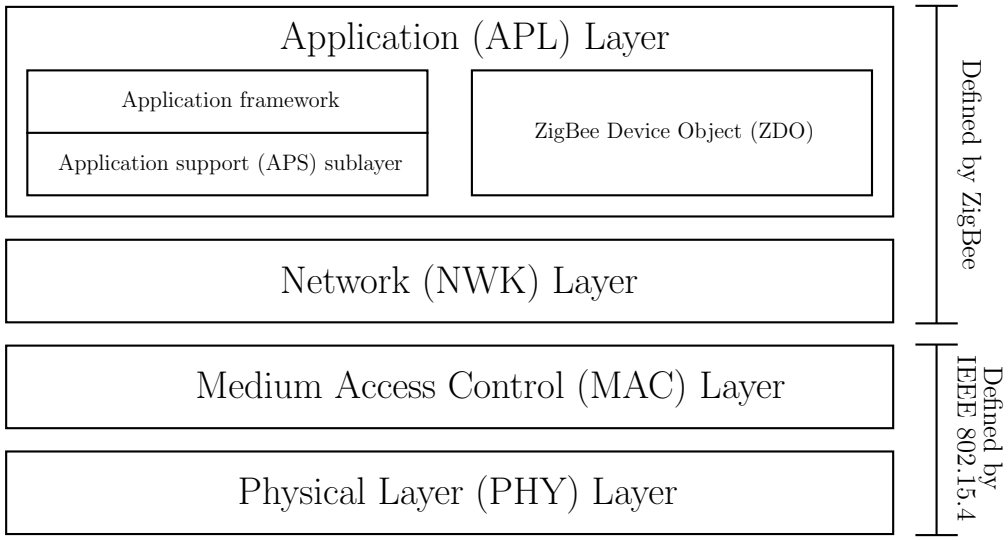

Figure A.4: *Protocol stack of wireless sensors operating under ZigBee and IEEE 802.15.4*

on a *network manager* that is responsible for configuring the network, scheduling communication between devices, managing routes, and monitoring network health. The key feature here is that if a node goes down (e.g., its battery runs out of energy), another one can play its role in terms of undertaking the out-of-energy node's relaying tasks. As for the application layer, communications between nodes are represented as command requests and responses where commands are divided into three classes: (i) Universal commands; (ii) Common practice commands and (iii) Wireless commands [31].

ISA100.11a

ISA100.11a (official description: 'Wireless Systems for Industrial Automation: Process Control and Related Applications') is a specification targeting industrial automation. Regarding its approach on the physical layer, ISA100.11a falls right into line with wirelessHART and ZigBee by adopting the IEEE 802.15.4 specification. As for the data link layer, a hybrid method combining TDMA with CSMA is implemented [32] while *channel hopping* (i.e., a technique that periodically changes the operating frequency of the communication channel) is supported. An interesting point in the network layer is that it supports *IPv6* protocol, making use of the 6LoWPAN technique explained in the sequel.

BLE

BLE (Bluetooth Low Energy) is an extension of the Bluetooth technology which allows communication between low cost and small battery-powered devices (e.g., wireless mouses, wireless keyboards, etc.) with devices supporting Bluetooth (e.g., laptops, desktops, etc.). It implements an ultra-low-power idle mode for energy efficiency purposes, and it is designed to extend its predecessor applications range in more fields, such as healthcare and sports.

IEEE 802.15.6

IEEE 802.15.6 is a standard defining the physical and the data link layer's MAC sub-layer for low-power devices placed on or inside the human body; thus nodes operating under 802.15.6 consist a *Body Area Network* (BAN), implemented for medical or other applications. 802.15.6 suggests the use of three physical layers under a unique MAC. These are: (i) *Narrowband* (NB); (ii) *Human Body Communications* (HBC) and (iii) *Ultra-wideband* (UWB) [33]. Regarding the MAC sub-layer, three modes of channel access are concerned: (i) beacon mode with superframes; (ii) non-beacon mode with superframes and (iii) non-beacon mode without superframes.

6LoWPAN

6LoWPAN stands for 'IPv6 over Low power Wireless Personal Area Networks'. It enables IEEE 802.15.4 low power wireless network devices to send and receive IPv6 packets. Various specifications already developed include header compression and neighbor discovery optimization, while an extra adaption layer is implemented to allow the transmission of IPv6 datagrams over 802.15.4 networks. This adaption layer is unavoidable because the vital requirement for IPv6 to be implemented over 802.15.4 considers the *maximum transmit unit* (MTU) to be at least 1280 byte packets, while in IEEE 802.15.4 standard the packet size is 127 octets [34].

RPL

Another IPv6 based technique is RPL which is a *distance vector routing protocol* [35] for low power networks compliant with IPv6. It is optimized for many-to-one communications for collecting data, but it supports one-to-many and one-to-one communications too. Under RPL, a *Directed Acyclic Graph* (DAG) [36] anchored at a border router of the wireless sensor network is created. Regarding the routing table of nodes, they can maintain more than one parents, thus constructing several routes towards the sink node. Having many choices, a node selects its preferable one,

based on an objective function that requires routing metrics (e.g., nodes' remaining energy, number of transmissions, etc.).

A.1.3 Energy Consumption Optimization Mechanisms

All standards and technologies briefly described in A.1.2 have taken into consideration the optimization of energy consumption. These techniques, along with many other approaches in the literature ([37], [38], [39], [40] are excellent surveys of them) are based on the mechanisms briefly reviewed in this subsection. Making a brief review of these mechanisms will smoothly lead to the proposed approaches in this thesis, connecting them with the related work that is given in Section A.2 and the contribution explained in Section A.3.

The primary existing energy consumption optimization mechanisms [37], [18] can be divided into three categories: (i) Network-based mechanisms; (ii) node-based mechanisms and (iii) recharging mechanisms. All three categories have the same goal which is the prolongation of the network's lifetime and their characteristics are described next.

Network-Based Mechanisms

Mechanisms in this category aim at achieving energy efficiency by dealing with issues that consider the network as an entity; thus, mechanisms here apply to the whole network. These mechanisms are: (i) optimal node deployment; (ii) topology control; (iii) cluster architectures and (iv) optimal sink placement.

Optimal node deployment: Optimal deployment of nodes can lead in a better view of the cost, coverage, average consumption and other characteristics of the network and prolong the network's lifetime [41], [42]. For example, in [43], a scheme is proposed that distributes the sensor nodes uniformly considering Euclidean distance and coverage redundancy among the mobile nodes. After determining the uncovered sensing areas, it selects the best mobile nodes to be moved to minimize the gap in hole.

Topology control: When sensors are redundantly deployed — especially when the nodes are randomly deployed, the administrator does not have any control over the design of network — it is possible to periodically deactivate some nodes that are not necessary for ensuring connectivity or coverage. For example, Misra *et al.* [44] propose the activation only of a subset of nodes in the network in order to prolong the network's lifetime, while Bachir *et al.* in their work [45] consider a distributed temperature aware algorithm that when

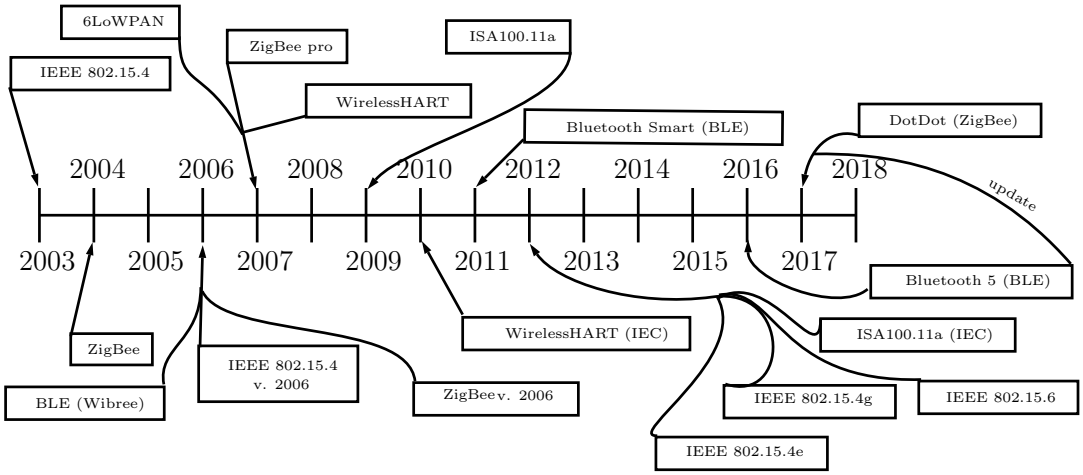

Figure A.5: *The presented technologies' progress over time*

temperature is lower than a threshold, allows some nodes to go to sleep while guaranteeing both coverage and connectivity.

Cluster architectures: Clustering aims at dividing the network into clusters each one managed by a node called *cluster head*, the latter being responsible for coordinating the cluster's containing nodes and communicating with other cluster heads. Cluster techniques can improve the network's lifetime [46] in many ways, e.g., by reducing the communication range of nodes inside the cluster and balancing energy consumption among nodes via cluster head rotation. Many works have proposed clustering algorithms, an example of a distributed one to be the *LEACH* algorithm [47]. In the latter, a randomized rotation of cluster heads and clusters is applied, thus balancing the energy consumption.

Optimal sink placement: Finding the optimal location to place the sink among the network nodes (i.e., the sink placement problem) has been proven to be NP-Complete [48]. Many studies suggest heuristics to find near-optimal solutions. Optimal sink placement is further studied in this thesis.

Node-Based Mechanisms

Mechanisms comprising the second category are applied on the wireless sensor network's power management plane, earlier described in A.1.1. This category consists of: (i) radio optimization; (ii) data aggregation and compression; (iii) sink node mobility (iv) energy-aware routing and (v) sleep/wake-up schemes.

Radio optimization: The radio module is one the most energy consuming components of sensor nodes and researchers have tried to optimize radio

parameters in order to reduce its consumption. Radio optimization can be further divided into many sub-categories such as coding and modulation schemes, power transmission, sleep/wake-up schemes and antenna direction, being thoroughly discussed in Rault's work [18].

Data aggregation and compression: Data aggregation and compression are data reduction techniques that aim at reducing large amounts of data, preserving only their meaningful parts. For example, Dong *et al.* [49] propose an approach that sends data to the sink node by converging multi-path routes of event monitoring nodes into a one-path route to aggregate data. On the other hand, Liu *et al.* [50] propose a compression data collection scheme for wireless sensor networks where data are compressed 'on the fly' under an opportunistic routing scheme.

Sink node mobility: Several works have proposed the sink node to have the ability to move and change its location in the network. As a result, nodes that are close to it, thus being severely affected by the *energy hole problem*, continuously change. A useful survey about these techniques is the one provided by Di Francesco *et al.* [51], whereas the more recent works by Zhang *et al.* in [52] and Yetgin *et al.* in [53] give a more up to date view of the field.

Energy-aware routing: Routing has special requirements in wireless sensor networks that should be met, the most significant being the efficient energy consumption. Pantazis *et al.* in their survey [38] have made a classification of the routing protocols for wireless sensor networks into four central schemes: (i) Network structure; (ii) Communication model; (iii) Topology-based and (iv) Reliable routing.

Sleep/wake-up schemes: Sleep/wake-up schemes are mainly protocols applied at the medium access control sub-layer of the nodes that are capable of deactivating and activating a node considering the given circumstances. For example, Ye *et al.* in their work [54] have proposed the so-called *Sensor Media Access Control* (S-MAC) protocol which by applying a *periodic listen and sleep* approach, tries to reduce idle listening of nodes by periodically putting them into sleep state where their radio is turned off.

Recharging Mechanisms

Recharging mechanisms aim at recharging wireless sensors' batteries based on (i) energy harvesting techniques or (ii) wireless charging.

Energy harvesting techniques: Energy harvesting techniques allow the sensors to make use of energy supplied by their surrounding environments such as solar, wind and even body heat [55]. Based on the source they harvest energy from, these techniques can be divided into [56]: (i) Ambient environment, where the sources are exclusively environmental (e.g., solar, thermal, wind, etc.) and (ii) eternal sources, where the sources are either mechanical (e.g., vibration) or human (e.g., activity). All these techniques are thoroughly discussed by Shaikh *et al.* [56].

Wireless charging: Recent technological advances in wireless energy transfer [6], [7] have enabled for the wireless sensor nodes the possibility to have their batteries wirelessly charged. The latter, is further studied in this thesis.

Discussion

In Section A.1.3, where the proposed recharging mechanisms categorization is given, two of the techniques are said to be further studied in this thesis; thus, giving an insight about in which of these mechanisms the proposed approaches of the thesis belong in. More specifically, the approaches here are based on two of the discussed mechanisms: (i) optimal sink placement which is part of the network-based mechanisms and (ii) wireless charging which is part of the recharging mechanisms. Given the latter mentions, the related work section (A.2) next gives an insight on these mechanisms, as well as on the past work that specifically relates to the proposed approaches.

A.2 Related Work

Akyildiz *et al.* survey the basics of wireless sensor networks in [1] and [2]. A review on energy consumption is given by Anastasi *et al.* [37]. Li and Mohapatra [57] and Liu *et al.* [58] study the energy hole problem and its impact on a network's lifetime. In the past decade, a vast amount of research has addressed network lifetime extension by reducing the effects of the energy hole problem, focusing on the sensor nodes (e.g., positions of relaying nodes), the sink(s) (e.g., multiple sinks, sink movements, sink positioning) and the need for recharging sensor network nodes (see e.g., [59] by Mathuna *et al.*), as discussed in the following.

A.2.1 Sensor Nodes as Relay Nodes

Younis and Akkaya [60] survey the various methods regarding the use of powerful relay nodes with special capabilities (e.g., enhanced battery capacity). The problem of minimizing the number of relay nodes by employing approximation algorithms is visited by Lloyd and Xue [61]. Hou *et al.* [62] propose relay nodes' placement by formulating a mixed-integer nonlinear programming problem, while Halder and Bit [63] propose the deployment of heterogeneous relay nodes for uniform energy consumption. The deployment of special data-aggregate-capable relay nodes is studied by Chen *et al.* [64]. In [65], a relay node deployment strategy based on artificial intelligence is proposed. Other approaches include content delivery in hybrid mobile social networks, e.g., [66].

A.2.2 Sink Placement

Efrat *et al.* [67] consider two optimal placement problems regarding the base station (i.e., the sink following the terminology of this thesis) to prolong network lifetime and cover a certain area given line-of-sight constraints. Bogdanov *et al.* [68] formulate the placement problem as a maximum flow one, while Oyman and Ersoy [69] focus on design issues. Li *et al.* [70] evaluate coordinating data transmissions for communication cost reduction, and Keskin *et al.* [71] propose a model which integrates sensor placement, scheduling, routes, and trajectories of mobile sinks.

Multiple sinks, as proposed by Vincze *et al.* [72], are shown to reduce the energy consumption by decreasing the average path length toward a corresponding sink. Basagni *et al.* [73] go a step further by introducing controlled sink movement, thus increasing the network's lifetime considering also the limitations of such movement. Luo and Habaux [74] proposed a sink mobility strategy along the periphery of the network for balancing energy consumption. Wang *et al.* [75] considered the practical limitations of moving a sink, while Shi and Hou [76] give further analytical insights on sink movement and network lifetime. Papadimitriou and Georgiadis [77] propose a routing algorithm capable of dealing with routing problems introduced by the mobility of the sink. A similar idea is presented by Luo *et al.* [78]. In their seminal paper [79], Luo and Habaux formulate the problem of maximizing network lifetime by suitable sink trajectories and prove its NP-hardness. In [80], an algorithm selecting relay nodes based on opportunistic routing theory is designed to virtually derive the optimal transmission distance for energy saving and maximizing the lifetime of the entire network.

A.2.3 Energy Consumption Problem as a Facility Location Problem

The energy consumption problem in this thesis is tackled from a facility location perspective and therefore, is different from the previously mentioned approaches (various initial results regarding facility location are surveyed by Mirchandani and Francis [81]). Facility location approaches are inherently suitable for solving placement issues and even though they result in NP-hard problems, recent approximation approaches are suitable for network environments, e.g., the distributed approximation by Smaragdakis *et al.* [82]. The closest work to the approach of this thesis is the one by Krivitski *et al.* [83] and by Oikonomou and Aïssa in a related work in [84]. In both studies, a facility formulation with respect to the sink node position is proposed. In particular, Krivitski *et al.* [83] introduce facility location modeling focusing on minimizing distances in sensor environments. Their approach indirectly reduces energy consumption because the shorter the distance, the less the energy consumed for transmission purposes. However, in Krivitski's work, the authors differentiated two significant points: (i) the authors focused mostly on approximation methods to solve the optimization problem while here the focus is mostly on the facility location modeling part; (ii) for the facility location modeling part they describe, they do not take into consideration important factors (e.g., the traffic load) that are the basis of this thesis modeling part. On the other hand, Oikonomou and Aïssa [84], proposed 1-median modeling to reduce the energy hole effects; their main focus was on the sink's movements to achieve their goal.

A.2.4 Recharging Sensor Nodes

After the recent growth in wireless power transfer technology, the concept of implementing mobile rechargers in wireless sensor networks was newly introduced by Kurs *et al.* [6], showing that under a novel technique called magnetic resonant coupling, wireless power transfer (i.e., the ability to transfer electric power from one storage device to another without any plugs or wires) is both feasible and practical. The benefit of recharging batteries in wireless networks in general, and in wireless sensor networks specifically is shown by Gatzianas *et al.* in [85] and by Angelopoulos *et al.* in [3], respectively.

The wireless charging models presented in the literature can be divided into point-to-point (e.g., [86], [87], [88], [89]) and point-to-multipoint models (e.g., [90], [91], [92], [93]). In the former case, a mobile recharger can charge a single sensor node while in the latter, the mobile recharger can charge more than one sensor nodes simultaneously.

In [94], Di Fransesco *et al.* survey the mobile data collection in wireless sensor networks, while Zhao *et al.* make a step further in [92] by jointly optimizing wireless energy provisioning and data gathering. In the same spirit, in [95], [96] and [97], schemes of joint wireless energy provisioning and data gathering by the mobile recharger are also presented.

An energy replenishing schedule in a deterministic and periodic fashion (i.e., *offline strategy* [98]) is proposed in [99] where Xie *et al.* introduced the concept of *renewable energy cycle* in which the residual energy level in a device exhibits some periodicity over a time cycle. Similar to the previous, a non-linear programming problem to optimize the travel path is formulated in [100]. The study in [101] extends the work in [99] by investigating point-to-multipoint charging. On the other hand, *on-demand strategies* (i.e., strategies that allow a mobile recharger to receive new charging requests and construct or adjust its travel path in an on-demand basis) are proposed in [102], [103], [104], [105] and [106]. In the latter, He *et al.* analyze the *On-Demand Mobile Charging* problem using a *Nearest-Job-Next with Preemption* (NJNP) discipline for the mobile recharger.

The mobile recharger's capability of recharging sensor nodes while moving, has been recently studied in [107] while in [108] and [109] the mobile rechargers are cooperating with each other while holding the ability to transfer energy between themselves. The problem of minimizing the number of rechargers, in case of multiple rechargers in the network, is considered by Dai *et al.* in [110] and in the same manner an attempt to reduce the number of rechargers is described by Pang *et al.* in [111]. Wang *et al.* [112] focus on scheduling aspects and the problem of the most suitable paths selected by a mobile recharger is studied in [113] and [114] by Han *et al.* and Li *et al.* respectively.

A.3 Contribution

The contribution of this thesis will be clearer if the problem tackled is described first.

A.3.1 Problem Definition and Motivation

Small and low-cost sensor nodes allow for developing wireless sensor networks in large-scale environments. On the other hand, small devices are typically supplied with small batteries; being wireless, they generally operate in the absence of an infrastructure, thus depending their operation on the energy supplied by their limited batteries. Even though energy consumption is of crucial importance in wireless

networks, it becomes more of a concern in their sensor counterparts [37] mostly due to the energy hole problem [57]. In particular, sensor nodes also act as relays for data generated by other nodes that need to reach the sink node, i.e., the particular node that is responsible for collecting all sensed information. For example, in Figure A.6 nodes A and B are responsible not only for sending their data packets but for forwarding the more distant nodes' packets as well, towards the sink node. As a result, they are going to run out of energy faster than the other nodes.

Consequently, nodes that are close to the sink node have to relay a significant amount of traffic load, and therefore their energy consumption is higher compared to other nodes with a less intense traffic load. This characteristic of wireless sensor networks has a significant impact on the energy consumed by the sensor nodes and specifically on network lifetime (i.e., the time until the network stops operating due to exhausted nodes' batteries [115]).

A.3.2 Proposed Approaches and Solutions

Two approaches are proposed in this thesis, in order to tackle the energy hole problem's effects and to prolong the network's lifetime. Both of them are intimately connected to *facility location theory* [81] the elements of which that are important for this thesis are given in Chapter B.

Energy Efficient Sink Placement

The first proposed approach formulates the sink placement problem (i.e., to select the particular node that the sink will be placed on) as a k-median facility location problem [81] (k is the number of sinks in the network), and shows that when the sink nodes are selected according to the solution of the median problem, then the (average) consumed energy in the network is minimized, thus allowing use of the saved energy to prolong the network's lifetime. Note that if replenishing techniques are implemented alongside with the proposed solution, the benefits from the available (i.e., saved) energy are also enhanced. Such techniques are energy harvesting [116], [117], [118] and recharging [6], [7], [119], [3], the latter taking advantage of wireless energy transfer technologies [6], [7] and utilizing recharging equipment (e.g., [3]) to fulfill their purpose.

The first challenge is to analytically model network lifetime and the available energy in a network, given that they both depend on numerous factors (e.g., transmission characteristics at the physical layer, medium access control and retransmission policies at the data link layer, routing approaches at the network layer, among others, under the protocol stack terminology earlier given). The motivation here is

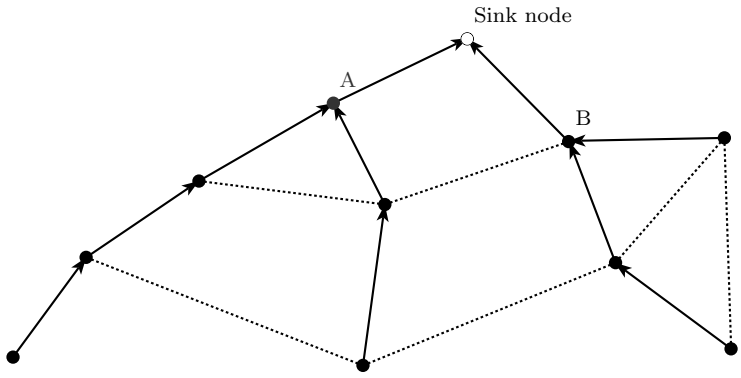

Figure A.6: *Simple example network. Arrowed lines correspond to the next hop of a data packet towards the sink node.*

to derive an effective but straightforward analytical model suitably representing a system's idiosyncrasies.

The mean and variance of the energy available in the network nodes are analyzed, and analytical expressions are also derived considering tree topologies as a case study motivated by the fact that data are forwarded over routing trees toward sink nodes. The next step is the formulation of the energy consumption problem as a facility location one, based on the proposed analytical model. It is demonstrated that when the sinks are placed according to the k-median solution, the network's overall consumed energy is minimized, thus enabling green use [120]. This is a key contribution as it relates the energy consumption problem to a facility location one and consequently, it allows application of tools and ideas from the area of facility location theory to energy consumption problems in the considered wireless sensor networks.

While dealing with the NP-hard nature of the facility location problems [81] is not within the scope of this thesis, approximate approaches do exist as well as distributed ones, e.g., [82], that can be employed to a particular network environment. A literature review about their computational complexity and approximate approaches is given in Section B.2.

In addition, the proposed analytical modeling and the analysis results are validated via simulation results, assuming geometric random graphs [121], suitable for representing wireless sensor network topologies. A contribution of the simulation results amounts to showing that the employed analytical model effectively captures certain basic aspects of the network's behavior. Regarding the analytical findings,

it is observed from the simulation scenarios that energy consumption is minimized when the sinks are located at those nodes recommended by the analysis and that the corresponding energy savings significantly increase network lifetime.

Recharging Distance Minimization

In the second approach, the increased energy consumption due to the energy hole problem is tackled by the implementation of a *mobile recharger* able to move within the network when a request is applied by one or more sensor nodes in need for a battery replenishment. The mobile recharger remains stationed at the sink node's location when inactive, and moves according to shortest path's branches upon an energy request, according to the given recharging policy. Two recharging policies are considered, both relying on local information, i.e., the mobile recharger receives intelligence regarding the recharging requests of the network nodes only when it arrives at the sink node. More specifically, these policies are: (i) a simple recharging policy under which a request is sent to the sink node to initiate a recharging process if the battery level of a sensor node is below a fixed recharging threshold; (ii) a recharging policy that enhances the previous one, recharging all nodes en route to the node that has requested for a recharge. When the mobile recharger under the second proposed policy arrives at the node (that has requested for a recharge) location, it recharges its battery and then moves to those neighbor nodes with the lowest energy level.The latter step is repeated until there is no energy left at the mobile recharger's battery to recharge any further.

As it is shown, the recharging distance, i.e., the distance covered by the mobile recharger, under the first recharging policy, corresponds to a facility location problem and particularly to a 1-median one [81]. This is an important contribution since it relates battery replenishing problems in wireless networks to facility location problems. Simulation results validate the analytical findings and show that when the sink is located at the solution of the 1-median problem formulated here, then the distance covered by the mobile recharger is minimized. For the simulation purposes, geometric random graphs are also considered. The effect of the recharging threshold is investigated and particularly, how it affects the energy level of the sensor nodes' batteries and the distance covered by the mobile recharger. It is also shown that the value of recharging threshold does not affect the optimal position of the sink; thus the minimum recharging distance remains constant as also expected by the analysis. Furthermore, this simple policy is enhanced by allowing the recharging device to replenish the nodes' battery along the trajectory towards the particular node that initiated the recharging request in the first place. As it is expected, the results are further improved in compliance with the analysis.

The second proposed policy is evaluated using simulation results against a well-known policy in the literature, the NJNP policy [106] and a variation of the latter – to be referred to hereafter as the *r-NJNP* policy – that, similarly to the proposed recharging policy, recharges all nodes en route. First, the median problem is also considered here, and it is demonstrated that, depending on the location of the sink, the performance of all three considered recharging policies changes; the best location being the solution of the median problem. This enhances the contribution derived by the first policy's approach since it confirms the relation of the battery replenishment problems in wireless sensor networks to facility location problems. Second, the location of the sink for the simulation experiments is assumed the one that corresponds to the solution of the particular median problem. The simulation results also demonstrate the fact that the proposed policy operates close to the NJNP and the r-NJNP policies and in some cases it outperforms them both, in terms of (mobile recharger's) covered distance, average and variance of the battery level in the network nodes, total (mobile recharger's) vacation period, pending of recharging requests and termination time. This is a significant result since the proposed recharging policy relies on local information as opposed to the existing NJNP and r-NJNP policies that require global knowledge. Note that the simulator parameters are configured based on the specifications of an existing wireless system (i.e., MICA2 mote [122]) in order to provide for a realistic simulation environment.

A.3.3 Contribution Summary

Summarizing the contribution of the thesis, two approaches are described here in order to minimize the energy consumption in wireless sensor networks and maximize the network lifetime, in order to counter the energy hole problem's effects. The first approach formulates the sink placement problem as a k-median facility location problem, while the second establishes a relation between the k-median facility location problems and battery replenishment, along with proposing a new policy for recharging the network nodes.

The establishment of a relation between facility location problems (particularly the k-median problem) to energy consumption and battery replenishment is a significant contribution that is expected to trigger future work in the area and reveal further aspects of the energy consumption issues and how lifetime may be prolonged in wireless sensor networks.

A.4 Thesis Structure

The present chapter (Chapter A) is the introductory part of the thesis, where a brief description of wireless sensor network applications. Existing technologies and mechanisms are also given aiming to optimize energy consumption in wireless sensor networks, which is also the goal of this thesis. As the proposed approaches here are related to two of the mechanisms mentioned, the above correlation is a springboard for reviewing the most recent research effort by the scientific community on related issues. Finally, this chapter presents the motivation and definition of the problem addressed and the proposed approaches to tackle its effects.

In Chapter B, basic elements of *facility location theory* are given, as the contribution of the thesis is based mainly on it. In particular, the facility location problem is described in its original form and is followed by further analysis of its various aspects: (i) *capacitated facility location problem*; (ii) *uncapacitated facility location problem*, and (iii) *k-median problem*. For ease of reading, an example of a facility location problem is given, which in each relevant section of the chapter is transformed into an example of a capacitated facility location problem, an uncapacitated facility location problem and a k-median problem, thus, giving an insight of the basic differences between the problems and their solutions. Note that the solutions are given for each aspect of the example and are calculated using a free tool. In addition, the computational complexity of facility location problems is given, as well as a review of the relevant existing research.

Chapter C describes all the elements that affect the operation of a wireless sensor network, as well as a set of assumptions that allow for a tractable analysis. All the approaches of the thesis are based on the model and assumptions being described in this chapter, while possible modifications are later mentioned in the text, where they take place. The components of the proposed system model described in this chapter are (i) topology, (ii) energy consumption, (iii) medium access control and retransmission, (iv) routing, (v) traffic load, (vi) battery of the devices and (vii) life of the system.

In Chapter D the first of the two approaches of the thesis is elaborated. It focuses on the study of the sink placement at an existing node (i.e., the node carrying the collector is responsible for collecting all the measurements of all network nodes) of the wireless sensor network, in such a way as to optimize the power consumption of the network and extend its lifetime. The basic feature of this approach is that it addresses the sink placement problem as a facility location problem (of a certain number of facilities), indicating that under the latter approach the power consumption of the network nodes is minimized. This chapter provides a theoretical analysis

of the above approach as well as the results of the simulations aiming at confirming the theoretical analysis. More specifically, in the first section of the chapter, the theoretical approach of the available energy of the network at the moment of its termination is presented. The available energy is studied from the point of view of the average available energy and the variation of available energy at the time of its termination. At the end of the first section, it is shown that based on the theoretical analysis given above, energy consumption can be optimized by moving the sink (between nodes). The motivation mentioned above is studied in the second section of the chapter with regard to the optimal placement of the sink (or sinks). The results obtained are further confirmed by the simulations carried out in the third section. There, after analyzing the scenarios developed and the parameters used, the theory is applied to the data used for the needs of the simulations (geometric random graphs, the use of a protocol for the medium access control), as well as analysis of the traffic load. The main points studied by the simulations are: (i) the available energy; (ii) the location of the sink; (iii) the lifetime of the network and (iv) networks with more than one sink.

The second approach of the thesis is given in Chapter E. The latter approach concerns the study of recharging the batteries of the wireless sensor devices by developing relevant policies that rely on the use of mobile rechargers. The main contribution highlighted here is the correlation between the reduction of the total distance that the mobile recharger travels, with the facility location theory. More specifically, in this chapter it is theoretically shown and reinforced by the relevant simulations, that when the starting point of the mobile recharger is the location of the sink node chosen through the logic of the facility location theory, then the distance covered by the mobile recharger decreases. Chapter E describes: (i) the two proposed recharging policies; (ii) the theoretical analysis associated with them (recharging period, distance traveled by the recharging device); (iii) the mechanisms under which they operate and (iv) the simulations that enhance the theoretical analysis.

Chapter F presents the overall contribution of the thesis. In particular, the general conclusions are presented and commented, while the chapter concludes with future research thoughts.

Appendices of the thesis are given in an extra part, where there are presented (i) the proofs of the various theorems, lemmas and corollaries being described and (ii) a description of the main elements of the simulator used to develop all the simulation scenarios of the thesis.

Chapter B

Discrete Facility Location Theory Elements

FACILITY location problems, as their name indicates, deal with selecting the best location for placing facilities in order to best meet the demanded constraints, where fixed costs exist for every possible facility's location. Facility location problems apply to a variety of fields, e.g., *operational research* [123], [124], *computational biology* [125], *computer vision* [126], [127], *data mining* [128], *network design* [129], etc.

For example, consider a supermarket's chain owner has decided to expand his supermarkets' network in a new country. After having decided about the cities the new supermarkets are going to be placed on, it remains to decide how many warehouses to be *opened* and at which locations, among several candidates. The problem here is to find the best locations for opening new warehouses so as to give the highest profit choice to the owner. The solution to this problem has to take into account parameters such as: (i) fixed costs for every location, e.g., acquiring land or buildings costs; (ii) distance that has to be traveled by the suppliers to reach every potential new warehouse location and (iii) demand the new supermarkets will have from warehouses so as to work properly.

In the primary form of the facility location problems, the number and locations of facilities have to be parts of the solution, while variations of facility location problems also exist. In some of them, potential facilities are bounded by a *capacity* threshold, that is the maximum demand that a facility can supply. Additionally, in some problems, the selection of the location of the new facility can be any location within the space, while in some other the set of facilities' possible locations is predefined. Moreover, in many problems, the number of facilities to be opened is fixed, and it does not have to be jointly derived along with the locations as part of the solution.

Problems in which the facilities locations' set of choices is not given belong to *continuous* facility location theory. In this thesis, for all approaches being presented, it is supposed that each facility is 'hosted' by a network's node; thus the facility's location is the same with the already defined node's location. In this case, approaches are based on *discrete* facility location theory, i.e., the number of possible locations of the facilities are discrete as they are reduced to the network nodes' locations.

B.1 Capacitated and Uncapacitated Facility Location Problems

Back to the example given in the second paragraph of the current chapter, suppose that the new supermarkets has been decided to be placed at the locations depicted in Table B.1 (Latitude (y) and Longitude (x)) and the warehouses' locations are going to be selected among the same set of locations, i.e., the set of the candidate locations for the warehouses to be opened, consists of the locations that already have been selected to place the new supermarkets[1]. Additionally, suppose that: (i) each supermarket demands a specific number of products to work properly; (ii) each warehouse will have a maximum number of products it can supply the supermarkets (including the one located in the same location with it) and (iii) the cost for opening (or setting up) a new warehouse differs among the candidate locations (e.g., buying land or building costs are not the same). All the locations' characteristics related to the supermarkets and warehouses are depicted in Table B.1. Note that there is a cost for each warehouse to serve a supermarket (called *service cost*) and it denotes the distance between a supermarket and a potential warehouse's location. The latter is calculated here by the Euclidean distance between the two locations, based on the given latitude and longitude.

Problems like this, where each potential facility may serve at most a maximum number of demands (i.e., facilities have a fixed capacity), are considered as *capacitated facility location problems*. The capacitated facility location problem is defined as follows:

Given:

- a finite set V and distances (or service costs) $\mathsf{c_{ij}} \geq 0$ $(\mathsf{i}, \mathsf{j} \in \mathsf{V})$ with $\mathsf{c_{ij}} + \mathsf{c_{jk}} \geq \mathsf{c_{ik}}$ (triangle inequality) for all $\mathsf{i}, \mathsf{j}, \mathsf{k} \in \mathsf{V}$;
- a set $\mathsf{D} \subseteq \mathsf{V}$ of clients;

[1]Note that in the sequel a supermarket will actually correspond to a node and a warehouse to a facility.

Table B.1: *Locations of the supermarkets and possible locations of the warehouses.*

Location	Latitude (y)	Longitude (x)	Demand	Capacity	Setup cost
A	38.957988739	20.7514095306	2	2	7000
B	39.1587715149	20.979850769	3	7	600
C	39.6685791016	20.8563804626	4	7	6000
D	39.5126495361	20.2583808899	2	3	6500
E	39.2854690552	20.4019298553	2	4	5600
F	39.7696609497	21.18268013	2	3	5500
G	38.7852783203	21.1128997803	2	4	5000
H	39.5415916443	20.513999939	3	7	700

- a set $\mathsf{F} \subseteq \mathsf{V}$ of potential facilities;
- a fixed cost $\mathsf{f_i} \geq 0$ for opening each facility $\mathsf{i} \in \mathsf{F}$;
- a capacity $\mathsf{u_i} \geq 0$ for each facility;
- a demand $\mathsf{d_j} \geq 0$ for each client.

The goal is to find:

- a subset $\mathsf{S} \subseteq \mathsf{F}$ of facilities to 'open';
- an assignment x of clients' demand to open facilities, where $\sum_{\mathsf{i}\in\mathsf{S}} \mathsf{x_{ij}} = \mathsf{d_j}$ for all $\mathsf{j} \in \mathsf{D}$

such that the sum of facility costs and service costs is minimized:

$$\min \sum_{\mathsf{i}\in\mathsf{S}} \mathsf{f_i} + \sum_{\mathsf{i}\in\mathsf{S}} \sum_{\mathsf{j}\in\mathsf{D}} \mathsf{x_{ij}} \mathsf{c_{ij}} \tag{B.1}$$

In Figure B.1, the solution to the example capacitated facility location problem is depicted. Locations B and H are the cheapest to open a facility - warehouse to and following their being placed closer to the network's center (thus minimizing distances from the other locations), their selection does make sense. On the other hand, their capacities are not large enough to serve all supermarkets' demands by themselves. In this case, one more facility - warehouse has to be opened. Note that, for the solution of the problem, *FLP Spreadsheet Solver* [130] is used, which is based on *Tabu search heuristic algorithm* [131] and variations of it.

Let us assume, in the given example that the warehouses have an infinite maximum capacity, the problem is now reformulated to an *uncapacitated facility location*

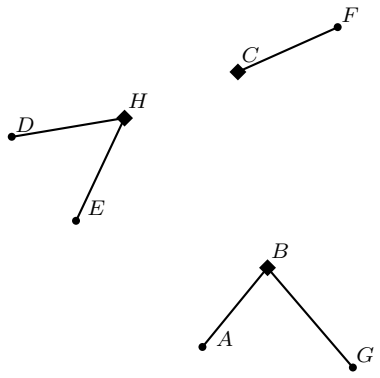

Figure B.1: *Solution to the example problem formulating a capacitated facility location problem. Diamonds (i.e., B, C, H) indicate locations where facilities are selected to be placed, while lines show the supermarkets each facility (warehouse) serves.*

problem [132]. In these problems, facilities, having infinite capacity, can suffice all demands by themselves.

The uncapacitated facility location problem is defined as follows:
Given:

- a finite set V and distances (or service costs) $\mathsf{c_{ij}} \geq 0$ $(\mathsf{i}, \mathsf{j} \in \mathsf{V})$ with $\mathsf{c_{ij}} + \mathsf{c_{jk}} \geq \mathsf{c_{ik}}$ (triangle inequality) for all $\mathsf{i}, \mathsf{j}, \mathsf{k} \in \mathsf{V}$;

- a set $\mathsf{D} \subseteq \mathsf{V}$ of clients;

- a set $\mathsf{F} \subseteq \mathsf{V}$ of potential facilities;

- a fixed cost $\mathsf{f_i} \geq 0$ for opening each facility $\mathsf{i} \in \mathsf{F}$;

The goal is to find:

- a subset $\mathsf{S} \subseteq \mathsf{F}$ of facilities to 'open';

- an assignment σ of clients to open facilities

such that the sum of facility costs and service costs is minimized:

$$\min \sum_{\mathsf{i} \in \mathsf{S}} \mathsf{f_i} + \sum_{\mathsf{j} \in \mathsf{D}} \mathsf{c_{\sigma(j)j}} \tag{B.2}$$

Reformulating the example problem in an uncapacitated one will make the solution ignore the demand and capacity given in Table B.1. Implementing the new (uncapacitated) setup to FLP Spreadsheet Solver, the solution now is depicted in

Figure B.2. Note that even if a single facility could serve all supermarkets, two of them are selected to be opened instead, as a result of the solution's taking into account the distance costs among locations. It seems to be more profitable to open one more facility than traveling from a single one to all supermarkets. For example, location G distance costs (i.e., the Euclidean distances) from C, D, E, H are 128.62, 135.42, 110.4 and 140.81 respectively. Summing the costs and multiplying the result by 2 (it is a two-way cost) will give 1030.50 as a result, which is more expensive than 'opening' a facility to H to serve them.

As already mentioned, approaches in this thesis are based on discrete facility location theory, because the number of possible locations of the facilities is discrete as they are reduced to the network nodes' locations. Additionally, existing solutions for capacitated and uncapacitated facility location problems are asymptotically the same. In the case of wireless sensor networks, the costs for a facility location problem to be solved would consist of the cost of communication between nodes. The latter cost can be dependent on the physical distance between nodes (as a longer wireless link requires higher transmit power and thus increased energy consumption), on the number of hops in a multi-hop network graph, or on interference and network congestion ([133]), as well as on the traffic load. Thus, facility location problems in wireless sensor networks are commonly dealt with solutions provided by discrete uncapacitated facility location problems.

B.2 Computational Complexity of Facility Location Problems

Facility location problems, as demonstrated by Krarup and Pruzan back in 1983 [134] are considered as part of combinatorial optimization problems class, termed NP-hard. Capacitated facility location problems are NP-hard [135] even in the case of setting the maximum facility capacity to ∞ (case of uncapacitated facility location problems) [136], [137], [135], [132]. In [138], Guha and Khuller showed that it is hard to approximate uncapacitated facility location problems within a factor of 1.463, assuming $NP \nsubseteq DTIME(n^{\log\log n})$. Three years later, Jain *et al.* in [139] introduced that the existence of a (λ_f, λ_c) - approximation algorithm with $\lambda_c < 1 + 2e^{-\lambda} f$ implies $NP \subseteq DTIME(n^{\log\log n})$. An algorithm is a (λ_f, λ_c) - approximation algorithm if its solution has total cost at most $\lambda_f \times F^* + \lambda_c \times C^*$, where F^* and C^* denote the facility and the assignment cost of an optimal solution, respectively.

Despite its NP-hardness, various approximation algorithms have been proposed

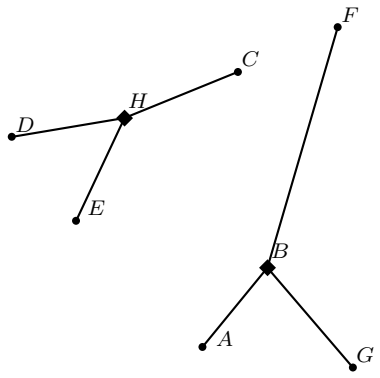

Figure B.2: *Solution to the example problem formulating an uncapacitated facility location problem. Diamonds (i.e., B, H) indicate locations where facilities are selected to be placed, while lines show the supermarkets each facility (warehouse) serves.*

and can be used to reduce the complexity of the problem. Back in 1982, Hochbaum in [140] introduced a greedy algorithm with $O(log(n))$-approximation guarantee for it, where n is the number of clients. In 1997, Shmoys *et al.* in [141], based on the Lin's & Vitter's *filtering and rounding technique* (LP-rounding) [142], showed a polynomial-time algorithm that finds a solution within a factor of 3.16 of the optimal. In 2001, Jain and Vazirani in [143] presented the first *primal-dual* approximation algorithm that was later improved by Jain *et al.* in 2003 [144] to find a solution within a factor of 1.861. Byrka and Aardal in their works in 2007 and 2010 [145], [146] proposed an algorithm parameterized by γ and used it with $\gamma \approx 1.6774$, obtaining an algorithm that gives expected approximation ratio 1.5. This work was a modification of the $(1 + 2/e)$ approximation algorithm of Chudak and Shmoys [147] and improved the 1.52-approximation algorithm by Mahdian *et al.* [148], [149]. Li, in [150], has shown that if the above γ is randomly selected, then the approximation ratio can be improved to 1.488, thus cutting the gap with the 1.463 factor shown by Guha and Khuller by almost 1/3.

Various techniques have been used as the basis for constructing approximation algorithms. For example, as already mentioned, Lin's and Vitter's filtering and rounding technique is one of them (e.g., in [151] and [147]) and primal-dual technique is another (e.g., in [143]). Some algorithms in the literature are based on a *greedy procedure* (e.g., in [138] and [152]), while *dual-fitting* is the chosen one by Li in [150]. In addition, combinations of the above techniques have been proposed, such as in [139] where Jain *et al.* presented a greedy algorithm that uses the LP-relaxation implicitly to obtain a lower bound for a primal-dual analysis, achieving

an approximation guarantee of 1.61. Mahdian *et al.* in their earlier mentioned work (i.e., [149]), used Jain *et al.* algorithm combined with a greedy procedure. Byrka and Aardal in [146] have also combined Jain *et al.* with an LP-rounding based algorithm, and subsequently, their algorithm and Jain *et al.* algorithm were remixed (by randomizing γ) to give the 1.463 approximation of Li, in [150].

B.3 The Case of Uncapacitated k-Median Problem

Suppose in the supermarkets' example, in its uncapacitated version, that the owner is obligated to open at maximum one warehouse to serve all supermarkets and that there is no cost for opening them (or the cost is equal for all locations). In cases of uncapacitated facility location problems and the number of facilities to be opened is fixed, with no cost for opening them, then the problem is reformulated in a *k-median problem*, where k is the number of facilities to be opened.

The k-median problem is defined as follows:

Given:

- a finite set V and distances (or service costs) $\mathsf{c_{ij}} \geq 0$ $(\mathsf{i}, \mathsf{j} \in \mathsf{V})$ with $\mathsf{c_{ij}} + \mathsf{c_{jk}} \geq \mathsf{c_{ik}}$ (triangle inequality) for all $\mathsf{i}, \mathsf{j}, \mathsf{k} \in \mathsf{V}$;
- a set $\mathsf{D} \subseteq \mathsf{V}$ of clients;
- a set $\mathsf{F} \subseteq \mathsf{V}$ of potential facilities;
- a fixed number of facilities k to open;

The goal is to find:

- a subset $\mathsf{S} \subseteq \mathsf{F}$, $|\mathsf{S}| = \mathsf{k}$ of facilities to 'open';
- an assignment σ of clients to open facilities;

such that the sum of service costs is minimized:

$$\min \sum_{\mathsf{j} \in \mathsf{D}} \mathsf{c}_{\sigma(\mathsf{j})\mathsf{j}} \tag{B.3}$$

In Figure B.3 the solution of the example problem is presented when taking into consideration that only one warehouse is going to be opened, i.e., it is a 1-median problem. Location B is chosen here, as it is one of the cheapest solutions in terms of distance cost (being placed almost in the center).

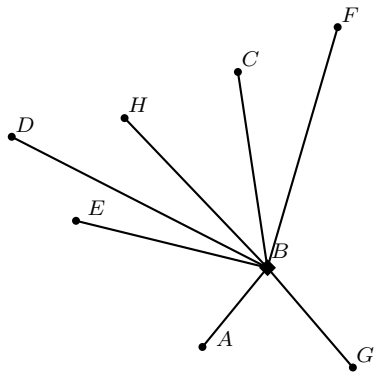

Figure B.3: *Solution to the example problem formulating a k-median problem. Diamonds (i.e., B) indicate locations where facilities are selected to be placed, while lines show the supermarkets each facility (warehouse) serves.*

B.3.1 Facility Location Notation

As already mentioned, the approaches in this thesis are based on uncapacitated facility location problems. In addition, the number of sinks (that will correspond to facilities) here are supposed to be known, so the k-median version of the uncapacitated facility location problems will be considered for the rest of this thesis.

Note that the approach here, is to study the sink placement problem (among the network nodes locations) from two perspectives: (i) the average consumed energy of the network is minimized (Chapter D) and (ii) the distance traveled by a mobile recharger is minimized (Chapter E). The cost for selecting a node to play the role of the *sink node* (i.e., the node that holds the sink) will be given by the sum of products $\lambda_u \mathtt{d}(u, \mathtt{s}(u))$ in the first case and $\Lambda_u \mathtt{d}(u, \mathtt{s}(u))$ in the second, where u denotes a node in the network, $\mathtt{s}(u)$ is the sink node (that serves node u), $\mathtt{d}(u, \mathtt{s}(u))$ is the shortest path distance from u to $\mathtt{s}(u)$ and λ_u (Λ_u) is the traffic load (aggregate traffic load) of node u.

Chapter C

Wireless Sensor Networks System Model and Notation

THE various factors that affect the operation and behavior of a wireless sensor network (e.g., topology, energy consumption, etc.) are described in this chapter, along with a set of assumptions that allow for a tractable analysis. The presented system model is considered throughout this thesis and possible variations are mentioned where applied. For the shake of readability, brief descriptions of parts of this section are given later whenever necessary.

C.1 Topology Model

The network topology is represented by a connected undirected graph $\mathbb{G}$ [121], where $V(\mathbb{G})$ is the set of nodes and $E(\mathbb{G})$ is the set of links among them. The size of set V, denoted by n, corresponds to the number of nodes in the network (i.e., $n = |V(\mathbb{G})|$). If a link (u, v) exists between two nodes u and v (i.e., $(u, v) \in E(\mathbb{G})$), then these nodes are neighbors and a transmission can take place between them directly. It is assumed that each node u occupies a physical location determined by position coordinates (two dimensional without loss of generality). If $(u, v) \in E(\mathbb{G})$, let $\chi(u, v)$ denote the corresponding Euclidean distance between nodes u and v. If $(u, v) \notin E(\mathbb{G})$ (i.e., nodes u and v are not neighbors), there exists a shortest path between these nodes, and let $\mathtt{x}(u, v)$ denote the summation of the Euclidean distances of the individual links between nodes u and v over the shortest path (referred to as the shortest path Euclidean distance). If $(u, v) \in E(\mathbb{G})$, then $\mathtt{x}(u, v) = \chi(u, v)$.

Sink nodes collect all the sensed information within the wireless sensor network and forward it outside the network. Therefore, it is reasonable to assume that each sink node is attached to some type of infrastructure (e.g., one having adequate

connectivity and abundant power supply). It is assumed that k sinks are located at k different positions in the network. Let $\mathtt{s}$ denote a particular sink placement, i.e., the particular set of nodes acting as sinks (obviously, $|\mathtt{s}| = k$). Each node $u \in V(\mathbb{G})$ is served by only one sink (i.e., u transmits its packets toward the same sink throughout the network operation), denoted by $\mathtt{s}(u)$, that is the one closest to node u in terms of the lowest Euclidean distance, i.e., $\mathtt{x}(u, \mathtt{s}(u)) = \min_{s \in \mathtt{s}} \mathtt{x}(u, s)$.

C.2 Energy Consumption Model

Assuming that node u is about to transmit to its neighbor node v (i.e., $(u, v) \in E(\mathbb{G})$), let $w(u, v)$ denote the energy consumed for this transmission. Symmetric links are considered here, thus the energy consumed for a transmission from node u to node v is the same for the reverse. A commonly used model ([153]) regarding the energy consumption is given by: $w(u, v) = \mu\chi^{\gamma}(u, v) + \nu$, where: (i) ν is a constant amount of energy consumed for the operation of the device (e.g., sensing) and independent of the distance; (ii) μ is a constant factor; and (iii) γ is the path loss factor that is mainly determined by the surrounding environment (for open space $\gamma = 2$, while for more dense environments, such as buildings, its value can be as high as five [153]). Given that the dominating factor in wireless transmissions is the energy consumed for the actual transmission so that ν is negligible when compared to $\mu\chi^{\gamma}(u, v)$ [154], then

$$w(u, v) = \mu\chi^{\gamma}(u, v). \tag{C.1}$$

The consumed energy $w(u, v)$ will be treated as the weight of the link between node u and v and will be referred to as the link weight of link (u, v). Assuming a shortest path among two nodes u and v, the summation of the weights of the links along this path will be referred to as the *energy distance* and is denoted by $\mathtt{d}(u, v)$. Obviously, $\mathtt{d}(x, y)$ corresponds to the overall consumed energy for a data packet being transmitted over the particular shortest path. That is, $\mathtt{d}(x, y)$ equals the sum of the energy consumed by the node that created the packet and the energy consumed by the nodes that forwarded the packet toward the sink node. Note that a shortest path among two nodes u and v, when considering the shortest path Euclidean distances $\mathtt{x}(u, s)$, is also a shortest path when link weights $w(u, v)$ are taken into account (assuming that μ and γ are the same for all network links). This is due to the fact that both $w(u, v)$ and $\mathtt{x}(u, s)$ depend on the Euclidean distance $\chi(u, v)$ (note that if $f > g + h$, then $f^e > g^e + h^e$, for any positive f, g, h and $e \geq 1$).

C.3 MAC and Retransmission Model

The employed MAC policy and other factors such as retransmissions, also affect the consumed energy [155]. For example, if a MAC policy that allows for collisions is employed (e.g., contention-based), then retransmissions are unavoidable. Even if a collision-free TDMA-based MAC is employed, there might be erroneous transmissions caused by the wireless medium (e.g., bad channel conditions, interference by nearby nodes) resulting in the need for retransmitting the same data packet. As the focus here is not on medium access control, for the analytical parts it is assumed that the employed MAC protocol is capable of successfully delivering data packets with no collisions. For the simulation parts, possible variations are explained in the respective sections. It should be noted that both the employed MAC and retransmission policy affect *time delay* and *packet loss*, which are critical parameters of the overall behavior of a network. For example, delayed data packets may become obsolete due to time constraints, thus resulting in unnecessarily consumed energy. The same applies for packet losses that require retransmissions. The approach followed is to reduce the overall energy consumption by selecting the sinks' locations and therefore further investigation of the MAC and retransmission policies are beyond the scope of this work.

C.4 Routing Model

Routing supports data packet relaying among neighbor nodes toward the sink nodes. Even though numerous sophisticated energy-aware routing protocols have been proposed over the years (e.g., [156], [157], [158], [159]) in this thesis a simple shortest path routing approach is employed [160], assuming link weights $w(u, v)$, as given by Equation (C.1). This fundamentally energy-aware and simple routing policy is adopted here, even though the analysis can be applied to any routing policy that creates routing trees.

Assuming node u, then a shortest path tree is created rooted at the corresponding sink node $\mathtt{s}(u)$. Given that there are $k \geq 1$ sink nodes in a network, there are k different shortest path trees, their root being a (different) sink node. For a sink placement $\mathtt{s}$, let $\mathbb{T}^{\mathtt{s}}(u)$ denote a subtree (of root node u) of the shortest path tree created by the previously mentioned shortest path routing policy. Under this notation, the shortest path tree (to be referred to also as the routing tree) rooted at sink node $\mathtt{s}(u)$ is denoted by $\mathbb{T}^{\mathtt{s}}(\mathtt{s}(u))$. An example of a routing tree is depicted in Figure C.1.

C.5 Traffic Load Model

When a data packet generated at some node u arrives at some node v, then node v, in its turn, should forward it further toward the sink node $\mathtt{s}(u)$, in addition to any data packets generated by node v itself. It is assumed that the node's internal memory is adequate for any queuing requirements.

Let λ_u denote the probability that a data packet is generated at some node u at any time unit, referred to as the traffic load of node u. Given a sink placement $\mathtt{s}$, let $\Lambda^{\mathtt{s}}(u)$ denote the aggregate traffic load of node u, given by

$$\Lambda^{\mathtt{s}}(u) = \sum_{v \in \mathbb{T}^{\mathtt{s}}(u)} \lambda_v. \tag{C.2}$$

Figure C.1 depicts an example network and graphically illustrates a shortest path tree, assuming the root sink node $\mathtt{s}(u)$, where $\mathbb{T}^{\mathtt{s}}(u)$ and $\Lambda^{\mathtt{s}}(u)$ for some node u. The illustrated dense arrows correspond to the paths over which data packets are forwarded through the network links toward the sink node.

C.6 Battery Model

Let $\mathcal{B}_u^{\mathtt{s}}(t)$ denote the amount of energy remaining at node u's battery at time t for a given sink placement $\mathtt{s}$. Let $\mathcal{B}_{\max}$ denote the capacity of a node's battery. Assuming that at the beginning of a network's life (i.e., $t = 0$) all nodes are fully charged, then $\mathcal{B}_u^{\mathtt{s}}(0) = \mathcal{B}_{\max}$, $\forall u \in V(\mathbb{G})$.

Given that transmissions represent the dominant energy consumption factor, if a transmission takes place from node u toward node v, it is expected that the energy level of node u's battery will be reduced by $w(u, v)$. Assuming that there are no transmission errors and that the employed MAC policy is capable of avoiding collisions, then for a time period $[0, t]$, node u is expected to transmit (on average) $\Lambda^{\mathtt{s}}(u)t$ data packets, thus consuming (on average) $\Lambda^{\mathtt{s}}(u)w(u, v)t$ energy units. Therefore, the average energy level in the node's battery at time t, is given by

$$\mathcal{B}_u^{\mathtt{s}}(t) = \mathcal{B}_{\max} - \Lambda^{\mathtt{s}}(u)w(u, v)t, \tag{C.3}$$

where $(u, v) \in E(\mathbb{G})$. For the purposes of the analysis, it will be assumed that link weights are equal for all network links, therefore, they are normalized to 1, or, $w(u, v) = 1$, $\forall (u, v) \in E(\mathbb{G})$, or $\mathcal{B}_u^{\mathtt{s}}(t) = \mathcal{B}_{\max} - \Lambda^{\mathtt{s}}(u)t$.

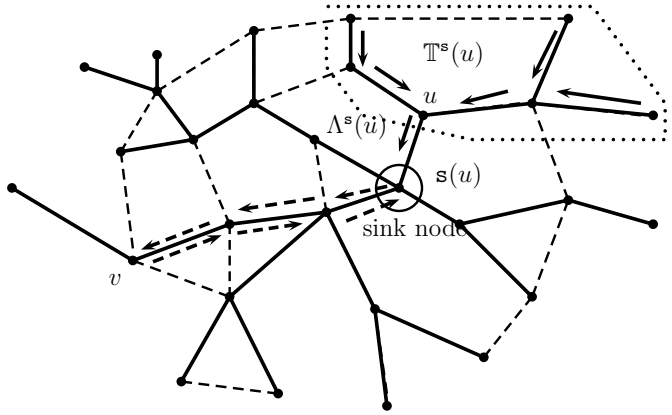

Figure C.1: *Illustrative example network (link weights equal to* 1*). Dense lines correspond to the shortest path (routing) tree links when the root is the sink node* $\mathtt{s}(u)$ *(within the circle). Dashed lines correspond to the remaining network links, i.e.,* $E(\mathbb{G}) \setminus E(\mathbb{T}^{\mathtt{s}}(\mathtt{s}(u)))$*. The area within the dotted shape pertains to subtree* $\mathbb{T}^{\mathtt{s}}(u)$*. The dense arrows correspond to the aggregate traffic load and the dashed ones to a recharging device that moves to node* v *and then returns to the sink node. For this example,* $\mathtt{s}(u) = \mathtt{s}(v)$*.*

C.7 Network Lifetime Model

A good indication regarding network lifetime refers to the time until the first node in the network runs out of battery power; it is soon expected to be followed by more nodes and therefore, the network will become non-operational [115]. Let $\mathcal{T}(\mathtt{s})$ denote this indicated network lifetime for sink placement $\mathtt{s}$, referred to as the termination time, and defined as the time until the first node in the network runs out of battery, i.e., $\mathcal{B}_u^{\mathtt{s}}(\mathcal{T}(\mathtt{s})) = 0$, for some node $u \in V(\mathbb{G})$. Given Equation (C.3) and equal link weights, any node u's battery will be exhausted at time $\frac{\mathcal{B}_{\max}}{\Lambda^{\mathtt{s}}(u)}$. Assuming that a sink node forwards the received information (e.g., wirelessly to an internet service provider facility), then sink node $\mathtt{s}(u)$ is expected to exhaust its battery before node u, due to its increased aggregate traffic load (i.e., the energy hole problem). Let $s \in \mathtt{s}$ be the particular sink node whose battery is the first to be exhausted. Consequently, its termination time is

$$\mathcal{T}(\mathtt{s}) = \frac{\mathcal{B}_{\max}}{\Lambda^{\mathtt{s}}(s)}. \tag{C.4}$$

$\mathcal{T}(\mathtt{s})$ is only an indication of a network's lifetime and even though it is common for a sink node to be attached to an external infrastructure and be plugged to an energy socket, it will reflect the network's lifetime behavior, as will be demonstrated using simulation results.

Chapter D

Energy - Efficient Sink Placement

IN this chapter, the first approach in this thesis is elaborated, showing the analytical analysis, along with the simulation results that confirm it. Under this approach, the sink placement problem is formulated as a k-median problem, showing that when the sink nodes are selected according to this problem's solution, then the (average) consumed energy in the network is minimized. The analytical models for both the network lifetime and the available energy are given, taking into consideration their dependencies regarding numerous factors, such as transmission characteristics, medium access control, retransmission policies and routing approaches. The motivation here is to derive a simple but effective analytical model suitably representing a system's idiosyncrasies.

The mean and variance of the energy available in the network nodes are analyzed and analytical expressions are also derived considering tree topologies as a case study, motivated by the fact that data are forwarded over routing trees toward sink nodes. Based on the analytical model proposed here, the energy consumption problem is formulated as a k-median problem and it is shown that when the sinks are placed according to the latter's solution, then the network's overall consumed energy is minimized.

Additionally, simulation results are given, validating the proposed analytical modeling and the analysis. For the simulation scenarios, geometric random graphs are assumed as suitable for representing wireless sensor network topologies. From the scenarios implemented, it is observed that energy consumption is minimized when the sinks are located at those nodes recommended by the analysis and that the corresponding energy savings significantly increase the network lifetime.

D.1 Available Energy Analysis

The energy available in the network at termination time, $\mathcal{T}(\mathtt{s})$, is key to further understand the effects of energy consumption in wireless sensor networks. Given Equation (C.3) and Equation (C.4), and assuming equal link weights, the energy left at any node u in the network at time $\mathcal{T}(\mathtt{s})$, is given by

$$\mathcal{B}_u^{\mathtt{s}}(\mathcal{T}(\mathtt{s})) = \mathcal{B}_{\max}\left(1 - \frac{\Lambda^{\mathtt{s}}(u)}{\Lambda^{\mathtt{s}}(s)}\right). \tag{D.1}$$

D.1.1 Mean Available Energy

The focus here is on the mean available energy in the network at time t, $\mathbb{E}[\mathcal{B}_u^{\mathtt{s}}(t)]$, as a function of the mean aggregate traffic load $\mathbb{E}[\Lambda^{\mathtt{s}}(u)]$, where $\mathbb{E}[\cdot] = \frac{1}{n}\sum_{u\in V(\mathbb{G})}(\cdot)$. Given Equation (C.3),

$$\mathbb{E}[\mathcal{B}_u^{\mathtt{s}}(t)] = \mathcal{B}_{\max} - \mathbb{E}[\Lambda^{\mathtt{s}}(u)]t. \tag{D.2}$$

From Equation (C.4), the following lemma is proved.

Lemma 1 *The mean available energy at time $t = \mathcal{T}(\mathtt{s})$, is given by*

$$\mathbb{E}[\mathcal{B}_u^{\mathtt{s}}(\mathcal{T}(\mathtt{s}))] = \mathcal{B}_{\max}\left(1 - \frac{\mathbb{E}[\Lambda^{\mathtt{s}}(u)]}{\Lambda^{\mathtt{s}}(s)}\right). \tag{D.3}$$

To further understand the nature of $\frac{\mathbb{E}[\Lambda^{\mathtt{s}}(u)]}{\Lambda^{\mathtt{s}}(s)}$ (and consequently, $\mathbb{E}[\mathcal{B}_u^{\mathtt{s}}(\mathcal{T}(\mathtt{s}))]$), l-ary tree topologies are considered as a case study. For simplicity, the case of only one sink node ($k = 1$) is considered for the l-ary tree case studies, even though the following results can be easily extended to cover the general case of $k \geq 1$. An l-ary tree, such as the one depicted in Figure D.1, is characterized by the number of levels m and the number of descendants of each node l, the root being the sink node. The number of nodes is given by $n = \sum_{i=0}^{m-1} l^i$. The example depicted in Figure D.1 corresponds to a l-ary tree of $l = 2$ and $m = 3$ levels with the number of nodes $n = 7$.

The motivation behind the introduction of l-ary trees as a special topology case is the existence of the routing tree that determines the paths over which data packets arrive to the corresponding sink node. Even though an l-ary tree may not be an exact approximation of a routing tree for some topologies, the analytical results are capable of capturing the network's behavior, as will be demonstrated later via simulation results.

Lemma 2 *Assuming constant traffic load λ for all network nodes and the case of an l-ary tree of m levels, the aggregate traffic load for a node at level i ($i = 1, \ldots, m-1$) of the l-ary tree, denoted as Λ_i, is given by $\frac{l^{m-i}-1}{l-1}\lambda$.*

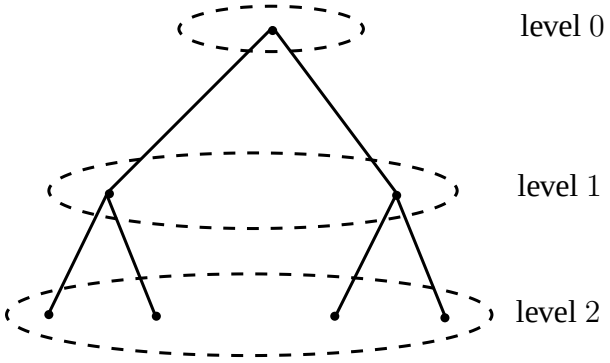

Figure D.1: *An l-ary tree ($l = 2$) example with $m = 3$ levels and $n = 7$ nodes.*

Proof *The proof is given in Appendix A.1.*

Figure D.2 depicts Λ_i as a function of the level i of a 3-ary tree of 5 levels. The corresponding number of nodes of level i (i.e., l^i) is also depicted. The interesting observation here is that large values of Λ_i (i.e., small values of i) characterize a small number of nodes, and as Λ_i decreases, the corresponding number of nodes increases exponentially. This is actually a graphical illustration of the energy hole problem, as a few nodes close to the sink node experience increased aggregate traffic load when compared to nodes not close to the sink.

Theorem 1 *Assuming one sink node, constant traffic load λ for all network nodes and the case of an l-ary tree of m levels, then it can be shown that* $\frac{\mathbb{E}[\Lambda^s(u)]}{\Lambda^s(s)} = \frac{(n(l-1)+1)\log_l(n(l-1)+1)-n}{n^2(l-1)}$.

Proof *The proof is in Appendix A.2.*

Theorem 1 provides for an analytical expression regarding $\frac{\mathbb{E}[\Lambda^s(u)]}{\Lambda^s(s)}$ as a function of n and l. The next step is to consider special cases of l, such as binary trees (i.e., 2-ary trees) and the complete graph (i.e., all nodes connected to all nodes) as given by the following corollary.

Corollary 1 *For one sink node and a 2-ary tree of m levels,* $\frac{\mathbb{E}[\Lambda^s(u)]}{\Lambda^s(s)} = \frac{(n+1)\log_2(n+1)-n}{n^2} \rightarrow \frac{\log_2(n)}{n}$, *and for the complete graph,* $\frac{\mathbb{E}[\Lambda^s(u)]}{\Lambda^s(s)} = \frac{2n-1}{n^2} \rightarrow \frac{2}{n}$.

Proof *The proof is in Appendix A.3.*

Theorem 1 and Corollary 1 shed further light on the behavior of $\frac{\mathbb{E}[\Lambda^s(u)]}{\Lambda^s(s)}$, which is an essential part of the energy left in the network, as shown in Equation (D.3). An illustration is given in Figure D.3. In particular, the left y-axis depicts $\frac{\mathbb{E}[\Lambda^s(u)]}{\Lambda^s(s)}$, as

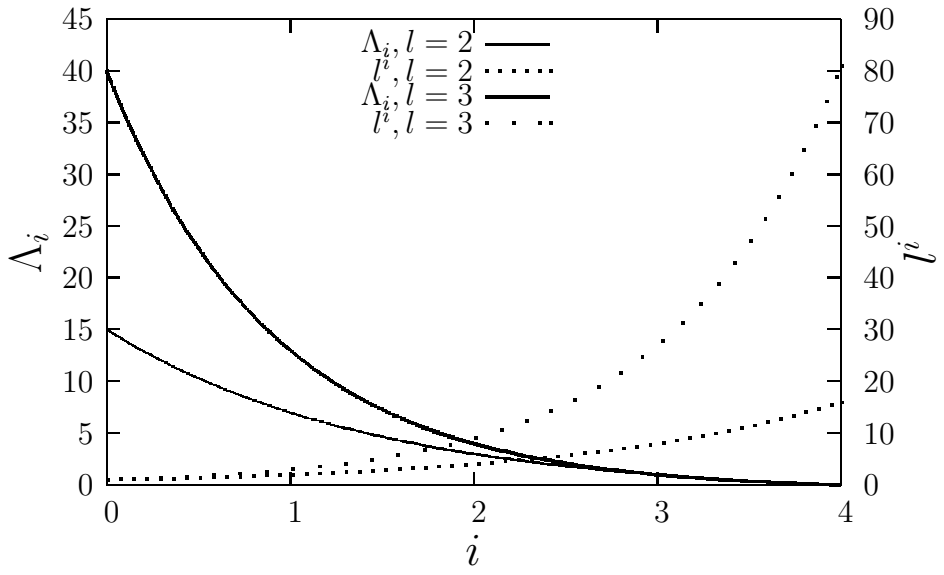

Figure D.2: *Aggregate traffic load* $\Lambda_i = \frac{l^{m-i}-1}{l-1}$ *of a node at level* i *and the number of nodes* l^i *at level* i*, as a function of* i*, for* $l = 2, 3$*, and* $m = 5$*.*

given by Theorem 1, as a function of l ($l \geq 2$, because the case of $l = 1$ corresponds to a single line topology) and $n = 1000$. For small values of l, the obtained value is close to the $\frac{\log_2(n)}{n}$ given by Corollary 1. As l increases, the (dense) curve converges to a certain point, i.e., limit $\frac{2}{n}$ given by Corollary 1. Actually, as l increases, the number of neighbor nodes in the network also increases, the upper limit being the complete graph.

D.1.2 Variance of Available Energy

Lemma 1 establishes a relationship between $\mathbb{E}[\Lambda^{\mathtt{s}}(u)]$ and $\Lambda^{\mathtt{s}}(s)$. In particular, the closer $\mathbb{E}[\Lambda^{\mathtt{s}}(u)]$ is to $\Lambda^{\mathtt{s}}(s)$, the less energy remains in the network. Note that one effect of the energy hole problem amounts to some nodes having exhausted their batteries while others' remain almost unused, thus indicating an unbalanced energy level [63]. A measure of this "unbalance" is the variance of the available energy, $Var[\mathcal{B}_u^{\mathtt{s}}(t))] = \mathbb{E}[(\mathcal{B}_u^{\mathtt{s}}(t))^2] - \mathbb{E}^2[\mathcal{B}_u^{\mathtt{s}}(t)]$, discussed below.

Lemma 3 *The variance of the available energy in the network at time* $t = \mathcal{T}(\mathtt{s})$*, is given by*

$$Var[\mathcal{B}_u^{\mathtt{s}}(\mathcal{T}(\mathtt{s}))] = \mathcal{B}_{\max}^2 \frac{Var[\Lambda^{\mathtt{s}}(u)]}{\left(\Lambda^{\mathtt{s}}(s)\right)^2}. \tag{D.4}$$

Proof *The proof is in Appendix A.4.*

The following theorem focuses on the l-ary tree case.

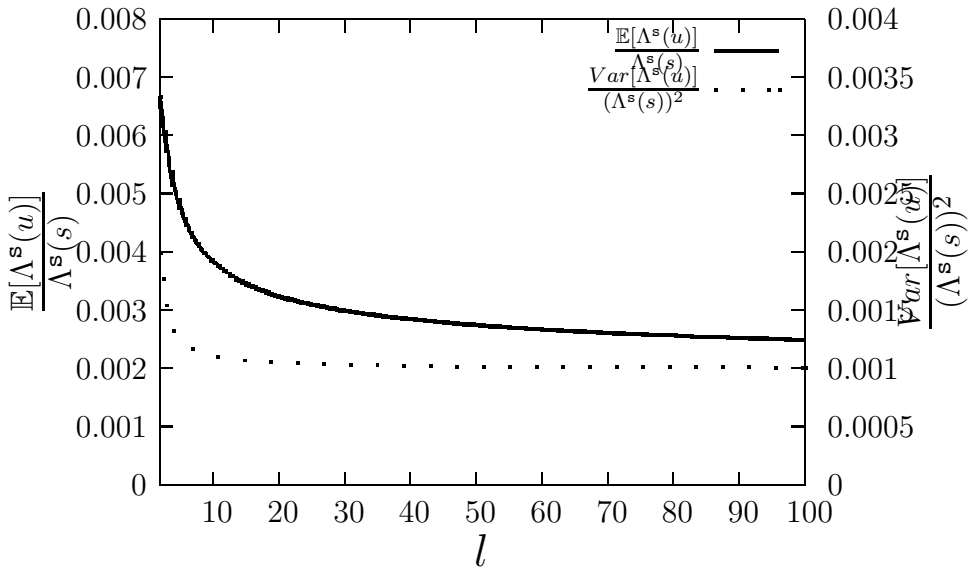

Figure D.3: $\frac{\mathbb{E}[\Lambda^s(u)]}{\Lambda^s(s)}$ *and* $\frac{Var[\Lambda^s(u)]}{(\Lambda^s(s))^2}$ *as a function of* $l \geq 2$ *(assuming* l*-ary trees) and* $n = 1000$*.*

Theorem 2 *Assuming one sink node, constant traffic load* λ *for all network nodes, and the case of an* l*-ary tree of* m *levels, it can be shown that* $\frac{Var[\Lambda^s(u)]}{(\Lambda^s(s))^2} = (n(l-1)+1)\,\frac{n^2 l-(n(l-1)+1)\log_l^2(n(l-1)+1)}{n^4(l-1)^2}$.

Proof *The proof is in Appendix A.5.*

Theorem 2 allows for an analytical expression regarding $\frac{Var[\Lambda^s(u)]}{(\Lambda^s(s))^2}$ that helps to further understand the energy available in the network for given values of l and n. Boundaries corresponding to binary trees (i.e., 2-ary tree) and the complete graph (i.e., all nodes connected to all nodes) are given next.

Corollary 2 *For one sink node and a 2-ary tree of* m *levels,* $\frac{Var[\Lambda^s(u)]}{(\Lambda^s(s))^2} = (n+1)\frac{2n^2-(n+1)\log_2^2(n+1)}{n^4} \to \frac{2}{n}$*, and for the complete graph,* $\frac{Var[\Lambda^s(u)]}{(\Lambda^s(s))^2} = \frac{(n-1)^3}{n^4} \to \frac{1}{n}$.

Proof *The proof is in Appendix A.6.*

Theorem 2 and Corollary 2 shed further light on the behavior of $\frac{Var[\Lambda^s(u)]}{(\Lambda^s(s))^2}$ for particular values of l and n. This is also graphically illustrated in Figure D.3. In particular, the right y-axis of Figure D.3 also depicts $\frac{Var[\Lambda^s(u)]}{(\Lambda^s(s))^2}$, as given by Theorem 2, as a function of l and $n = 1000$. For small values of l, the obtained value is close to $\frac{2}{n}$ given by Corollary 2. As l increases, the (dotted) curve converges to a certain point, i.e., limit $\frac{1}{n}$ given by Corollary 2.

D.1.3 Energy Consumption vs Sink Placement

A change in the sink placement may result in different energy consumption in the network, as established by the following lemma. Let $\mathtt{s}_1$ denote a certain sink placement and $\mathtt{s}_2$ a different one. Given Equation (D.2), then $\mathbb{E}[\mathcal{B}_u^{\mathtt{s}_1}(t)] = \mathcal{B}_{\max} - \mathbb{E}[\Lambda^{\mathtt{s}_1}(u)]t$ and $\mathbb{E}[\mathcal{B}_u^{\mathtt{s}_2}(t)] = \mathcal{B}_{\max} - \mathbb{E}[\Lambda^{\mathtt{s}_2}(u)]t$. The following lemma is presented and proved.

Lemma 4 *For any two different sink placements, say* $\mathtt{s}_1$ *and* $\mathtt{s}_2$*, it holds that at time* $0 < t \leq \mathcal{T}(\mathtt{s})$*,*

$$\mathbb{E}[\Lambda^{\mathtt{s}_1}(u)] < \mathbb{E}[\Lambda^{\mathtt{s}_2}(u)] \Leftrightarrow \mathbb{E}[\mathcal{B}_u^{\mathtt{s}_1}(t)] > \mathbb{E}[\mathcal{B}_u^{\mathtt{s}_2}(t)].$$

Obviously, it is possible to minimize the consumed energy by changing the location of the sinks. This motivates the sink placement analysis presented in the next section.

D.2 Energy Consumption Minimization

The motivation given by Lemma 4 is further studied with respect to the optimal position of the sinks, i.e., the particular sink placement that maximizes the mean available energy in the network at any time t. Consequently, the requirement is the solution of equation

$$\mathbb{E}[\mathcal{B}_u^{(\mathtt{s}_\mathcal{E})}(t)] = \max_{\mathtt{s}} \mathbb{E}[\mathcal{B}_u^{\mathtt{s}}(t)], \tag{D.5}$$

where $\mathtt{s}_\mathcal{E}$ denotes the optimal energy sink placement.

To proceed with the analysis, assume an arbitrary data packet generated at any node u. This data packet will be forwarded toward sink node $\mathtt{s}(u)$ over the routing tree rooted at $\mathtt{s}(u)$. Thus, the consumed energy is given by the energy distance $\mathtt{d}(u, \mathtt{s}(u))$. On average, λ_u packets per time unit are generated at node u; thus, the average energy consumed for data packets generated at node u is equal to $\lambda_u \mathtt{d}(u, \mathtt{s}(u))$. For sink placement $\mathtt{s}$ and for all network nodes, the average network consumed energy, denoted by $\mathcal{E}(\mathtt{s})$, is given by

$$\mathcal{E}(\mathtt{s}) = \sum_{u \in V(\mathbb{G})} \lambda_u \mathtt{d}(u, \mathtt{s}(u)). \tag{D.6}$$

The following theorem reveals a rather useful relationship between the mean available energy at time t and the consumed energy in the network.

Theorem 3 *For any two sink placements in the network, say* $\mathtt{s}_1$ *and* $\mathtt{s}_2$*, it holds that*

$$\mathbb{E}[\Lambda^{\mathtt{s}_1}(u)] < \mathbb{E}[\Lambda^{\mathtt{s}_2}(u)] \Leftrightarrow \mathcal{E}(\mathtt{s}_1) < \mathcal{E}(\mathtt{s}_2).$$

Proof *The proof is in Appendix A.7.*

Given Theorem 3 and Lemma 4, Corollary 3 is proved.

Corollary 3 *For any two sink placements in the network, say* $\mathtt{s}_1$ *and* $\mathtt{s}_2$*, it holds that*

$$\mathbb{E}[\mathcal{B}_u^{\mathtt{s}_1}(t)] > \mathbb{E}[\mathcal{B}_u^{\mathtt{s}_2}(t)] \Leftrightarrow \mathcal{E}(\mathtt{s}_1) < \mathcal{E}(\mathtt{s}_2).$$

Given that Corollary 3 is also satisfied for $t = \mathcal{T}(\mathtt{s})$, then it is concluded that the optimal energy sink placement $\mathtt{s}_\mathcal{E}$ that satisfies $\mathbb{E}[\mathcal{B}_u^{(\mathtt{s}_\mathcal{E})}(\mathcal{T}(\mathtt{s}))] = \max_\mathtt{s} \mathbb{E}[\mathcal{B}_u^{(s)}(\mathcal{T}(\mathtt{s}))]$, also satisfies $\mathcal{E}(\mathtt{s}_\mathcal{E}) = \min_\mathtt{s} \mathcal{E}(\mathtt{s})$.

Eventually, the problem of maximizing the available energy in the network (i.e., Equation (D.5)), is transformed to a minimization problem based on the average consumed energy in the network as given by Equation (D.6). A closer look on Equation (D.6) reveals that the mentioned optimization problem is actually a facility location one, and more specifically, a k-median problem [81], the latter observation being the basic contribution of this approach in the thesis.

As described in Section B.2, the k-median problem is a difficult optimization problem (e.g., NP-complete) requiring global information and thus impractical in wireless sensor environments. Various approximation techniques can be used to reduce the complexity of the problem depending on the case. For example, easily implemented distributed "hill-climbing" techniques, e.g., [82], [161], can be employed to reduce both the need for increased computational power and global information, while at the same time adapt to dynamic network changes. Note that these approximations and distributed approaches are investigated under analysis of the facility location area and are not within the scope of this work.

D.3 Simulation Results and Evaluation

The OMNeT++ simulator [162] is used for developing the simulation scenarios. Sink nodes are assumed as part of the infrastructure, with constantly recharged batteries, and are the roots of the corresponding shortest path routing trees. The simulation scenarios parameters and their corresponding values are shown in Table D.1. More specifically, each node u generates data packets according to its traffic load λ_u and each packet is forwarded toward the corresponding sink node over the routing tree. Traffic load λ_u takes random values uniformly distributed within the range $[0, 1/n]$, where n is the number of nodes, thus, the mean value is $\mathbb{E}[\lambda_u] = \frac{1}{2n}$. When a data packet transmission takes place, energy is consumed according to Equation (C.1) with the assumption that the consumed energy is the same for every node, and without loss of generality, $\gamma = 3$ and $\mu = 1$ are the selected values in Equation (C.1) for the simulation scenarios, unless otherwise mentioned. In particular, if a data

packet transmission is to take place from node u to node v, $(u, v) \in E(\mathbb{G})$, then the battery level at node u is reduced by $w(u, v) = r_c^3$. The initially available energy at each node is set at $\mathcal{B}_{\max} = 1$.

D.3.1 Simulation Elements

The developed simulation scenarios rely on certain software packets available in the OMNeT++ simulator [162] libraries. For the simulation part, a more realistic scenario will be assumed based on carrier sense multiple access with collision avoidance (CSMA/CA), thus, collisions will occur as well as retransmissions. The CSMA/CA MAC is part of the OMNeT++ simulator libraries, and more specifically of the INET framework [163]. According to CSMA/CA, collisions may occur during the simulations resulting in retransmissions of data packets. Moreover, the CSMA/CA's acknowledgment (ACK) feature within the OMNeT++ simulator is enabled, in which a node u sends an ACK (acknowledgement) message to node v after a packet has been successfully received. The energy consumed by transmitting an ACK is set at one-fifth of the energy consumed by transmitting a (larger) data packet. In the case of no ACK being received after a transmission, a retransmission takes place. In the following, to simplify the presentation of the simulation results, the case of one sink node ($k = 1$) is initially considered, whereas the results for multiple sinks ($k > 1$) are presented in a separate subsection at the end.

Table D.1: *Simulation Network Parameters.*

Parameter	Value
Network area	$[0, 1] \times [0, 1]$
Number of nodes n	1000
Connectivity radius r_c	0.06
Traffic load λ_u	$[0, 1/n]$
Nodes' initial energy $\mathcal{B}_{\max}$	1
Packet transmission energy $w(u, v)$	r_c^3
ACK transmission energy	$\frac{r_c^3}{5}$

D.3.2 Geometric Random Graph Topologies

Connected geometric random graph topologies [121] of $n = 1000$ nodes in the $[0, 1] \times [0, 1]$ network area are considered for the simulations as the most suitable to capture the sensor network's topology idiosyncrasies [164]. In these topologies, a link exists

between two nodes if their Euclidean distance is less than or equal to the connectivity radius r_c.

Given Equation (C.3), an analytical expression can be derived with respect to the available energy $\mathcal{B}_u^{\mathtt{s}}(t)$, given that the Euclidean distance between any neighbor nodes is upper bounded by r_c in geometric random graphs. Furthermore, an additional one-fifth of the energy spent for the actual data packet transmissions is used for the subsequent acknowledgments. The total energy consumed by retransmitted packets is considered small owing to the small number of collisions for such low values of load $\mathbb{E}[\lambda_u] = \frac{1}{2n}$. Therefore, it holds that for geometric random graphs and $\mathcal{B}_{\max} = 1$, $\mathcal{B}_u^{\mathtt{s}}(t) = 1 - \Lambda^{\mathtt{s}}(u) r_c^3 t - \frac{1}{5}\Lambda^{\mathtt{s}}(u) r_c^3 t$,

$$\mathcal{B}_u^{\mathtt{s}}(t) \cong 1 - 6/5\Lambda^{\mathtt{s}}(u) r_c^3 t. \tag{D.7}$$

This latter expression is used to derive further results, as in the following lemma.

Lemma 5 *For a connected geometric random graph of $n = 1000$ and $r_c = 0.06$, there is an expression with respect to termination time $\mathcal{T}(\mathtt{s})$ and the mean available energy $\mathcal{B}_u^{\mathtt{s}}(\mathcal{T}(\mathtt{s}))$ left at the network nodes, such that $\mathcal{T}(\mathtt{s}) \geq \frac{5}{3r_c^3}$, and $\mathbb{E}[\mathcal{B}_u^{\mathtt{s}}(\mathcal{T}(\mathtt{s}))] = 1 - 6/5\frac{(n+1)\log_2(n+1)-n}{2n^2} r_c^3 \mathcal{T}(\mathtt{s})$.*

Proof *The proof is in Appendix A.8.*

Although r_c can take values up to $\sqrt{2}$, it is certain that for these cases, the corresponding topologies are of small diameter and large numbers of neighbor nodes and do not resemble typical wireless sensor networks, where sensor nodes are expected to be widely spread with low transmission range. Table D.2 presents a snapshot of simulation results for the network diameter and the average number of neighbor nodes $2\frac{|E(\mathbb{G})|}{n}$ for geometric random graphs for various values of r_c. It appears that for $r_c > 0.75$ the network diameter is too small (close to 2) and each node has (on average) 79.4% of the network nodes as neighbors. Our focus will be on values of $r_c \leq 0.4$, as they correspond to network topologies of large diameter and low numbers of neighbor nodes.

Table D.2: *Diameter and $2\frac{|E(\mathbb{G})|}{n}$ for various values of r_c and $n = 1000$.*

r_c	0.06	0.1	0.2	0.4	0.75	1.0	$\sqrt{2}$
Diameter	30	16	8	4	2	2	1
$2\frac{\lvert E(\mathbb{G})\rvert}{n}$	10.8	28.3	102.6	340.9	794.2	972.2	999

D.3.3 Traffic Load

Figure D.4 depicts both simulation (lines with points) and analytical results (isolated points) with respect to $\frac{\mathbb{E}[\Lambda^{\mathtt{s}}(u)]}{\Lambda^{\mathtt{s}}(s)}$ and $\frac{Var[\Lambda^{\mathtt{s}}(u)]}{(\Lambda^{\mathtt{s}}(s))^2}$, as a function of r_c and $n = 1000$. The left y-axis corresponds to $\frac{\mathbb{E}[\Lambda^{\mathtt{s}}(u)]}{\Lambda^{\mathtt{s}}(s)}$, and the right y-axis to $\frac{Var[\Lambda^{\mathtt{s}}(u)]}{(\Lambda^{\mathtt{s}}(s))^2}$. The analytical results for the network topology correspond to plotting the analytical expression of Theorem 1, whereas the particular value of l is extracted by the simulation results.

For either case, it is observed that both the analytical and simulation results converge as r_c increases. As r_c increases, the topology begins to resemble the complete graph. For the case of $\frac{\mathbb{E}[\Lambda^{\mathtt{s}}(u)]}{\Lambda^{\mathtt{s}}(s)}$, the convergence value is $\frac{2}{n}$, i.e., the expected boundary given by Corollary 1, while for the case of $\frac{Var[\Lambda^{\mathtt{s}}(u)]}{(\Lambda^{\mathtt{s}}(s))^2}$, the convergence value is $\frac{1}{n}$ as given by Corollary 2. For low values of r_c, the network topology is far from the complete graph and even though it is not a tree [121], it is interesting to note that the boundaries given by Corollary 1 (i.e., $\frac{\log_2(n)}{n} \approx 0.0099$) and by Corollary 2 (i.e., $\frac{2}{n} = 0.002$) are close to the observed values in the simulations. This is an indication that the topology corresponding to $r_c = 0.06$ can be approximated by a binary tree.

D.3.4 Available Energy

Figure D.5 depicts simulation results pertaining to $\mathcal{B}_u^{\mathtt{s}}(t)$ at time $t = 5000$ for $r_c = 0.06$, for two different and arbitrarily selected sink placements, $\mathtt{s}_1$ and $\mathtt{s}_2$. The y-axis of Figure D.5 corresponds to $\mathcal{B}_u^{\mathtt{s}}(5000)$ and the x-axis corresponds to the aggregate

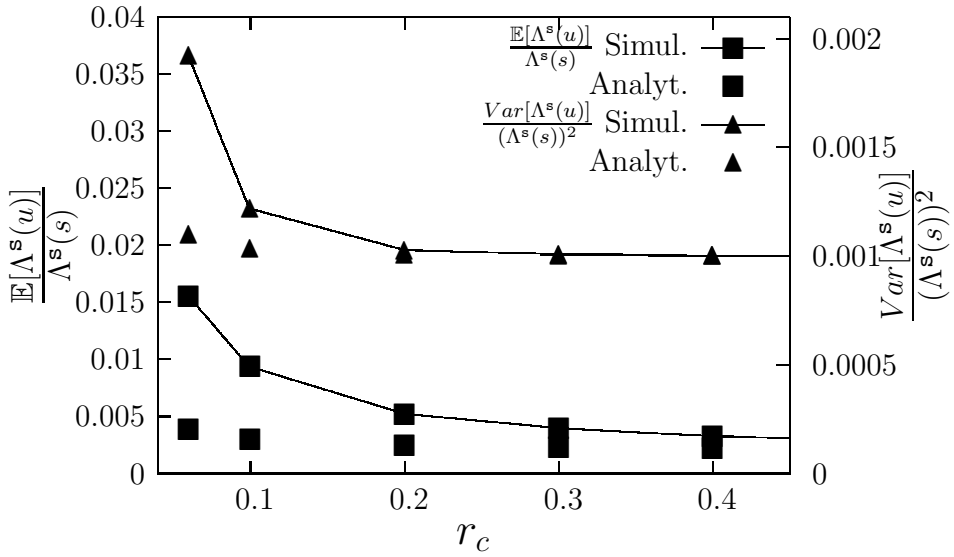

Figure D.4: $\frac{\mathbb{E}[\Lambda^{\mathtt{s}}(u)]}{\Lambda^{\mathtt{s}}(s)}$ *and* $\frac{Var[\Lambda^{\mathtt{s}}(u)]}{(\Lambda^{\mathtt{s}}(s))^2}$, *as functions of* r_c.

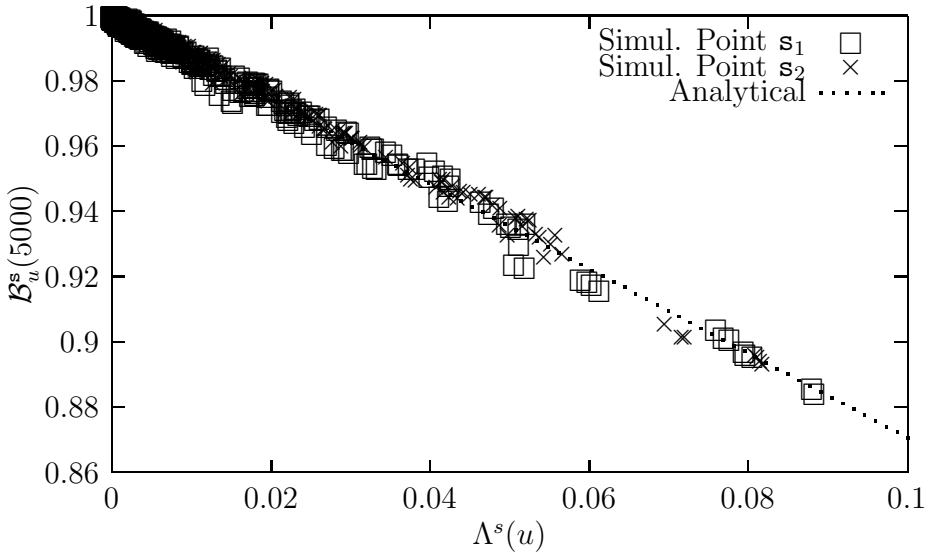

Figure D.5: $\mathcal{B}_u^{\mathbf{s}}(t)$ *at time* $t = 5000$*, as a function of* $\Lambda^{\mathbf{s}}(u)$ *for two arbitrarily chosen sink placements* $\mathbf{s}_1$ *and* $\mathbf{s}_2$*.*

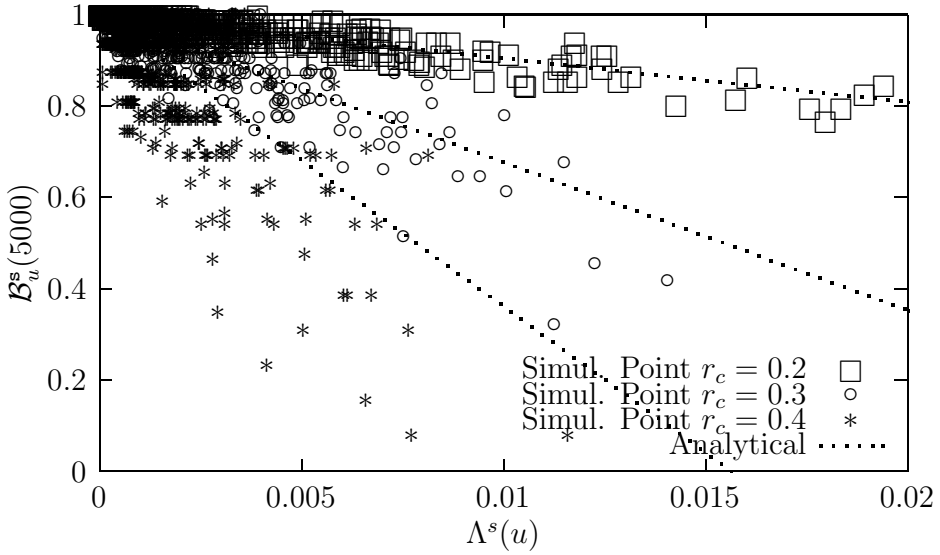

Figure D.6: $\mathcal{B}_u^{\mathbf{s}}(t)$ *at time* $t = 5000$*, as a function of* $\Lambda^{\mathbf{s}}(u)$*, for three values of* r_c *(*0.20*,* 0.30 *and* 0.40*).*

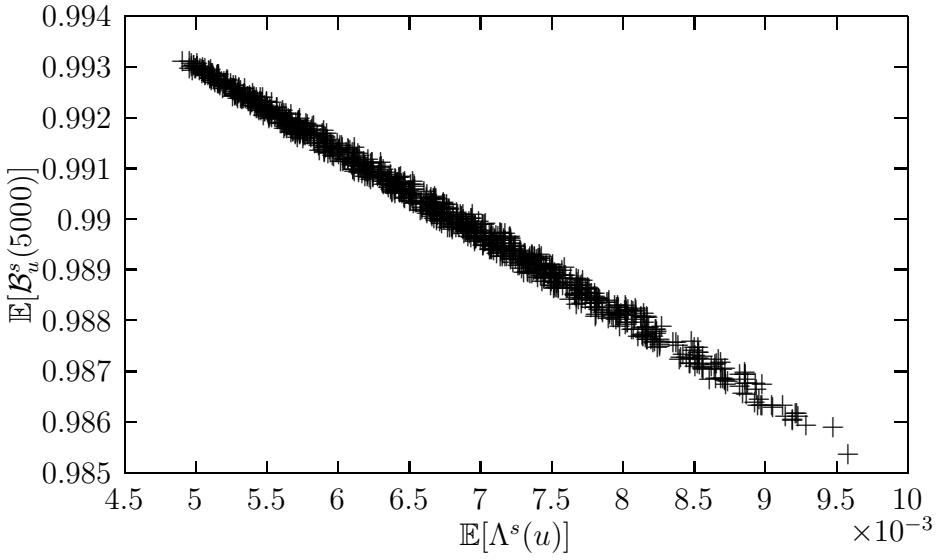

Figure D.7: $\mathbb{E}[\mathcal{B}_u^{\mathtt{s}}(5000)]$ *as a function of* $\mathbb{E}[\Lambda^{\mathtt{s}}(u)]$.

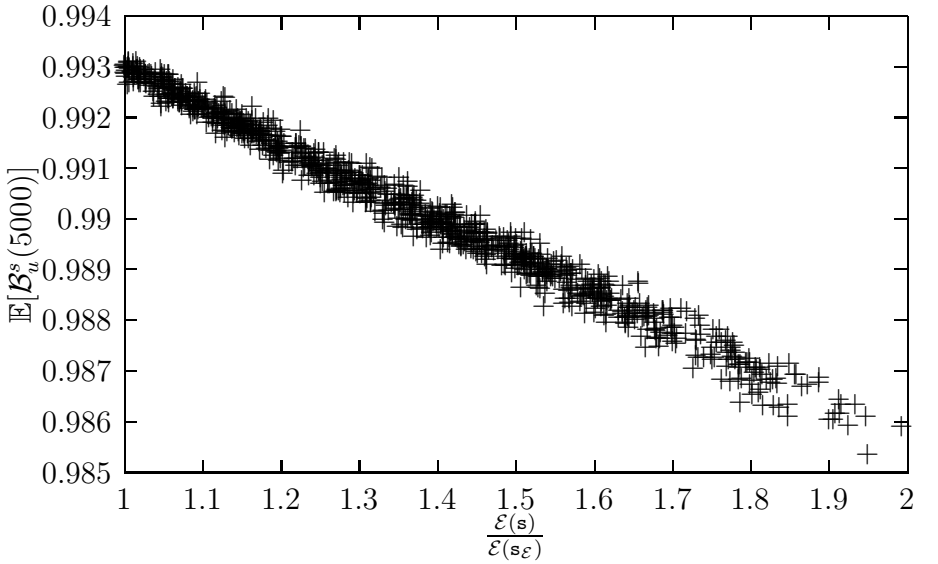

Figure D.8: $\mathbb{E}[\mathcal{B}_u^{\mathtt{s}}(5000)]$ *as a function of the energy ratio* $\frac{\mathcal{E}(\mathtt{s})}{\mathcal{E}(\mathtt{s}_\mathcal{E})}$.

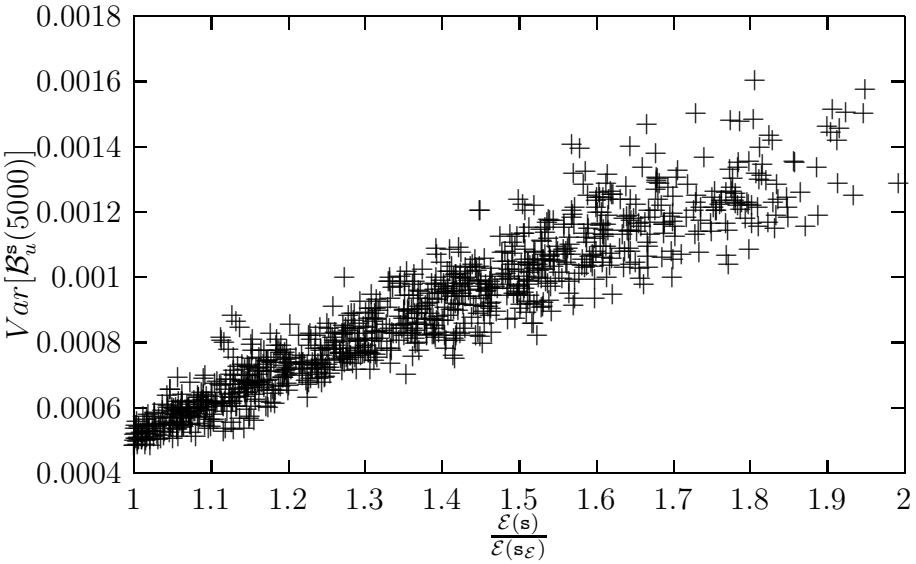

Figure D.9: *$Var[\mathcal{B}_u^{\mathbf{s}}(5000)]$ as a function of the energy ratio $\frac{\mathcal{E}(\mathbf{s})}{\mathcal{E}(\mathbf{s}_\mathcal{E})}$.*

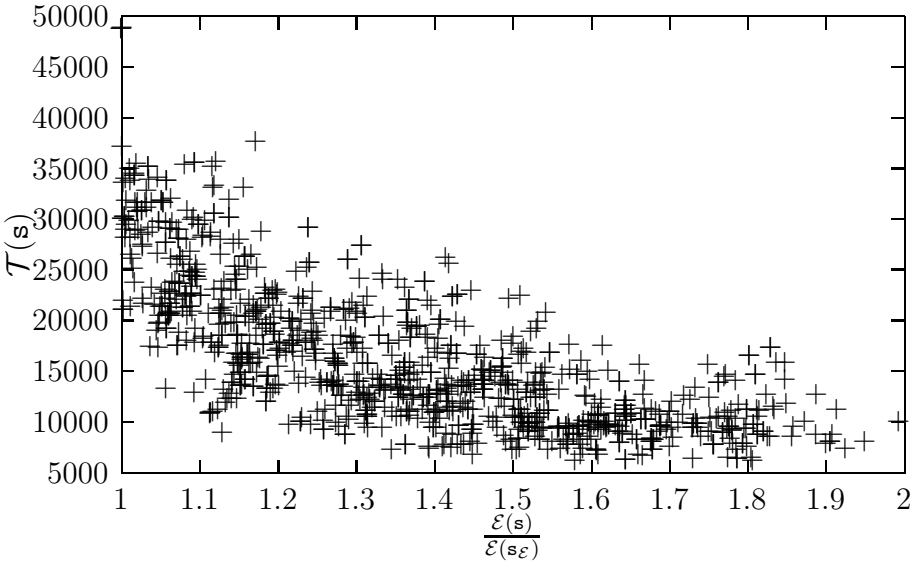

Figure D.10: *$\mathcal{T}(\mathbf{s})$ as a function of the energy ratio $\frac{\mathcal{E}(\mathbf{s})}{\mathcal{E}(\mathbf{s}_\mathcal{E})}$.*

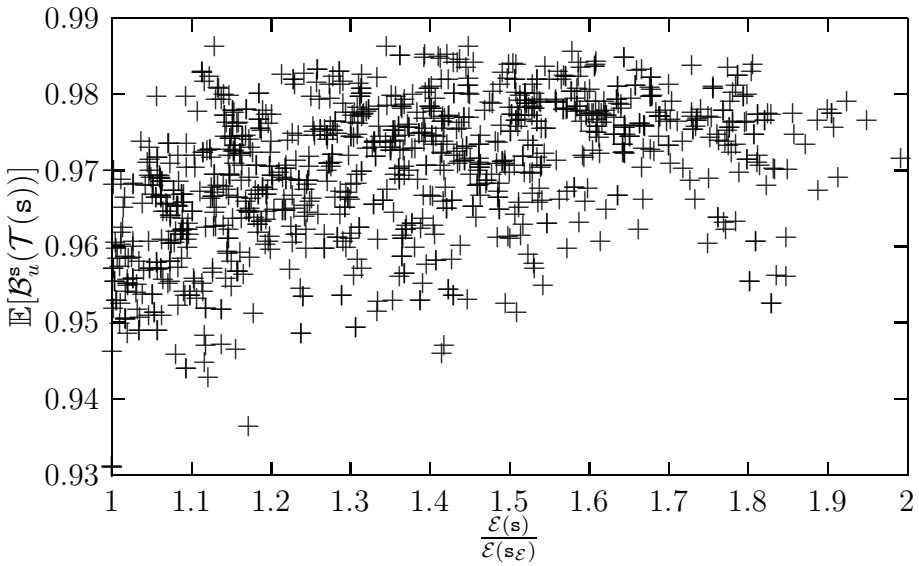

Figure D.11: $\mathbb{E}[\mathcal{B}_u^{\mathbf{s}}(\mathcal{T}(\mathbf{s}))]$ *at termination time* $\mathcal{T}(\mathbf{s})$*, as a function of the energy ratio* $\frac{\mathcal{E}(\mathbf{s})}{\mathcal{E}(\mathbf{s}_\mathcal{E})}$.

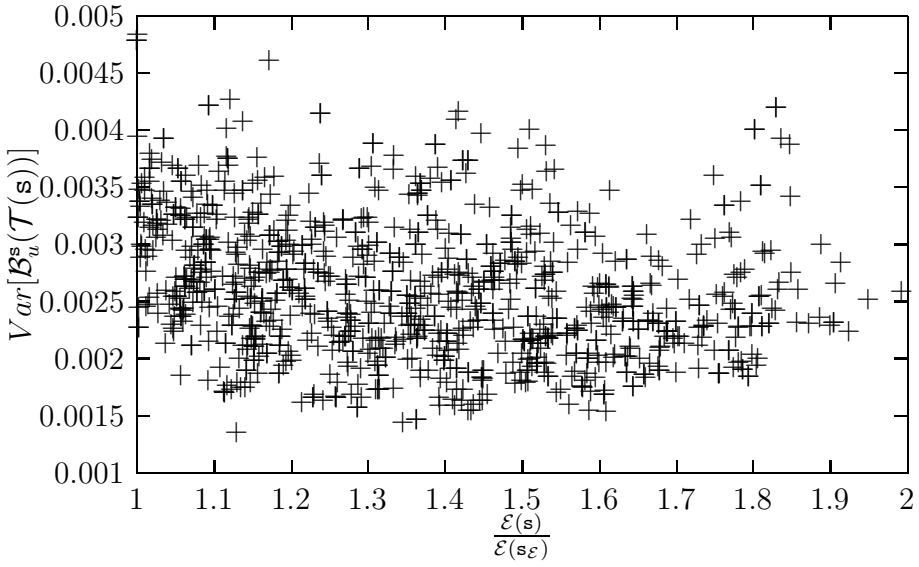

Figure D.12: $Var[\mathcal{B}_u^{\mathbf{s}}(\mathcal{T}(\mathbf{s}))]$ *at termination time* $\mathcal{T}(\mathbf{s})$*, as a function of the energy ratio* $\frac{\mathcal{E}(\mathbf{s})}{\mathcal{E}(\mathbf{s}_\mathcal{E})}$.

traffic load $\Lambda^{\mathtt{s}}(u)$ for each node u. Each depicted point corresponds to $\mathcal{B}_u^{\mathtt{s}}(5000)$ of an individual node for the particular sink placement (thus, 2000 simulation points are depicted, i.e., 1000 for sink placement $\mathtt{s}_1$ and 1000 for sink placement $\mathtt{s}_2$). A first observation is that the majority of the points concentrate on the upper left corner of the graph. This is in accordance with Lemma 2 and it is actually another graphical illustration of the energy hole problem, where some nodes consume a significantly larger energy proportion than others.

The analytical expression of Equation (D.7) is also depicted in Figure D.5 as a dotted line. The latter corresponds to function $1 - 6/5\Lambda^{\mathtt{s}}(u)r_c^3 t = 1 - 1.296\Lambda^{\mathtt{s}}(u)$, and as observed, it effectively approximates $\mathcal{B}_u^{\mathtt{s}}(5000)$ for a given value of $\Lambda^{\mathtt{s}}(u)$ for both sink nodes. Note that the analysis has taken place under certain assumptions (e.g., not taking into account retransmission issues), whereas the simulator program is closer to reality (e.g., data packets are queued, lost, retransmitted etc.) Yet the analysis is capable of capturing the behavior of the system as illustrated in Figure D.5. This is also illustrated in Figure D.6 for several values of the radius connectivity r_c and one arbitrarily selected sink node.

D.3.5 Sink Placement

So far, a sink's location was arbitrarily selected among the network nodes. In the following, the presented simulations take place for all possible n locations (permutations) of the sink. In particular, Figure D.7 depicts the mean available energy remaining at each network node at time $t = 5000$, denoted as $\mathbb{E}[\mathcal{B}_u^s(5000)]$, as a function of the mean aggregate traffic load $\mathbb{E}[\Lambda^s u]$. Each point corresponds to a different sink placement ($n = 1000$ in total). It is observed that as the mean aggregate traffic load increases, the mean available energy decreases, in accordance with Lemma 4.

Let $\frac{\mathcal{E}(\mathtt{s})}{\mathcal{E}(\mathtt{s}_\mathcal{E})}$ denote the energy ratio that shows how close to the optimal (i.e., $\frac{\mathcal{E}(\mathtt{s})}{\mathcal{E}(\mathtt{s}_\mathcal{E})} \rightarrow 1$) is the (average) network consumed energy for the particular sink placement $\mathtt{s}$ (obviously, $\frac{\mathcal{E}(\mathtt{s})}{\mathcal{E}(\mathtt{s}_\mathcal{E})} \geq 1$ for any sink placement). Figure D.8 depicts the same results as in Figure D.7, as a function of the energy ratio. It is obvious that as $\frac{\mathcal{E}(\mathtt{s})}{\mathcal{E}(\mathtt{s}_\mathcal{E})}$ increases, the mean available energy $\mathbb{E}[\mathcal{B}_u^{\mathtt{s}}(5000)]$ decreases, which is a clear indication that the energy remaining in the network at some time $t < \mathcal{T}(\mathtt{s})$ is higher when the sink placement is close to optimal (i.e., the solution of the k-median problem as given by Equation (D.6)). The corresponding variance $Var[\mathcal{B}_u^{\mathtt{s}}(10^4)]$, also depicted in Figure D.9, increases as the energy ratio increases, thus the energy remaining in the network's nodes is "more" uniform for the energy ratio closest to the optimal.

D.3.6 Network Lifetime

Figure D.10 depicts simulation results regarding termination time $\mathcal{T}(\mathtt{s})$ as a function of the energy ratio $\frac{\mathcal{E}(\mathtt{s})}{\mathcal{E}(\mathtt{s}_\mathcal{E})}$. An increment of approximately 10 times can be observed for some nodes (i.e., close to 5×10^4 for $\frac{\mathcal{E}(\mathtt{s})}{\mathcal{E}(\mathtt{s}_\mathcal{E})} \to 1$, when compared to 5×10^3 for $\frac{\mathcal{E}(\mathtt{s})}{\mathcal{E}(\mathtt{s}_\mathcal{E})}$ close to 2). Clearly, it is the nodes with energy ratio close to 1 that allow for a termination time increment. This demonstrates that the non-consumed energy is exploited to improve the network's lifetime.

Figure D.11 and Figure D.12 depict the mean (variance) of the available energy as a function of the energy ratio, in analogy to Figure D.8 and Figure D.9. Obviously, there is no pattern in Figure D.11 (Figure D.12) similar to Figure D.8 (Figure D.9). This is attributed to the fact that the unused available energy in the previous scenario has already been used in this scenario to extend the network's lifetime.

The mean available energy $\mathbb{E}[\mathcal{B}_u^{\mathtt{s}}(\mathcal{T}(\mathtt{s}))]$ remaining in the network at $t = \mathcal{T}(\mathtt{s})$, is depicted in Figure D.13 as a function of termination time $\mathcal{T}(\mathtt{s})$. The analytical solution of $\mathcal{B}_u^{\mathtt{s}}(\mathcal{T}(\mathtt{s}))$ as given by Lemma 5 for $r_c = 0.06$ is also depicted in Figure D.13 and captures the behavior of the system as shown by the simulation results.

Figure D.14 depicts termination time $\mathcal{T}(\mathtt{s})$ as a function of r_c. Each point corresponds to the termination time averaged over all n possible locations for the sink. For each point, the depicted upper bound corresponds to the maximum of $\mathcal{T}(\mathtt{s})$ for the particular scenario and the lower to the minimum, respectively. The analytical boundary $\mathcal{T}(\mathtt{s}) = \frac{5}{3r_c^3}$, given by Lemma 5, is also depicted. As r_c increases, termination time decreases.

D.3.7 Multiple Sinks

The case of $k > 1$ is presented in this subsection ($k = 2, 3, 4$). For readability purposes, the results presented for $k > 1$ correspond to the simulation scenarios already investigated for $k = 1$. Furthermore, to reduce the required computational power owing to the NP-hard nature of the k-median problem, an arbitrarily selected subset of $n = 1000$ permutations is considered, instead of the $\binom{n}{k}$ possible permutations.

Figure D.15 depicts the energy remaining in the sink nodes $\mathcal{B}_u^{\mathtt{s}}(t)$ at time $t = 5000$ as a function of $\Lambda^{\mathtt{s}}(u)$, in a similar scenario to the one presented in Figure D.5. The analytical expression is also plotted. It is obvious that for $k > 1$, the analysis still captures the network's behavior. The same observations hold for Figure D.16, which depicts $\mathbb{E}[\mathcal{B}_u^{\mathtt{s}}(\mathcal{T}(\mathtt{s}))]$ as a function of termination time $\mathcal{T}(\mathtt{s})$, in a similar scenario to the one presented in Figure D.13. As observed, the analytical expression successfully captures the network's behavior.

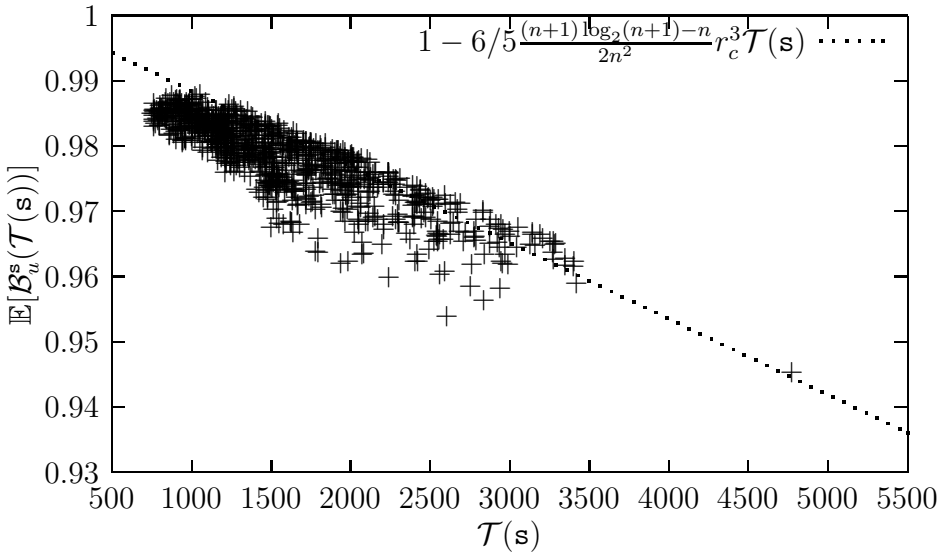

Figure D.13: $\mathbb{E}[\mathcal{B}_u^{\mathtt{s}}(\mathcal{T}(\mathtt{s}))]$ *as function of termination time* $\mathcal{T}(\mathtt{s})$ *for* $r_c = 0.06$.

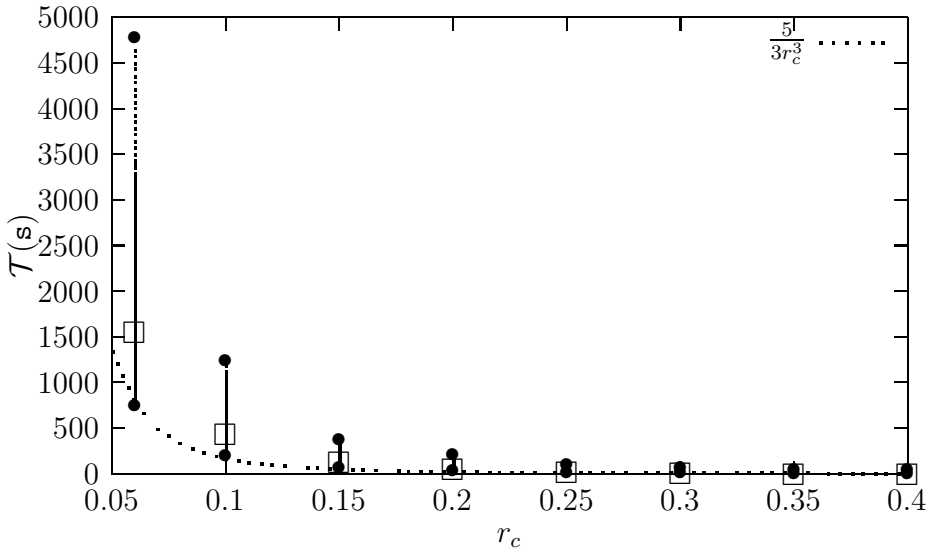

Figure D.14: $\mathcal{T}(\mathtt{s})$ *as a function of* r_c. *For each point, the maximum and minimum observed values of* $\mathcal{T}(\mathtt{s})$ *are also depicted. The dotted line corresponds to the analytical solution given by Lemma 5.*

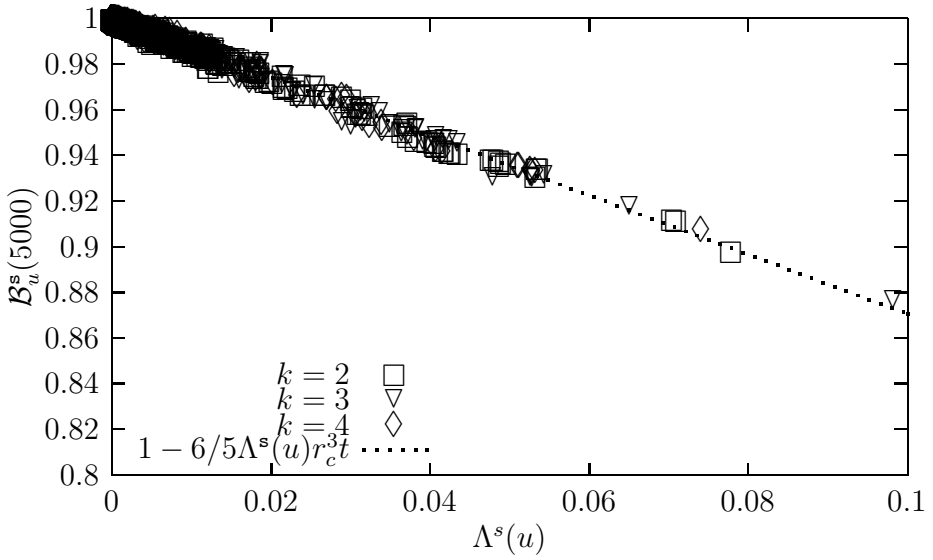

Figure D.15: $\mathcal{B}_u^{\mathtt{s}}(t)$ *at time* $t = 5000$ *as a function of* $\Lambda^{\mathtt{s}}(u)$.

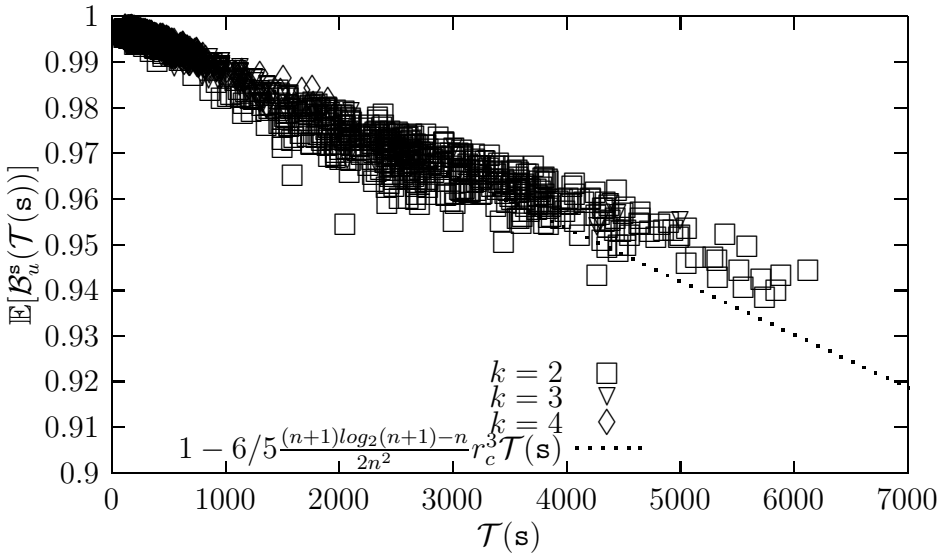

Figure D.16: $\mathbb{E}[\mathcal{B}_u^{\mathtt{s}}(\mathcal{T}(\mathtt{s}))]$ *as a function of termination time* $\mathcal{T}(\mathtt{s})$.

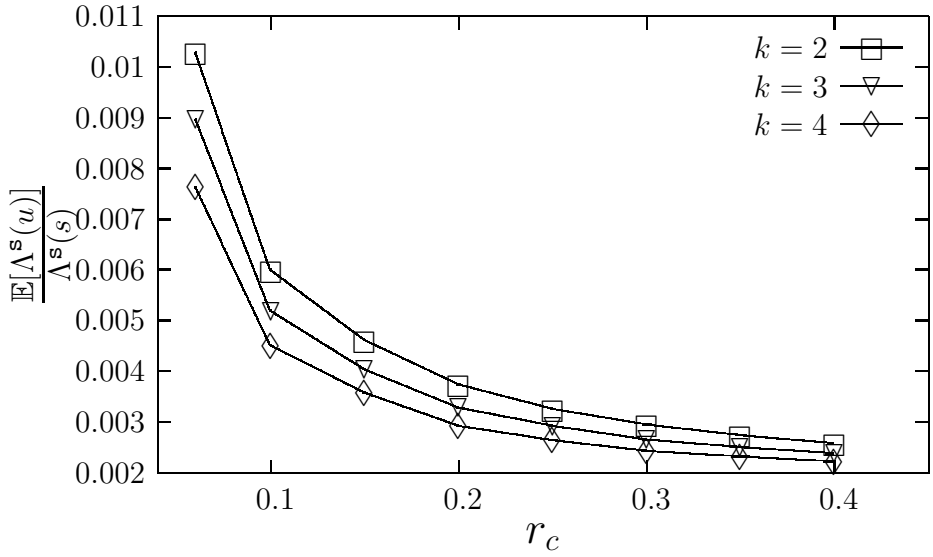

Figure D.17: $\frac{\mathbb{E}[\Lambda^{\mathbf{s}}(u)]}{\Lambda^{\mathbf{s}}(s)}$ *as a function of* r_c.

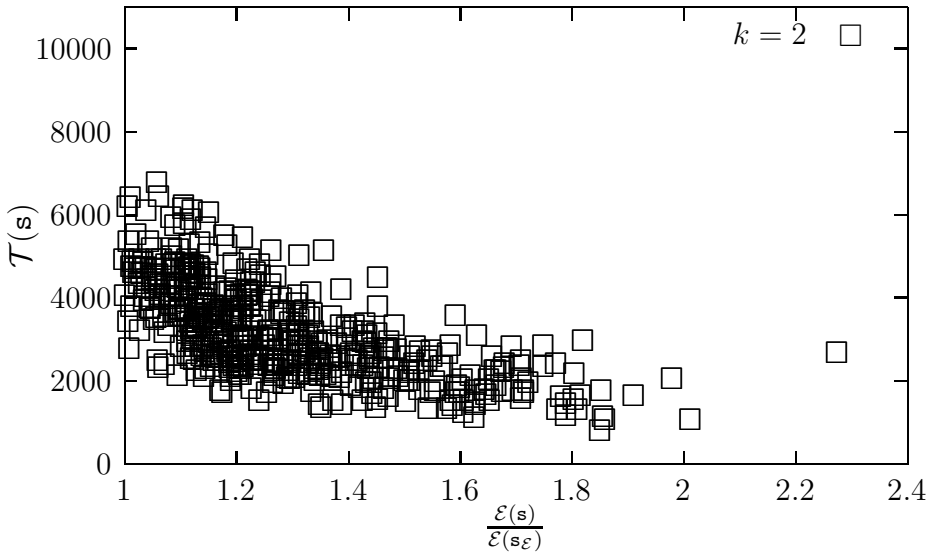

Figure D.18: $\mathcal{T}(\mathbf{s})$ *for* $k = 2$, *as a function of the approximate energy ratio* $\frac{\mathcal{E}(\mathbf{s})}{\mathcal{E}(\hat{\mathbf{s}}_{\mathcal{E}})}$.

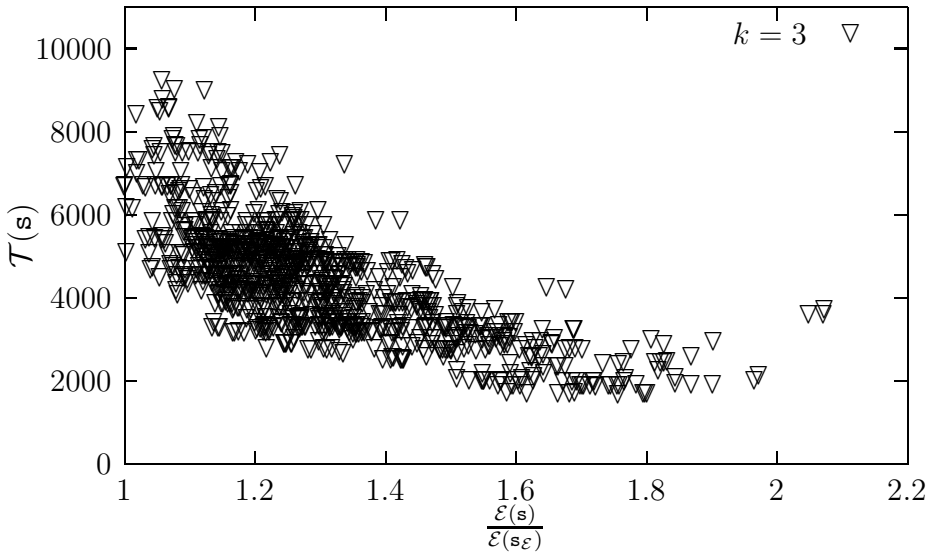

Figure D.19: $\mathcal{T}(\mathtt{s})$ *for* $k = 3$*, as a function of the approximate energy ratio* $\frac{\mathcal{E}(\mathtt{s})}{\mathcal{E}(\hat{\mathtt{s}}_{\mathcal{E}})}$.

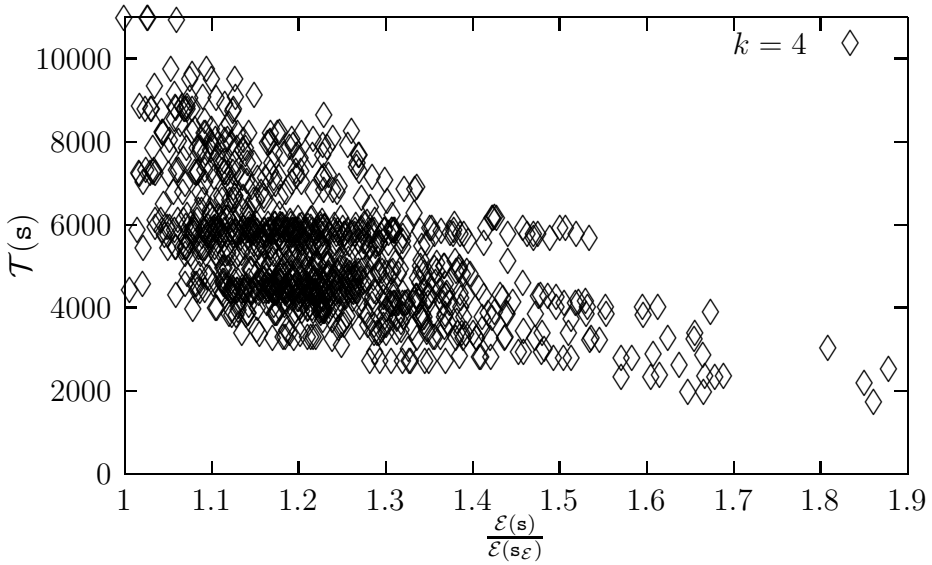

Figure D.20: $\mathcal{T}(\mathtt{s})$ *for* $k = 4$*, as a function of the approximate energy ratio* $\frac{\mathcal{E}(\mathtt{s})}{\mathcal{E}(\hat{\mathtt{s}}_{\mathcal{E}})}$.

Figure D.17 depicts $\frac{\mathbb{E}[\Lambda^{\mathtt{s}}(u)]}{\Lambda^{\mathtt{s}}(s)}$, as a function of r_c, similarly to the scenario presented in Figure D.4. All three curves converge toward $\frac{2}{n}$ as given by Corollary 1. For low values of r_c, they still converge toward $\frac{\log_2(n)}{n} \approx 0.009$, also given by Corollary 1. Note that as the number of sinks in the network increases, $\frac{\mathbb{E}[\Lambda^{\mathtt{s}}(u)]}{\Lambda^{\mathtt{s}}(s)}$ decreases. This is expected because as the number of sinks increases, the number of the corresponding routing trees increases and therefore, their size decreases. Eventually, the aggregate traffic load relayed by the nodes is decreased.

Figure D.18, Figure D.19 and Figure D.20 illustrate termination time $\mathcal{T}(\mathtt{s})$ as a function of the approximate energy ratio $\frac{\mathcal{E}(\mathtt{s})}{\mathcal{E}(\hat{\mathtt{s}}_{\mathcal{E}})}$, for $k = 2, 3, 4$, respectively, in a similar scenario to that of Figure D.10. It is obvious that for small values of the approximate energy ratio, termination time can be significantly increased. Furthermore, as k increases, the maximum value of $\mathcal{T}(\mathtt{s})$ also increases. This is attributed to the reduction of the energy hole problem effect when the number of sinks increases.

D.4 Discussion

The first proposed approach formulates the sink placement problem as a k-median facility location problem and shows that when the sink nodes are selected according to the solution of the median problem, then the (average) consumed energy in the network is minimized.

A simple but effective analytical model suitably representing a system's idiosyncrasies is given here. The mean and variance of the energy available in the network nodes are analyzed, and analytical expressions are also derived considering tree topologies. Based on the proposed analytical model, the energy consumption problem is formulated as a facility location one. It is demonstrated that when the sinks are placed according to the k-median solution, the network's overall consumed energy is minimized; thus relating the energy consumption problem to a facility location one and consequently, allowing for application and ideas from the area of facility location theory to be applied on energy consumption problems in the considered wireless sensor networks.

Simulation results validate the proposed analytical modeling and the analysis results show that the employed analytical model effectively captures certain important aspects of the network's behavior and that energy consumption is minimized when the sinks are located at those nodes recommended by the analysis.

Chapter E

Energy Replenishment Policies and Analysis

TWO policies are considered in this thesis, so as to reduce the energy hole problem's effects and prolong the network's lifetime. In the sequel, the two recharging policies are presented, along with their analysis and simulation results. In both policies, the increased energy consumption due to the energy hole problem effects is tackled by the implementation of a mobile recharger, initially stationed at the sink node's location, able to move within the network when a request is applied by one or more sensor nodes in need for a battery replenishment. The common characteristic of the two proposed policies is their being relied on local information that is acquired from the network's nodes.

Under the first proposed policy's study, it is shown that the recharging distance minimization problem corresponds to a facility location problem and particularly to a 1-median one, the latter contribution relating battery replenishing problems in wireless networks to facility location problems. This contribution is further validated by simulation results that also show that when the sink is located at the solution of the 1-median problem, then the distance covered by the mobile recharger is minimized, for both the proposed policy and an improved version of it. Additionally, it is shown that the value of recharging threshold does not affect the optimal position of the sink; thus the minimum recharging distance remains constant as also expected by the analysis.

The second proposed policy considers an enhanced version of the first, in terms of recharging all nodes en route to the node that has requested for a recharge, as well as of continuing operating after having recharged the battery of the node that has requested for the recharge, by moving in a hop-by-hop manner to those neighbor nodes of the lowest energy level. The second proposed policy is evaluated

using simulation results against a well-known policy in the literature, the NJNP policy [106] and a variation of it, both relying on global network knowledge. The contribution derived by the first policy's approach is enhanced here by confirming the relation of the battery replenishment problems in wireless sensor networks to facility location problems, while it is shown that, depending on the location of the sink, the performance of all three considered recharging policies change. The simulation results also demonstrate the fact that the proposed policy operates close to the NJNP and the r-NJNP policies and in some cases it outperforms them both, in terms of (mobile recharger's) covered distance, average and variance of the battery level in the network nodes, total (mobile recharger's) vacation period, pending of recharging requests and termination time, the latter result being significant since the proposed recharging policy relies on local information as opposed to the NJNP and r-NJNP policies that require global knowledge.

E.1 Recharging Policies

As aforementioned, there is a need for recharging the nodes' batteries in order to prolong the network's operation. The use of recharging devices like mobile rechargers, initially stationed at the sink node (thus, having abundant power supply) and moving to recharge nodes' exhausted batteries and then back to the sink node, requires a careful study of various aspects, such as the battery consumption process as well as the distance covered by the mobile recharger.

E.1.1 A Simple Recharging Policy

In C.6 the battery model was described and it is rediscussed here for the shake of readability. As denoted in Section C.6 $\mathcal{B}_u^{\mathtt{s}}(t)$ is the amount of energy remaining at node u's battery at time t, the sink node being $\mathtt{s}$. Let $\mathcal{B}_{\max}$ denote the capacity of a node's battery. Assuming that at the beginning of a network's life (i.e., $t = 0$) all nodes are fully charged, then $\mathcal{B}_u^{\mathtt{s}}(0) = \mathcal{B}_{\max}$, $\forall u \in V$.

Regarding the energy consumption when a data packet transmission takes place, energy is consumed according to Equation (C.1) with the assumption that the consumed energy is the same for every node, and without loss of generality, $\gamma = 3$ in Equation (C.1). In particular, if a data packet transmission is to take place from node u to node v, $(u, v) \in E(\mathbb{G})$, then the battery level at node u is reduced by

$$w = \mu r_c^3. \tag{E.1}$$

Given that transmitting is the dominating energy consumption factor, if one

transmission takes place from node u towards node v, it is expected that the energy level of node u's battery will be reduced by w. Assuming no transmission errors or collisions, then for a time period $[0, t]$, node u is expected to transmit (on average) $\Lambda^{\mathtt{s}}(u)t$ data packets, thus consuming (on average) $\Lambda^{\mathtt{s}}(u)wt$ energy units. Therefore, the battery's average energy level at time t is given by

$$\mathcal{B}_u^{\mathtt{s}}(t) = \mathcal{B}_{\max} - \Lambda^{\mathtt{s}}(u)wt, \tag{E.2}$$

where $(u, v) \in E$.

A simple recharging policy is considered, whereby there exists (i) one mobile recharger hosted at the sink node, (ii) capable of moving over the routing tree's branches, (iii) to any network node that is about to exhaust its battery, (iv) recharge it, and (v) move back to the sink node. The dashed arrows in Figure C.1 illustrate the path followed by the mobile recharger for replenishing the battery of a certain node v.

The Recharging Policy: The battery of a node $u \in V$ requires recharging, if at some time t, $\frac{\mathcal{B}_u^{\mathtt{s}}(t)}{\mathcal{B}_{\max}} \leq \rho$ is satisfied, where $0 \leq \rho \leq 1$ represents a recharging threshold common for all network nodes. The condition being satisfied, a recharging process is initiated and the mobile recharger, stationed at sink node $\mathtt{s}$, moves to node u over the routing tree, recharges its battery and returns back to sink node $\mathtt{s}$.

Under this policy, for some node u, sink node $\mathtt{s}$ is notified whether condition $\frac{\mathcal{B}_u^{\mathtt{s}}(t)}{\mathcal{B}_{\max}} \leq \rho$ is satisfied, by control information suitably piggybacked within data packets. If the condition is satisfied, then the mobile recharger moves a distance $\mathtt{x}(\mathtt{s}, u)$ to recharge node's u battery and then returns to sink node $\mathtt{s}$, thus having moved a total recharging distance of $2\mathtt{x}(\mathtt{s}, u)$. Node's battery is assumed to be recharged.

Even though the benefits of a recharging policy are obvious, there is a certain cost attributed to (i) the required amount of energy for recharging purposes, and (ii) the recharging distance. Given that the mobile recharger is normally stationed at the sink, it is reasonable to assume that it has access to power supply similarly to the sink node. Regarding the recharging distance, the purpose here is to minimize it and thus, improve certain aspects of the considered recharging policy (e.g., to minimize recharging delays). An enhancement of this recharging policy that allows the replenishment of nodes over the trajectory towards the particular node that triggered the recharging process, is also considered later in the simulation section. More sophisticated recharging policies, e.g., as in [113], are left for future work.

E.1.2 An Enhanced Recharging Policy

Taking a step further, a more sophisticated recharging policy is also considered so as to prolong the network's lifetime and to further elaborate on the recharging

distance minimization study. This recharging policy is based on local information, where the mobile recharger moves – upon request – to a node of reduced energy level and replenishes its battery. Under the proposed policy, the mobile recharger, after completing the recharging of the requested node, it moves in a hop-by-hop manner to the neighbor nodes of the lowest energy level, starting from the requested node. The effectiveness of this policy is investigated using simulation results and compared against an existing well-known on-demand recharging policy that exploits global knowledge (i.e., knowledge of both the energy level of all nodes and the network topology). It is shown that the proposed policy, even though based on local information, maintain the average energy level and termination time higher than that under the existing one that exploits global knowledge. Furthermore, it is observed that the network's lifetime is maximized when the basis of the mobile recharger is located at the solution of the mentioned median problem for all studied policies.

It is assumed that all nodes, apart from the sink node $\mathtt{s}$, are initially in idle mode, their triggering depending on sensing or receiving data. While idle, nodes are not sensing any information or transmitting their own data packets. However, they are still responsible for receiving and forwarding data packets arriving from other nodes. Traffic load λ_u, earlier mentioned in C.5 denotes the probability that a data packet is generated at some node u at any time unit. In this approach, λ_u plays the same role, but in the same time it denotes the probability of a node u to be triggered, where a node leaves the idle mode for sensing and sending a data packet.

Furthermore, in order to achieve an even closer to reality system model, it is assumed for the enhanced policy study that nodes consume energy not only for transmitting data packets but for processing information (e.g., sensing) and receiving data packets too. Additionally, energy consumed for the above actions is now counted in consumed energy per time unit. Let $\mathtt{p}$ denote this consumed energy per time unit being referred to hereafter as the processing cost. Let $\mathtt{e}$ denoted the particular energy for transmitting and $\mathtt{r}$ for receiving per time unit, respectively.

Energy stored in the mobile recharger's battery is also reduced to support mainly two actions: to move and to recharge nodes' batteries. The mobile recharger is equipped with one battery and the stored energy is used for both moving and recharging. It is assumed that the mobile recharger is initially hosted at the sink node $\mathtt{s}$ and is capable of moving over the shortest path tree branches to any network node with a constant velocity denoted as $\mathtt{v}$. Let $\mathcal{C}$ denote the initial capacity of the mobile recharger's battery. When the mobile recharger located at some node v moves towards another node u, it consumes an amount of energy per time unit $m \times \frac{x(u,v)}{\mathtt{v}}$, where m (i.e., moving consumption) is a constant. The recharging process

is not instantaneous, and therefore, let ψ denote the energy that can be transfered per time unit (called node recharging ratio) from the mobile recharger to any node battery. Finally, the process of refilling the mobile recharger's battery at the sink node is also not instantaneous. Let ϕ denote the energy per time unit for refilling the mobile recharger's battery. Note that full recharge is assumed in all cases and it is also assumed that the mobile recharger always reserves an amount of energy sufficient enough to travel back to the sink node.

E.2 Recharging Policies Analysis

In this section a further analysis of the policies is given. While the most significant analysis regarding the recharging policies is being conducted under the simple recharging policy's study (e.g., the recharging distance minimization's analysis), it is useful to analytically describe the second proposed policy's behavior too, because of its role in this thesis, which is the enhancement of the findings of the study of the first proposed policy.

E.2.1 Analysis of the Simple Recharging Policy

Assume that the system has started operating and some long enough time has elapsed for all nodes to have sent packets towards the sink node, i.e., the network operates at steady state mode. Let $\tau^{\mathtt{s}}(u) > 0$ denote the recharging period between a recharging event that took place at time t_1 and the need for a new recharging event at time t_2, or $t_2 = t_1 + \tau^{\mathtt{s}}(u)$ for node u and sink node $\mathtt{s}$.

Assuming the proposed recharging policy, $\frac{\mathcal{B}_u^{\mathtt{s}}(\tau^{\mathtt{s}}(u))}{\mathcal{B}_{\max}} = \rho$ is satisfied. Given that $\mathcal{B}_u^{\mathtt{s}}(t) \overset{\text{Equation (E.2)}}{=} \mathcal{B}_{\max} - \Lambda^{\mathtt{s}}(u)wt$, where v is the neighbor node of u towards the sink node $\mathtt{s}$ over the routing tree branches. Eventually, $\rho = \frac{\mathcal{B}_{\max} - \Lambda^{\mathtt{s}}(u)w\tau^{\mathtt{s}}(u)}{\mathcal{B}_{\max}}$ and the recharging period for node u is given by

$$\tau^{\mathtt{s}}(u) = (1-\rho)\frac{\mathcal{B}_{\max}}{\Lambda^{\mathtt{s}}(u)w}. \tag{E.3}$$

Obviously, at any time instance $t \geq 0$, there would be $\lfloor t/\tau^{\mathtt{s}}(u) \rfloor$ recharges. For each one, the mobile recharger covers a distance $2\mathtt{x}(u, \mathtt{s})$ to get to node u and then return back to its main position at the sink $\mathtt{s}$. Therefore, for node u at time t, distance $2\lfloor t/\tau^{\mathtt{s}}(u) \rfloor \mathtt{x}(u, \mathtt{s})$ is covered for recharging purposes. Consequently, for all network nodes, the covered distance by the mobile recharger at time t is given by $D^{\mathtt{s}}(t) = 2\sum_{u \in V} \lfloor t/\tau^{\mathtt{s}}(u) \rfloor \mathtt{x}(u, \mathtt{s})$, for sink node $\mathtt{s}$. Given Equation (E.3), the result

is

$$D^{\mathtt{s}}(t) = 2\sum_{u\in V}\left\lfloor (1-\rho)\frac{\Lambda^{\mathtt{s}}(u)w}{\mathcal{B}_{\max}}t\right\rfloor \mathtt{x}(u,\mathtt{s}). \tag{E.4}$$

The requirement is to determine the particular sink node for which $D^{\mathtt{s}}(t)$ is minimized irrespectively of time t.

In order to proceed with the analysis, a more tractable form of $D^{\mathtt{s}}(t)$, as given by Equation (E.4), is introduced, denoted as $\mathcal{D}(\mathtt{s})$. In particular, factor $2\frac{1-\rho}{\mathcal{B}_{\max}}wt$ is omitted being a constant (the objective is minimization with respect to sink placement), and without loss of generality $\lfloor\cdot\rfloor$ is also omitted. Therefore,

$$\mathcal{D}(\mathtt{s}) = \sum_{u\in V}\Lambda^{\mathtt{s}}(u)\mathtt{x}(u,\mathtt{s}), \tag{E.5}$$

to be referred to as the recharging distance.

The objective now is to find the particular optimal distance sink node $\mathtt{s}_{\mathcal{D}}$ such that

$$\mathcal{D}(\mathtt{s}_{\mathcal{D}}) = \min_{\mathtt{s}}\mathcal{D}(\mathtt{s}). \tag{E.6}$$

The resemblance of Eq. (E.6) and Eq. (E.5) to Eq. (D.5) and Eq. (D.6), respectively, is obvious. Therefore, it is concluded that the optimization problem of Eq. (E.6) is also a k-median one. For example, the aggregate traffic load $\Lambda^{\mathtt{s}}(u)$ is now taken into account for node u, instead of the traffic load λ_u and the summation of the shortest path euclidean distances $\mathtt{x}(u,v)$, instead of the energy distance $\mathtt{d}(u,v)$.

Similarly to Eq. (C.2), let $\mathtt{\Lambda}^{\mathtt{s}}(u)$ denote the aggregation of the aggregate traffic loads, or

$$\mathtt{\Lambda}^{\mathtt{s}}(u) = \sum_{v\in\mathbb{T}^{\mathtt{s}}(u)}\Lambda^{\mathtt{s}}(v) = \sum_{v\in\mathbb{T}^{\mathtt{s}}(u)}\sum_{z\in\mathbb{T}^{\mathtt{s}}(v)}\lambda_z. \tag{E.7}$$

Given the previously mentioned similarities with Theorem 3, in analogy to the proof in Appendix A.7, the following theorem evolves.

Theorem 4 *For any two sink placements in the network, say* $\mathtt{s}_1$ *and* $\mathtt{s}_2$*, it holds*

$$\mathbb{E}[\mathtt{\Lambda}^{\mathtt{s}_1}(u)] < \mathbb{E}[\mathtt{\Lambda}^{\mathtt{s}_2}(u)] \Leftrightarrow \mathcal{D}(\mathtt{s}_1) < \mathcal{D}(\mathtt{s}_2).$$

The following corollary relates the solutions of both facility location problems, i.e., sink placements $\mathtt{s}_{\mathcal{D}}$ and $\mathtt{s}_{\mathcal{E}}$.

Corollary 4 *For those cases that* $\mathbb{E}[\mathtt{\Lambda}^{\mathtt{s}_{\mathcal{E}}}(u)] = \mathbb{E}[\Lambda^{\mathtt{s}_{\mathcal{E}}}(u)]$*, or* $\mathbb{E}[\mathtt{\Lambda}^{\mathtt{s}_{\mathcal{D}}}(u)] = \mathbb{E}[\Lambda^{\mathtt{s}_{\mathcal{D}}}(u)]$*, then* $\mathtt{s}_{\mathcal{E}} \equiv \mathtt{s}_{\mathcal{D}}$*.*

Proof *The proof is in Appendix A.9.*

An example topology satisfying the $\mathbb{E}[\mathtt{\Lambda}^{\mathtt{s}_{\mathcal{E}}}(u)] = \mathbb{E}[\Lambda^{\mathtt{s}_{\mathcal{E}}}(u)]$ hypothesis of Corollary 4 is the complete graph.

E.2.2 Analysis of the Enhanced Recharging Policy

The main mechanism behind the second proposed recharging policy is based on a simple finite state machine depicted in Figure E.1, consisting of the following states:

State 0: *Vacation* is the particular (and initial) state of the mobile recharger when located at the sink node. If its battery energy level is not full, it replenishes it. Since the sink node receives all recharging requests, eventually, this knowledge is made available to the mobile recharger during the vacation state.

State 1: *Moving* to the next node. This node is selected according to the assumed recharging policy (e.g., it may be an intermediate node of the node that has requested for a recharge). The time required to arrive to a node depends on the euclidean distance and the mobile recharger's velocity. In addition, the movement consumes energy from the mobile recharger's battery. When the mobile recharger arrives at the destination, the next step is to start recharging according to the next state.

State 2: *Recharging* node starts by the time the mobile recharger arrives at its destination. The time required to complete a node's recharging depends on the node recharging ratio ψ and the energy left at the particular node's battery.

State 3: *Returning* to sink node $\mathtt{s}$ takes place when the recharger has no more nodes to recharge under the assumed recharging policy or its battery is running out of energy. The returning state is similar to the moving state, the difference being the destination which now is the sink node and not a node to be recharged. Similarly to the case of the moving state, this movement takes place over the shortest path tree's branches. The time needed to reach the destination is analogous to the velocity and the sum of the euclidean distances over the branches of the shortest path tree.

Changing states depends on the mobile recharger's remaining energy and the schedule being in use. If the mobile recharger's remaining energy is not enough to continue operating or it has finished its given schedule, then the returning state will be chosen. If more nodes have to be recharged and the recharger is capable to fulfill this goal (i.e., its remaining energy is enough to move to the next node and recharge it) the moving state will be chosen, thus moving the recharger to the next node according to the given policy.

Remember that $\mathcal{B}_u^{\mathtt{s}}(t)$ denotes the amount of energy remaining at node u's battery at time t, the sink node being $\mathtt{s}$ and $\mathcal{B}_{\max}$ denotes the capacity of a node's battery. Assuming that at the beginning of a network's life (i.e., $t = 0$) all nodes are fully charged, then $\mathcal{B}_u^{\mathtt{s}}(0) = \mathcal{B}_{\max}$, $\forall u \in V$. Depending on λ_u when a node u is triggered, it senses and processes the sensed information and reduces its battery's energy by $\mathtt{p}$ multiplied by the time this processing takes place. For the transmission taking place from node u towards node v over the shortest path tree, it is expected that the energy level of node u's battery will be reduced by $\mathtt{e}$ and node v's battery

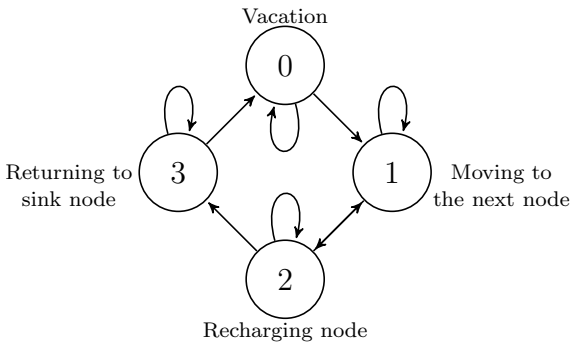

Figure E.1: *The recharging mechanism depicted as a finite state machine. The four states are: (0) Vacation; (1) Moving to the next node; (2) Recharging node; and (3) Returning to sink node* `s`.

will be reduced by `r` multiplied by the corresponding time period, respectively.

During the network's operation, when a node u is ready to transmit a packet towards the sink node `s` and its energy level is below a certain threshold, it piggybacks a recharging request within the data packet. In particular, let $0 \leq \rho \leq 1$ represent a recharging threshold common for all network nodes. A recharging request is sent when $\frac{\mathcal{B}_u^{\mathtt{s}}(t)}{\mathcal{B}_{\max}} \leq \rho$ holds. The mobile recharger becomes aware about the recharging requests when it is located at the sink node, i.e., State 0 (vacation).

At the beginning, the mobile recharger, being at State 0 (vacation), is full of energy. When the first recharging request arrives, the sink node informs the mobile recharger about the particular node that has requested for arecharge. Then, the mobile recharger switches to State 1 (moving state) and travels to the this node along the corresponding shortest path. Meanwhile, it recharges all en route nodes by switching between State 2 (recharging) and State 1 (moving) repeatedly. When it reaches the requested node it switches to State 2 (recharging) and when it finishes – assuming that there is enough energy left in its battery – it switches to State 1 (moving) and moves to the neighbor node of the smallest energy left in its battery. This process (moving hop by hop to neighbor nodes of the smallest energy and recharging their batteries) continues until the energy left in the mobile recharger's battery is barely enough to return to the sink node (i.e., switch to State 3).

Meanwhile, in the absence of the mobile recharger, if a new request arrives at the sink node, it is stored accordingly. When the mobile recharger returns to the sink node, it is informed about the pending recharging requests and moves to satisfy the oldest one, provided this node has not been replenished after the recharging request has been sent. If there are no recharging requests, the mobile recharger remains at State 0 (vacation), until a recharging request arrives.

E.3 Simulation Results and Evaluation

Simulation scenarios are developed using the OMNeT++ simulator [162] for both the simple and the enhanced recharging policy case. Each node u generates data packets according to its traffic load λ_u and each packet is forwarded towards the sink node over the said routing tree.

E.3.1 Evaluation of the Simple Recharging Policy

Simulation results regarding the simple recharging policy are given in the sequel.

Simulation Configuration

Traffic load λ_u takes random values uniformly distributed within range $[0, 1/n]$, where n is the total number of nodes. For the simulation purposes, $n = 1000$. When a transmission takes place, energy is consumed according to Equation (E.2) per (simulation) time unit. If a transmission is to take place from node u to node v, $(u, v) \in E$, then the battery level at node u gets reduced by $w = \mu r_c^3$ (Equation (E.1)), for various values of μ. The initially available energy at each node is set at $\mathcal{B}_{\max} = 1$. A uniformly distributed packet error rate of 10^{-6} is also considered for each network link (thus, corrupted packets are retransmitted).

Connected geometric random graphs topologies of $n = 1000$ nodes in the $[0 \dots 1] \times [0 \dots 1]$ square area, are considered for the simulations. The connectivity radius is $r_c = 0.06$, which corresponds to a connected network topology of 10.8 (on average) number of neighbor nodes per node and 30.2 (on average) diameter, which is a typical one for wireless sensor networks. When a node runs out of battery, then the simulation stops. The maximum possible number of simulation units for the OMNeT++ platform [162] is close to 9×10^6.

Recharging Policy Behavior

The proposed recharging policy is implemented considering a mobile recharger initially stationed at the sink node and then moving towards a node to recharge it upon receipt of a request for such. The time period (in time units) for the mobile recharger movement to take place, and consequently to return, is equal to twice the number of hops (in time units) this node is away from the sink plus one time unit for recharging. If, in the meantime, a request for replenishing the battery of another node is received, it gets queued in a first-in-first-out manner at the sink node.

Figure E.2, depict the average battery level $\overline{\mathcal{B}^{\mathtt{s}}}(t) = 1/n \sum_{\forall u \in V} \mathcal{B}_u^{\mathtt{s}}(t)$ for some arbitrarily selected sink node $\mathtt{s}$, as a function of time t for three different values of ρ

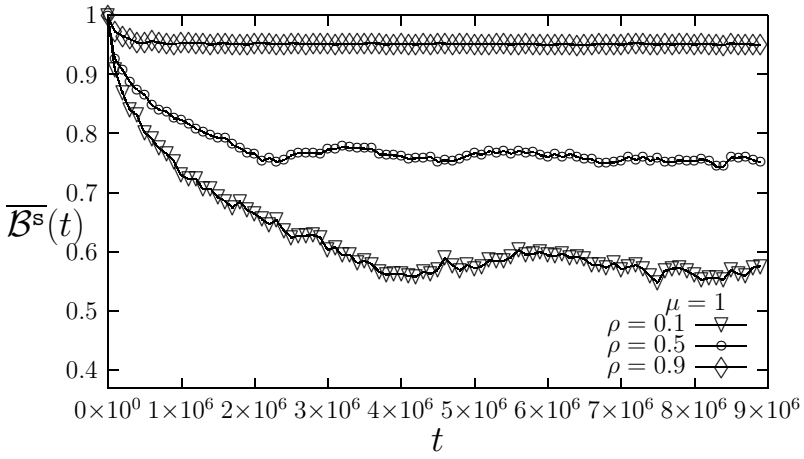

Figure E.2: *Simulation results regarding the average energy left at the networks nodes* $\overline{\mathcal{B}^{\mathrm{s}}}(t)$*, as a function of time* t *for three different values of the recharging threshold* ρ *(i.e.,* 0.1*,* 0.5 *and* 0.9*) and energy consumption constant* $\mu = 1$*, under the simple recharging policy.*

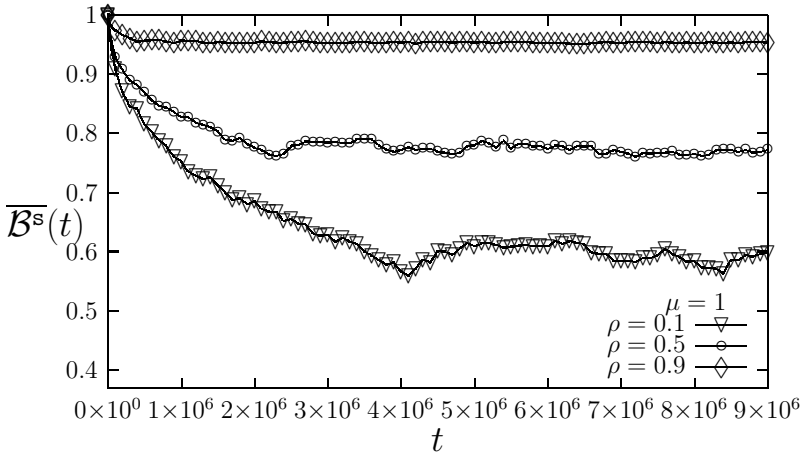

Figure E.3: *Simulation results regarding the average energy left at the networks nodes* $\overline{\mathcal{B}^{\mathrm{s}}}(t)$*, as a function of time* t *for three different values of the recharging threshold* ρ *(i.e.,* 0.1*,* 0.5 *and* 0.9*) and energy consumption constant* $\mu = 1$*, under the improved policy.*

(0.1, 0.5 and 0.9) and $\mu = 1$. It is observed that the average battery level decreases and eventually converges to a certain level, even for small values of ρ.

Figure E.3 depicts the same scenario considering an improved version[1] of the simple recharging policy presented in Section E.1. Under this improved recharging policy all nodes located en route towards the node that triggered the recharging process have their battery replenished. In particular: (i) one mobile recharger is hosted at the sink node; (ii) a network node that is about to exhaust its battery makes a request for recharging; (iii) the mobile recharger moves towards the node that has made a request over the tree's branches; (iv) it recharges all nodes located on path; (v) it recharges the particular node that initiated the process; and (vi) moves back to the sink node.

As it is observed from Figure E.3, the average battery level $\overline{\mathcal{B}^{\mathbb{s}}}(t)$ under the improved recharging policy is slightly higher compared to the simple recharging policy. This is expected due to the fact that overall, the remaining energy is increased under the improved version of the recharging policy due to the enhanced replenishing process.

Figure (E.4, E.5) and Figure (E.6, E.7) depict the same simulation as in Figure (E.2, E.3) considering $\mu = 3$ and 5 (instead of $\mu = 1$). The same observations apply as before when comparing the simple recharging policy (E.4) and the improved one (E.5). When comparing figures (E.2, E.3), (E.4, E.5) and (E.6, E.7) (i.e., as μ increases), it is obvious that the convergence period for each case is reduced. However, the particular convergence value does not change, an indication that it depends on ρ.

Figures E.8 and E.9 depict the total number of requested recharges and the total distance covered by the mobile recharger as a function of the recharging threshold ρ after 9×10^6 time steps and $\mu = 1$. As expected, the number of recharges as well as the covered distance increase as ρ increases. Furthermore, comparing the simple recharging policy (E.8) and the improved one (E.9), it is obvious that the number of requested recharges and the total covered distance is reduced under the latter policy.

Evaluation of the 1-median Problem Formulation

In order to evaluate the minimization of the recharging distance as a 1-median problem, it is sufficient to show that when the sink is located at the solution of the

[1]The improved version of the simple recharging policy is not the same with the enhanced recharging policy proposed in this thesis. They have a similarity based on their common characteristic, which is the recharging of the en route nodes, but the enhanced recharging policy has even more features given in E.1.2 subsection of the current section.

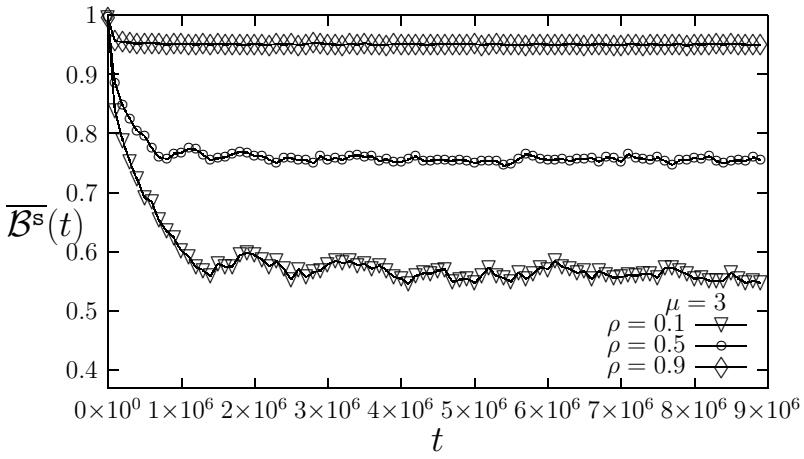

Figure E.4: *Simulation results regarding the average energy left at the networks nodes* $\overline{\mathcal{B}^{\mathrm{s}}}(t)$*, as a function of time* t *for three different values of the recharging threshold* ρ *(i.e.,* 0.1*,* 0.5 *and* 0.9*) and energy consumption constant* $\mu = 3$*. under the simple recharging policy.*

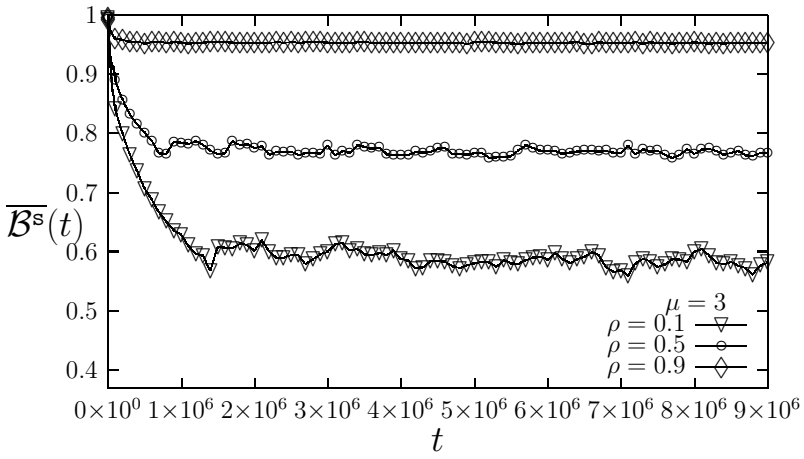

Figure E.5: *Simulation results regarding the average energy left at the networks nodes* $\overline{\mathcal{B}^{\mathrm{s}}}(t)$*, as a function of time* t *for three different values of the recharging threshold* ρ *(i.e.,* 0.1*,* 0.5 *and* 0.9*) and energy consumption constant* $\mu = 3$*, under the improved recharging policy.*

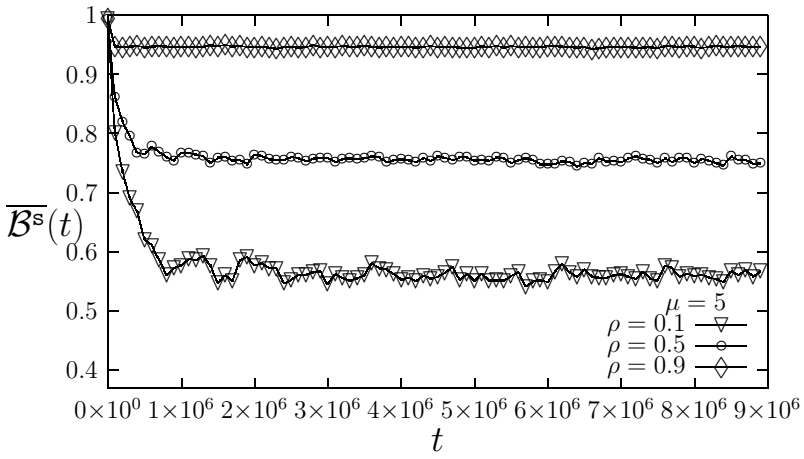

Figure E.6: *Simulation results regarding the average energy left at the networks nodes* $\overline{\mathcal{B}^{\mathrm{s}}}(t)$*, as a function of time* t *for three different values of the recharging threshold* ρ *(i.e.,* 0.1*,* 0.5 *and* 0.9*) and energy consumption constant* $\mu = 5$*, under the simple recharging policy.*

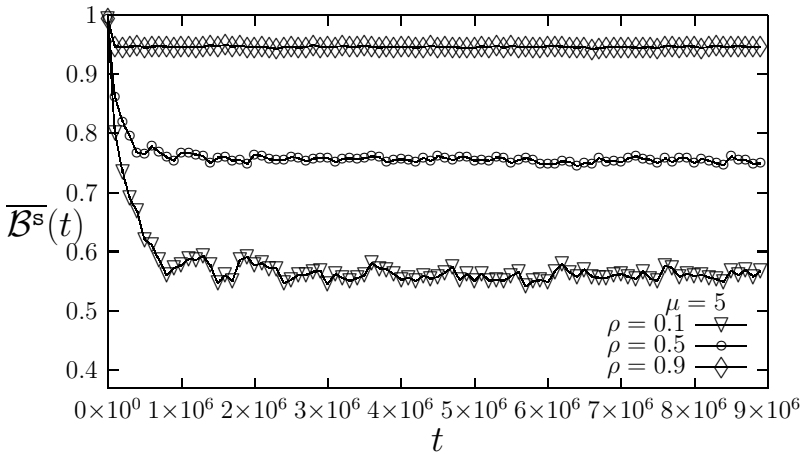

Figure E.7: *Simulation results regarding the average energy left at the networks nodes* $\overline{\mathcal{B}^{\mathrm{s}}}(t)$*, as a function of time* t *for three different values of the recharging threshold* ρ *(i.e.,* 0.1*,* 0.5 *and* 0.9*) and energy consumption constant* $\mu = 5$*, under the improved recharging policy.*

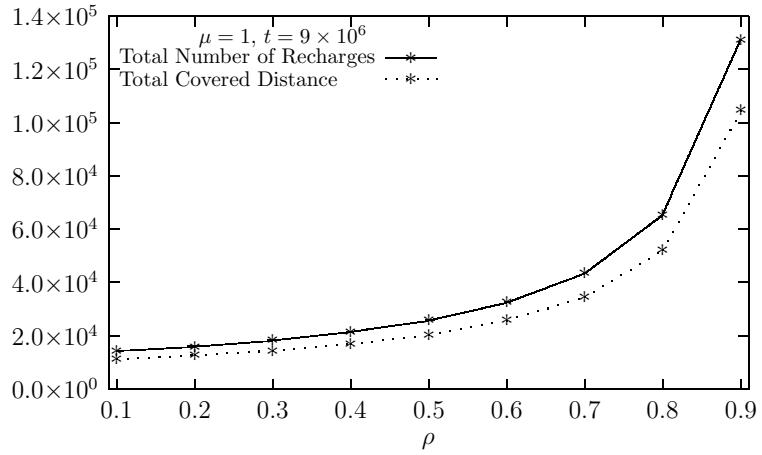

Figure E.8: *Total number of requests for recharges and total distance covered by the mobile recharger as a function of the recharging threshold ρ, at time $t = 9 \times 10^6$ and $\mu = 1$, under the simple recharging policy.*

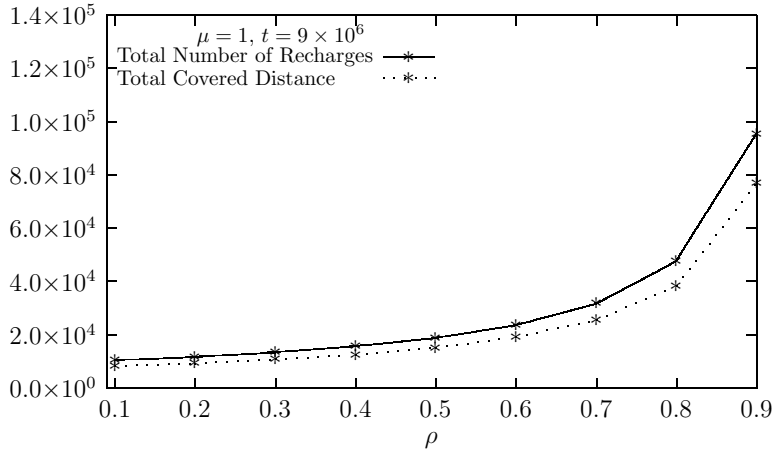

Figure E.9: *Total number of requests for recharges and total distance covered by the mobile recharger as a function of the recharging threshold ρ, at time $t = 9 \times 10^6$ and $\mu = 1$, under the improved recharging policy.*

median problem, then the covered distance is minimized. Let fraction $\frac{\mathcal{D}(\mathbf{s})}{\mathcal{D}(\mathbf{s}_{\mathcal{D}})}$ denote the distance ratio ($\frac{\mathcal{D}(\mathbf{s})}{\mathcal{D}(\mathbf{s}_{\mathcal{D}})} \geq 1$).

Figures E.10 and E.11 depicts $D^{\mathbf{s}}(t)$ at time $t = 10^3$ as a function of the distance ratio $\frac{\mathcal{D}(\mathbf{s})}{\mathcal{D}(\mathbf{s}_{\mathcal{D}})}$ for $\rho = 0.9$ and $\mu = 5$ for both the simple recharging policy E.10 and the improved one (E.11). Each point corresponds to the total recharging distance that took place when the sink was located at a node of the particular value regarding distance ratio. There are 1000 points that correspond to the 1000 nodes, each one being the sink. Obviously, the smaller the distance ratio, the smaller the total recharging distance, the minimum assumed at $\frac{\mathcal{D}(\mathbf{s})}{\mathcal{D}(\mathbf{s}_{\mathcal{D}})} = 1$ which is the solution of the previously formulated 1-median problem. It is clear that both the simple recharging policy and its improved version are in accordance with the analytical results. As observed, the recharging distance under the improved version is smaller than that under the simple recharging policy.

Figure E.12 depicts $D^{\mathbf{s}}(t)$ at time $t = 9 \times 10^9$ as a function of the distance ratio $\frac{\mathcal{D}(\mathbf{s})}{\mathcal{D}(\mathbf{s}_{\mathcal{D}})}$ for three different values of ρ (0.1, 0.5 and 0.9) and $\mu = 5$. The requirement for $t = 9 \times 10^9$ and the three values of ρ results in 27×10^6 more runs compared to the experiment that took place for the scenario of Figure E.10, pushing to the limits the simulation program and thus, considering only the simple recharging policy. As before, it is observed that the minimum is assumed at $\frac{\mathcal{D}(\mathbf{s})}{\mathcal{D}(\mathbf{s}_{\mathcal{D}})} = 1$ which is the solution of the previously formulated 1-median problem, while the depicted values are more concentrated compared to those depicted in Figures E.10 and E.11. Moreover, the covered distance depends on the recharging threshold ρ. However, its minimization is clearly independent of ρ as it can be concluded from the analytical results (i.e., Equation (E.5) does not depend on ρ) and observed by the simulation results as well.

The case of $\rho = 0.9$ is interesting and requires further elucidation. As before, for $\frac{\mathcal{D}(\mathbf{s})}{\mathcal{D}(\mathbf{s}_{\mathcal{D}})} \to 1$, the total recharging distance is minimized. However, as $\frac{\mathcal{D}(\mathbf{s})}{\mathcal{D}(\mathbf{s}_{\mathcal{D}})}$ increases and more specifically when $\frac{\mathcal{D}(\mathbf{s})}{\mathcal{D}(\mathbf{s}_{\mathcal{D}})}$ is larger than 1.5, the total distance does not follow the expected pattern. The reason is that for sink nodes of these particular values, the simulation execution terminates earlier than $t = 9 \times 10^6$ due to at least one node of exhausted battery. Consequently, the obtained value corresponds to the total distance not at time $t = 9 \times 10^6$ but at an earlier time and, as expected, is smaller.

The latter observation looks like a paradox, even though it is not. For $\rho = 0.9$, after some time, a large number of nodes would require to be recharged. Consequently, their recharging requests would be queued according to the previously mentioned first-in-first-out policy. As a result, there will be some nodes (the ones close to the sink) that will be severely affected by the energy hole problem and the energy left in their batteries will be consumed before the next recharging. The fact

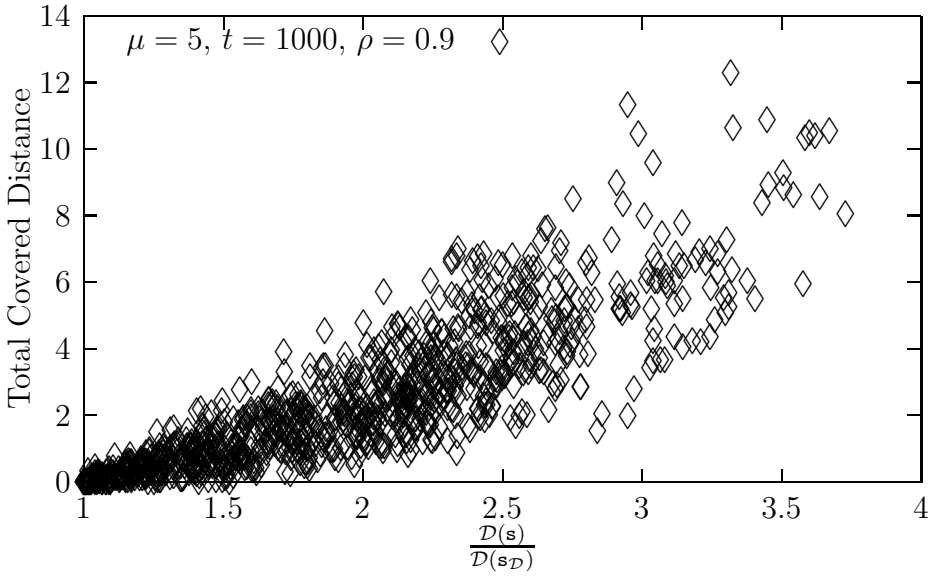

Figure E.10: *Total covered distance at time $t = 10^3$ as a function of the distance ratio $\frac{\mathcal{D}(\mathbf{s})}{\mathcal{D}(\mathbf{s}_\mathcal{D})}$, for $\rho = 0.9$) and $\mu = 5$, under the simple recharging policy.*

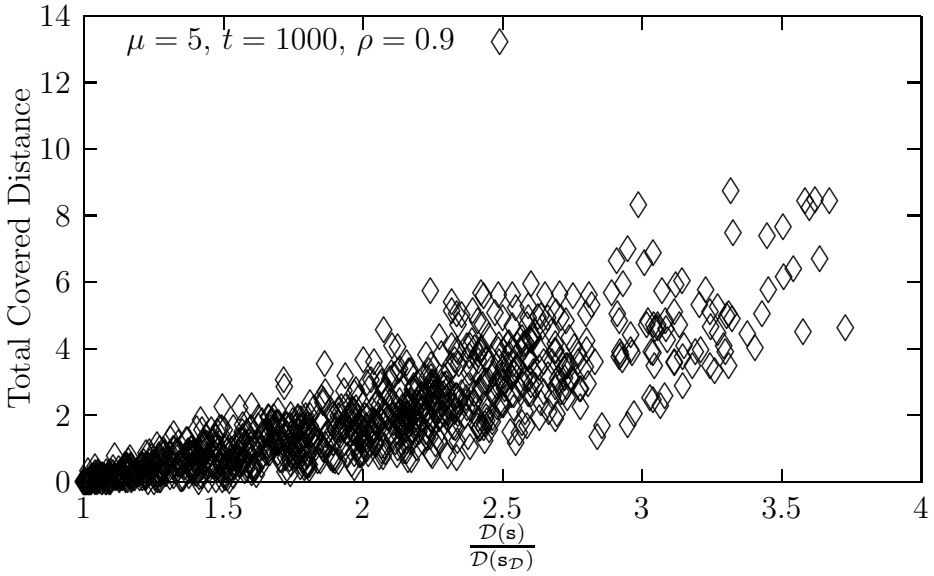

Figure E.11: *Total covered distance at time $t = 10^3$ as a function of the distance ratio $\frac{\mathcal{D}(\mathbf{s})}{\mathcal{D}(\mathbf{s}_\mathcal{D})}$, for $\rho = 0.9$) and $\mu = 5$, under the improved recharging policy.*

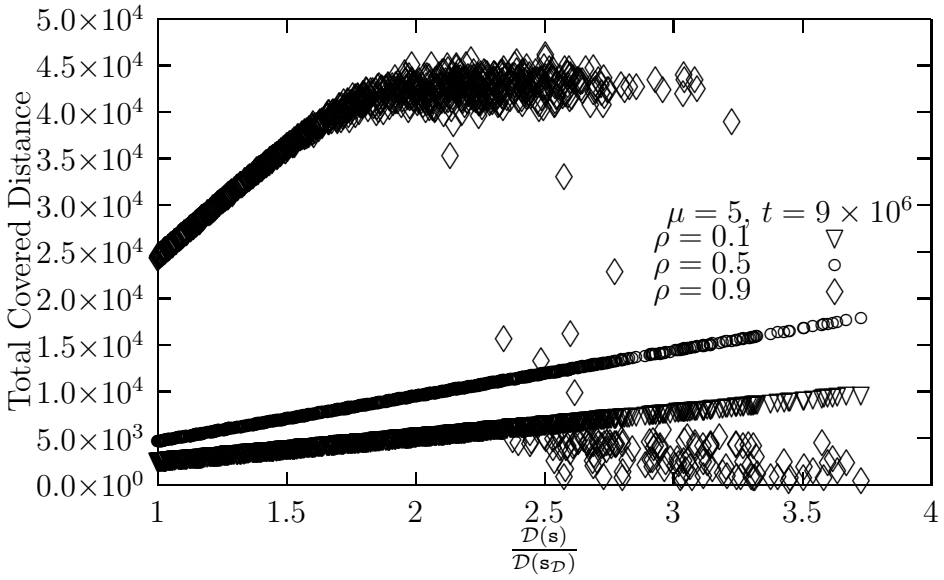

Figure E.12: *Total covered distance at time* $t = 9\times10^6$ *as a function of the distance ratio* $\frac{\mathcal{D}(\mathbf{s})}{\mathcal{D}(\mathbf{s}_\mathcal{D})}$*,for three different values of* ρ *(*0.1*,* 0.5 *and* 0.9*) and* $\mu = 5$*.*

that such a behavior is not observed for $\rho = 0.1$ or $\rho = 0.5$ is attributed to the fact that $t = 9 \times 10^6$, even thus the maximum, it is not enough to reveal this behavior. A possible improvement (left for future work) could be a replacement of the first-in-first-out policy with one considering the remaining battery level of each node that sends a recharging request. Note, however, that for all cases, when $\frac{\mathcal{D}(\mathbf{s})}{\mathcal{D}(\mathbf{s}_\mathcal{D})} \to 1$ there is no such a problem, which is another indication that the solution of the previously formulated 1-median problem efficiently captures the minimum recharging distance for the particular simple recharging policy.

E.3.2 Evaluation of the Enhanced Recharging Policy

The purpose here is to demonstrate the effectiveness of the enhanced recharging policy using simulation results. The NJNP policy as well as a variant that improves its performance and described later, are used for comparison purposes.

Simulation Configuration

The simulation platform OMNeT++ [162] is used to develop the simulation scenarios with respect to the network environment, the proposed policy and the policies that will serve as the comparison basis. Connected geometric random graphs topologies [121] of $n = 1000$ nodes in the $[0 \dots 1000] \times [0 \dots 1000]$ square area, are considered as the most suitable ones to capture the sensor networks' topology idiosyncrasies

Table E.1: *Simulation Network Parameters.*

Parameters	Value
Traffic load λ_u	$[0, 1/n]$
Number of nodes n	1000
Processing cost `p`	400 mA
Transmission `e`	27 mA
Reception `r`	10 mA
Connectivity radius r_c	150 m
Nodes' battery capacity $\mathcal{B}_{\max}$	100 mAh
Data packet's length	20 *bytes*
Data rate	38.4 *kbps*

[164]. Each node u senses and processes the sensed information and generates data packets according to its traffic load λ_u and each packet – piggybacked by the sensed information – is forwarded towards the sink node over the branches of a shortest path tree. Traffic load λ_u takes random values uniformly distributed within range $[0, 1/n]$.

In order to configure the simulation scenarios as close to reality as possible, the energy consumption parameters regarding the communication are set based on the data sheet of MICA2 (MPR400CB) mote [122], which operates with maximum transmitting and receiving current draw of 27 mA, and 10 mA, respectively. The data rate is 38.4 *kbps* while data packets' size is set to 20 *bytes*. Regarding the nodes' batteries, it is assumed that all nodes hold a rechargeable battery of capacity equal to 100 mAh. The consumed energy for processing is set to 400 mA. These parameters and the corresponding values are shown in Table E.1.

Regarding the mobile recharger, it recharges the nodes' batteries with a recharging ratio $\psi = 3000$ mA. In addition, it moves among nodes over the shortest path tree with a constant velocity `v` set to 1 m/s, while its initial battery capacity $\mathcal{C}$ equals 1000 mAh. The mobile recharger consumes $\Updownarrow = 100$ mA to move (i.e., moving consumption) and when in vacation, it fully recharges itself with a recharger recharging ratio $\phi = 3000$ mA. Mobile recharger's parameters are shown in Table E.2.

The NJNP and the r-NJNP Policies

The main characteristic of the NJNP recharging policy is the mobile recharger's capability of receiving all recharging requests irrespectively of its location. Even though a simple approach is to assume the transmission range of all networks nodes

Table E.2: *Simulation Mobile Recharger Parameters.*

Parameters	Value
Node recharging ratio ψ	3000 mA
Velocity $\mathtt{v}$	1 m/s
Initial battery capacity $\mathcal{C}$	1000 mAh
Moving consumption $\Updownarrow$	100 mA
Recharger recharging ratio ϕ	3000 mA

covers the entire network area, an energy efficient approach is to assume that it is only the sink that does so. In the former approach the energy consumption would be increased for nodes of already low battery energy level, while for the latter approach there is no such problem since the sink node is attached to an existing infrastructure. Eventually, this allows for a fair comparison between the NJNP policy and the proposed one.

As long as the mobile recharger is aware about pending recharging requests, it moves to the particular node of the nearest location among those nodes that have send a recharging request. The energy stored in the battery of the mobile recharger is reduced for both moving and replenishing the node's battery.

One characteristic of the proposed policy is its capability to charge all nodes en route to a node that has requested for a recharge. In order to get a fair comparison, this characteristic is added to the NJNP policy, thus introducing the r-NJNP policy. The latter holds the initial NJNP's characteristics (e.g., global knowledge, selection of the closer node to recharge next, etc.) along with the ability to charge en route nodes. Both the NJNP and the r-NJNP policies are implemented for comparison purposes against the proposed policy.

Evaluation of the 1-median Problem Formulation

The first step is to determine the particular node that the sink should be located at. By selecting different nodes as the sink placement, this eventually leads to different overall energy consumption and the recharging effectiveness is also affected. In some sensor network environments, the sink position may be predefined (e.g., close to infrastructure), whereas in some others there might be a possibility to select the sink position, even though it will remain fixed for the rest of the network's life. Having this in mind, Figures E.13, E.14 and E.15 depict the total consumed energy by the recharger for both operations (recharging nodes' batteries and traveling) until time $t = 2 \times 10^5$, as a function of the distance ratio $\frac{\mathcal{D}(\mathtt{s})}{\mathcal{D}(\mathtt{s}_\mathcal{D})}$ for the presented

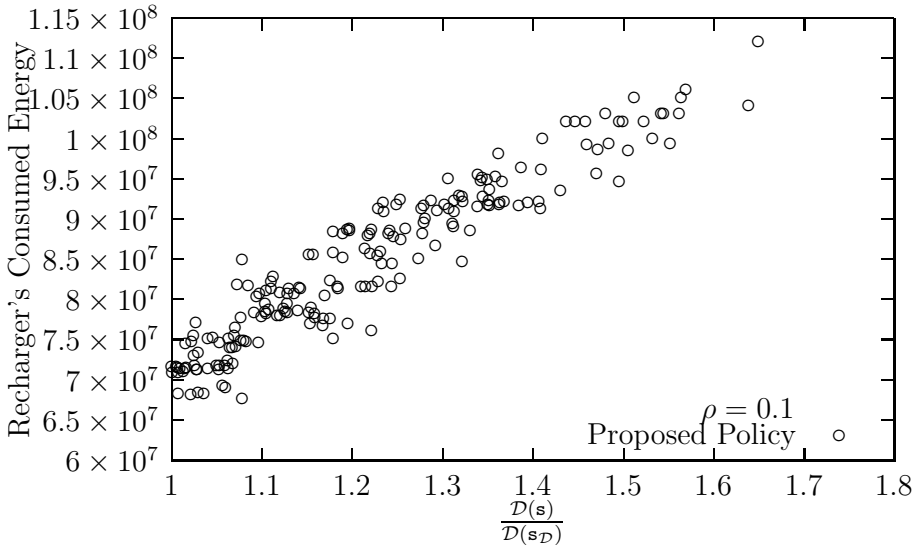

Figure E.13: *Recharger's consumed energy under the proposed recharging policy when each node assumes the role of the sink, as a function of the distance ratio* $\frac{\mathcal{D}(\mathbf{s})}{\mathcal{D}(\mathbf{s}_{\mathcal{D}})}$ *for* $\rho = 0.1$ *and* $t = 2 \times 10^5$.

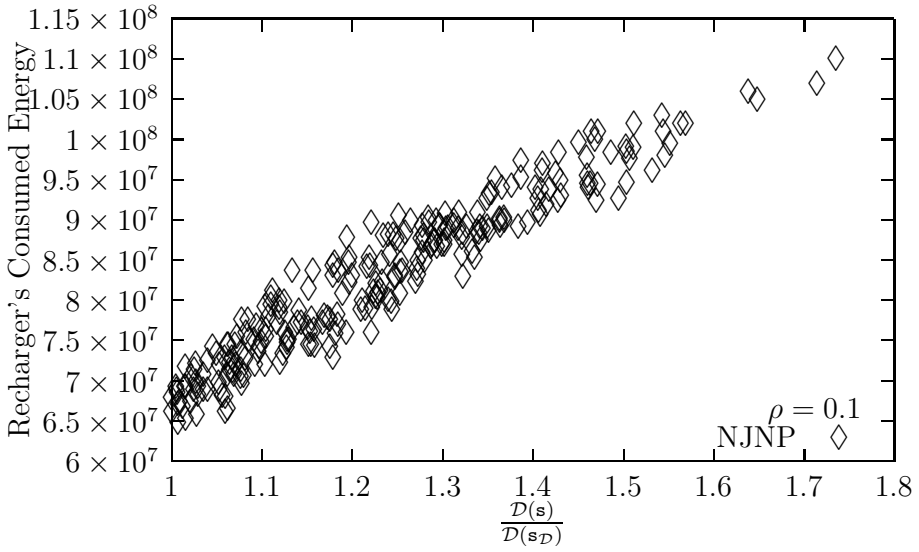

Figure E.14: *Recharger's consumed energy under the NJNP policy when each node assumes the role of the sink, as a function of the distance ratio* $\frac{\mathcal{D}(\mathbf{s})}{\mathcal{D}(\mathbf{s}_{\mathcal{D}})}$ *for* $\rho = 0.1$ *and* $t = 2 \times 10^5$.

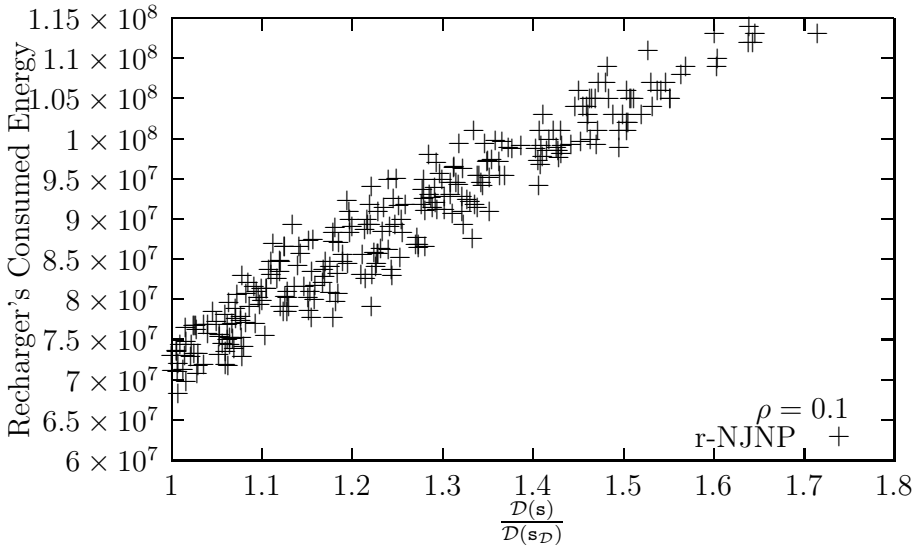

Figure E.15: *Recharger's consumed energy under the r-NJNP policy when each node assumes the role of the sink, as a function of the distance ratio* $\frac{\mathcal{D}(\mathbf{s})}{\mathcal{D}(\mathbf{s}_{\mathcal{D}})}$ *for* $\rho = 0.1$ *and* $t = 2 \times 10^5$.

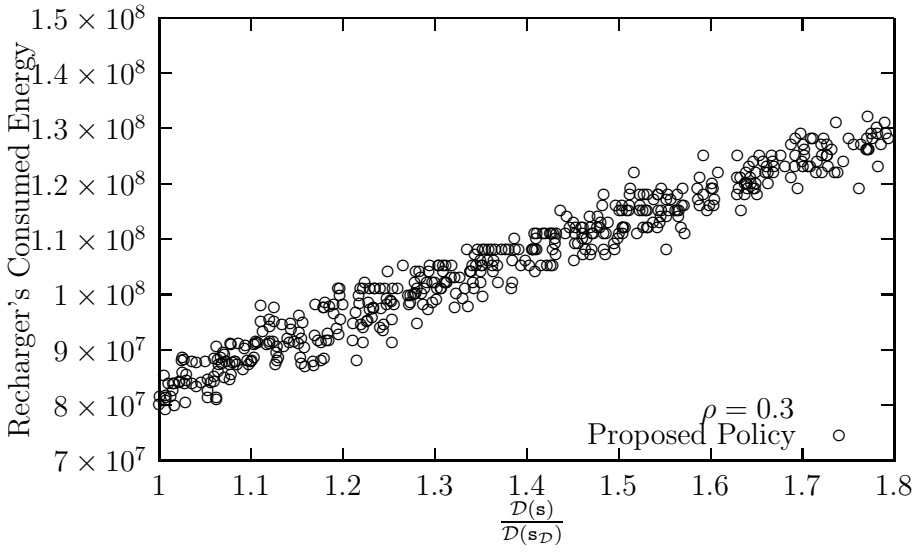

Figure E.16: *Recharger's consumed energy under the proposed recharging policy when each node assumes the role of the sink, as a function of the distance ratio* $\frac{\mathcal{D}(\mathbf{s})}{\mathcal{D}(\mathbf{s}_{\mathcal{D}})}$ *for* $\rho = 0.3$ *and* $t = 2 \times 10^5$.

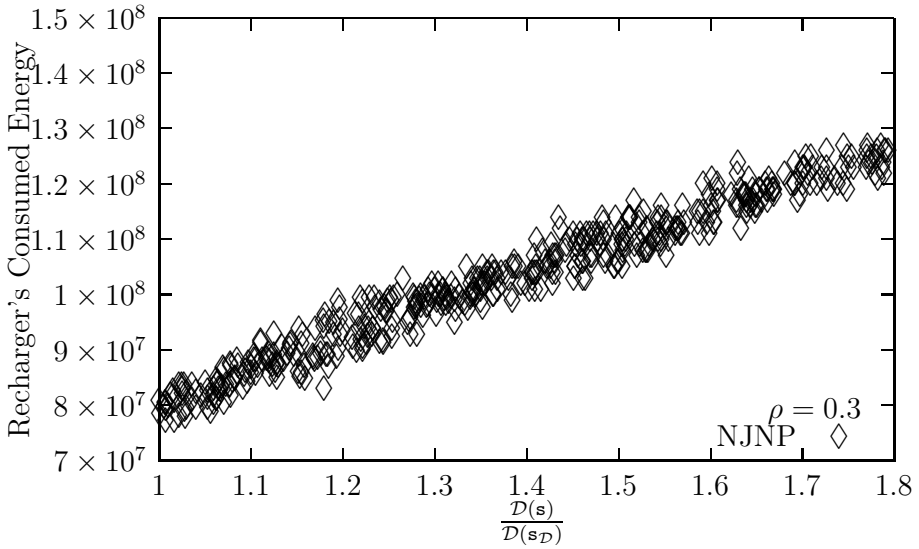

Figure E.17: *Recharger's consumed energy under the NJNP policy when each node assumes the role of the sink, as a function of the distance ratio* $\frac{\mathcal{D}(\mathbf{s})}{\mathcal{D}(\mathbf{s}_\mathcal{D})}$ *for* $\rho = 0.3$ *and* $t = 2 \times 10^5$.

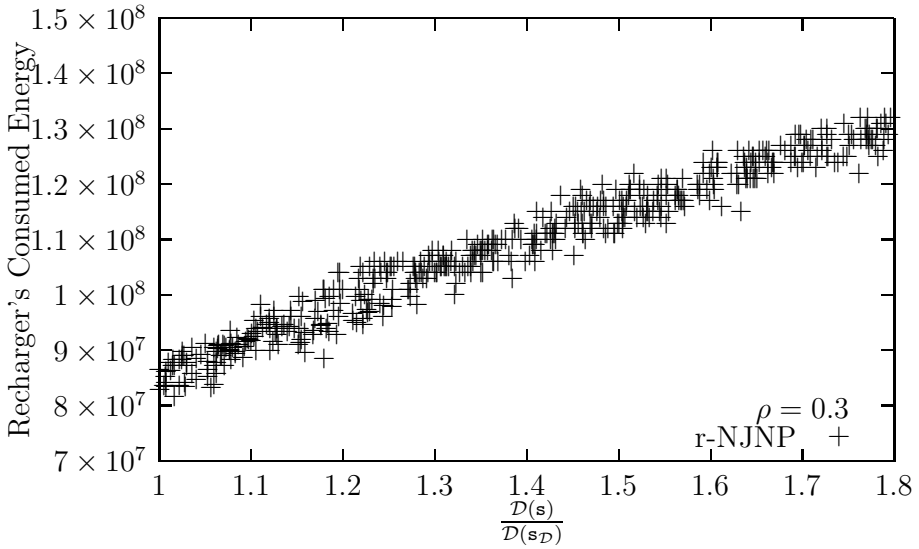

Figure E.18: *Recharger's consumed energy under the r-NJNP policy when each node assumes the role of the sink, as a function of the distance ratio* $\frac{\mathcal{D}(\mathbf{s})}{\mathcal{D}(\mathbf{s}_\mathcal{D})}$ *for* $\rho = 0.3$ *and* $t = 2 \times 10^5$.

policy, as well as for both the NJNP and r-NJNP policies and $\rho = 0.1$. In addition, Figures E.16, E.17 and E.18 are in the same spirit, differentiated in ρ's value which is set to 0.3 for them. Each point corresponds to the total consumed energy that took place when the sink is located at node $\mathtt{s}$ characterized by this distance ratio $\frac{\mathcal{D}(\mathtt{s})}{\mathcal{D}(\mathtt{s}_\mathcal{D})}$. There are 1000 depicted points that correspond to the 1000 nodes, each one being the sink for one simulation run. It is interesting to observe that for all policies, the best scenario, i.e., the minimum consumed energy, takes place for distance ratio values close to 1, i.e., to the solution of the 1-median problem.

In a similar manner, termination time is depicted in Figures E.19, E.20 and E.21 for $\rho = 0.1$ and in Figures E.22, E.23 and E.24 for $\rho = 0.3$ respectively. Clearly, when placing the sink node (and the mobile recharger) closer to the solution of the 1-median problem (i.e., $\frac{\mathcal{D}(\mathtt{s})}{\mathcal{D}(\mathtt{s}_\mathcal{D})} = 1$), the network's lifetime tends to be prolonged.

Figures E.25 and E.26 depict the total time period that the mobile recharger remained at vacation until time $t = 2 \times 10^5$ as a function of the distance ratio $\frac{\mathcal{D}(\mathtt{s})}{\mathcal{D}(\mathtt{s}_\mathcal{D})}$ for all three policies. Under all considered policies, the mobile recharger stays in vacation longer when the sink is closer to $\frac{\mathcal{D}(\mathtt{s})}{\mathcal{D}(\mathtt{s}_\mathcal{D})} = 1$ than when it is not. Staying longer at vacation is the outcome of both having less recharging requests and serving them faster. In this figure, it is clear that the mobile recharger under the proposed policy stays longer at vacation than the others.

Behavior of Recharging Policies

Having shown that all policies behave better at the solution of the 1-median problem, for the rest of the simulations, the sink node is the one that corresponds to the particular solution, i.e., $\frac{\mathcal{D}(\mathtt{s})}{\mathcal{D}(\mathtt{s}_\mathcal{D})} = 1$. Figures E.27 and E.28 depict the average battery level ratio $\frac{\overline{\mathcal{B}^{\mathtt{s}}}(t)}{\mathcal{B}_{\max}}$, where $\overline{\mathcal{B}^{\mathtt{s}}}(t) = 1/n \sum_{\forall u \in V} \mathcal{B}_u^{\mathtt{s}}(t)$ for sink node $\mathtt{s}$, as a function of time t for $\rho = 0.1$ and $\rho = 0.3$. Clearly, as time increases, the energy left in the network nodes decreases, but there is a tendency to converge towards a certain level (0.7 and 0.75). It is also observed that at the beginning all three policies are close but as time increases the highest remaining energy level is that under the proposed policy and the r-NJNP policy. Note, however, that both the NJNP and the r-NJNP policies are based on global knowledge, i.e., they have knowledge about nodes that need to be recharged, whereas the proposed policy is based on local information moving in a per hop basis and only when placed at the sink node it receives intelligence about which node should be recharged next.

Apart from the average value of the battery level ratio, the variance is another key parameter since it reflects the effectiveness of the recharging policy against the energy hole problem. The energy hole problem corresponds to some nodes having a

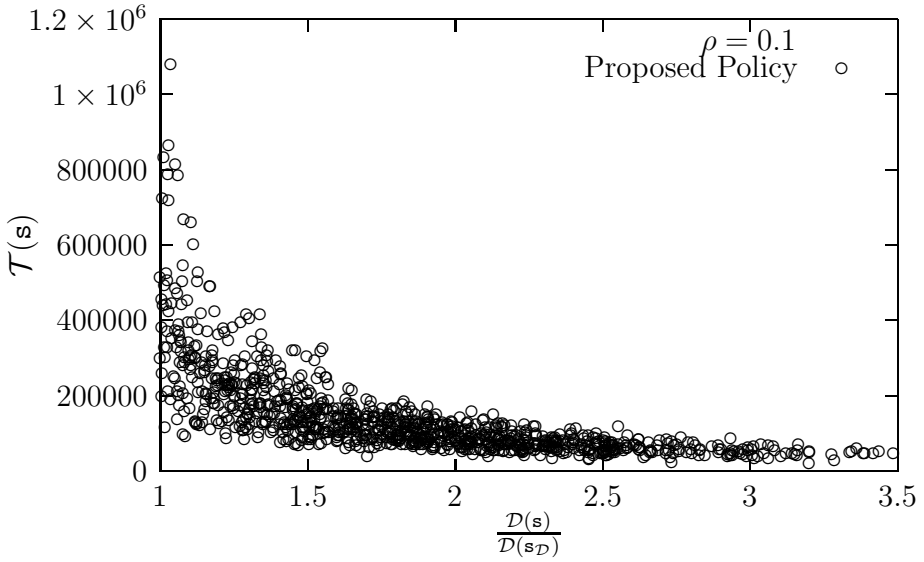

Figure E.19: *Termination time $\mathcal{T}(\mathtt{s})$ under the proposed recharging policy when each node assumes the role of the sink, as a function of the distance ratio $\frac{\mathcal{D}(\mathtt{s})}{\mathcal{D}(\mathtt{s}_\mathcal{D})}$ for $\rho = 0.1$.*

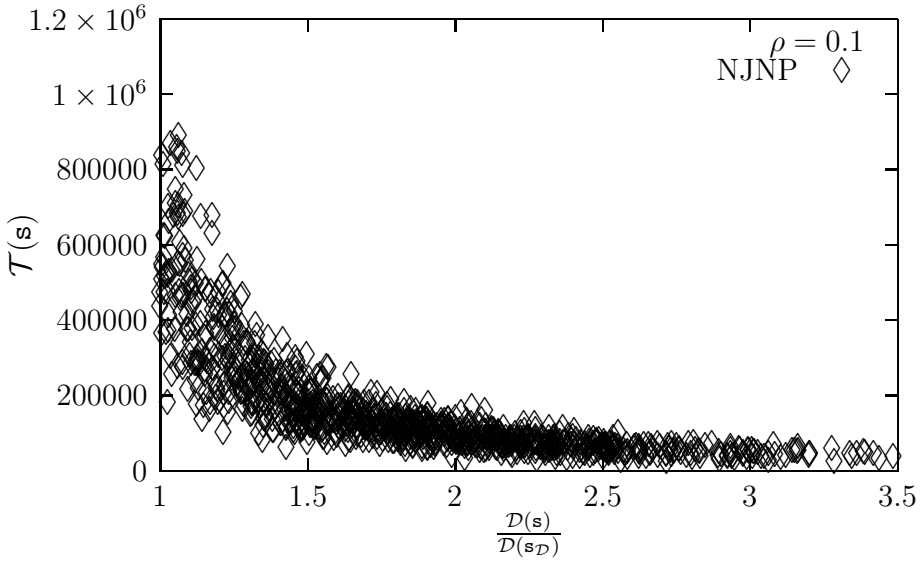

Figure E.20: *Termination time $\mathcal{T}(\mathtt{s})$ under the NJNP policy when each node assumes the role of the sink, as a function of the distance ratio $\frac{\mathcal{D}(\mathtt{s})}{\mathcal{D}(\mathtt{s}_\mathcal{D})}$ for $\rho = 0.1$.*

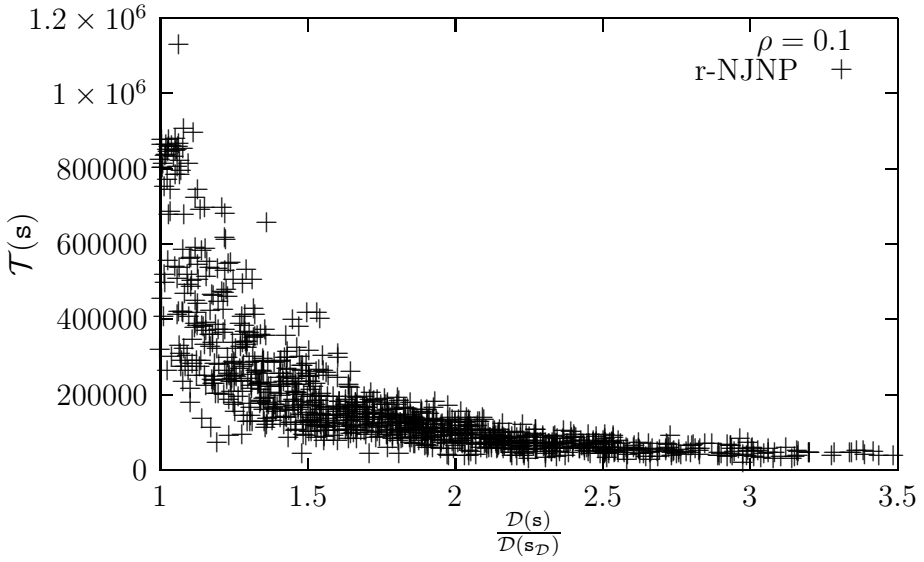

Figure E.21: *Termination time $\mathcal{T}(\mathtt{s})$ under the r-NJNP policy when each node assumes the role of the sink, as a function of the distance ratio $\frac{\mathcal{D}(\mathtt{s})}{\mathcal{D}(\mathtt{s}_\mathcal{D})}$ for $\rho = 0.1$.*

significantly low energy level, whereas other do not, thus the variance of the energy level is large. Clearly, the smaller the variance, the less the effectiveness of the energy hole problem. Figures E.29 and E.30 depict the variance of the nodes' remaining energy $Var[\mathcal{B}_u^{\mathtt{s}}(t)]$, as a function of time t for $\rho = 0.1$ and $\rho = 0.3$. As observed, the variance of the energy level under the proposed policy remains smaller than that under the other policies.

In Figure E.31 the distance covered by the recharger until $t = 3 \times 10^5$ is depicted as a function of ρ. It is observed that the mobile recharger under the proposed policy covers a smaller overall distance than under the other policies. Furthermore, regarding the maximum pending recharging requests as a function of ρ (until $t = 3 \times 10^5$) as depicted in Figure E.32, the proposed policy clearly serves the pending requests better than the other policies.

Termination time under the three considered policies is depicted in Figure E.33 as a function of ρ. As observed, network's lifetime is prolonged more effectively under the proposed policy than under the NJNP and r-NJNP policies. This is expected since the effects of the energy hole problem are reduced under the proposed policy when compared to the other ones.

E.4 Discussion

In the second approach of this thesis, presented in this chapter, the increased energy consumption due to the energy hole problem, is countered by the implementation

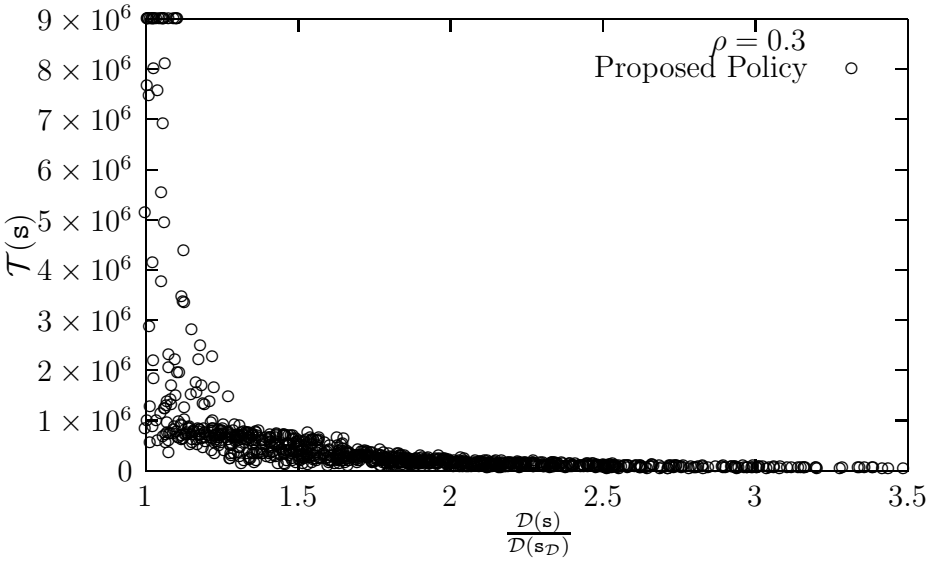

Figure E.22: *Termination time $\mathcal{T}(\mathtt{s})$ under the proposed recharging policy when each node assumes the role of the sink, as a function of the distance ratio $\frac{\mathcal{D}(\mathtt{s})}{\mathcal{D}(\mathtt{s}_\mathcal{D})}$ for $\rho = 0.3$.*

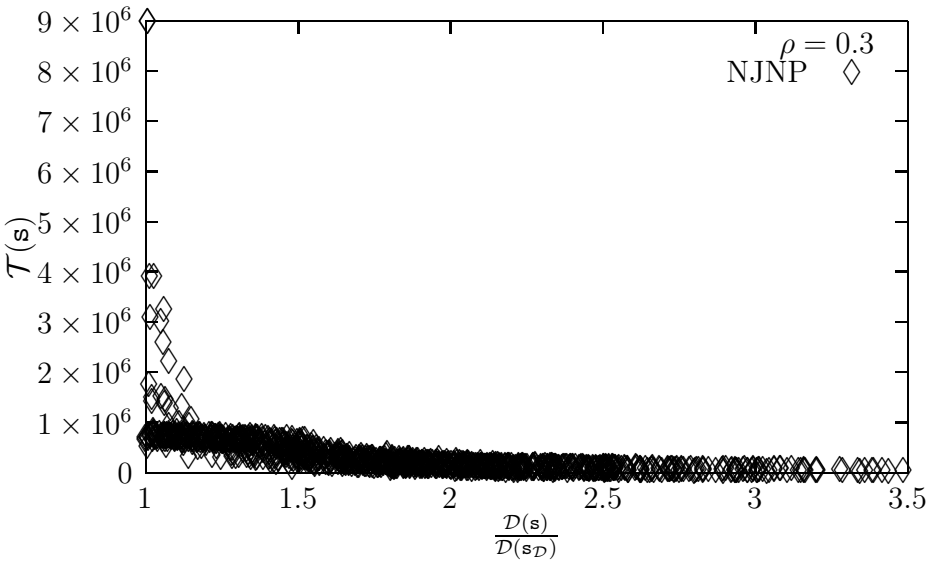

Figure E.23: *Termination time $\mathcal{T}(\mathtt{s})$ under the NJNP policy when each node assumes the role of the sink, as a function of the distance ratio $\frac{\mathcal{D}(\mathtt{s})}{\mathcal{D}(\mathtt{s}_\mathcal{D})}$ for $\rho = 0.3$.*

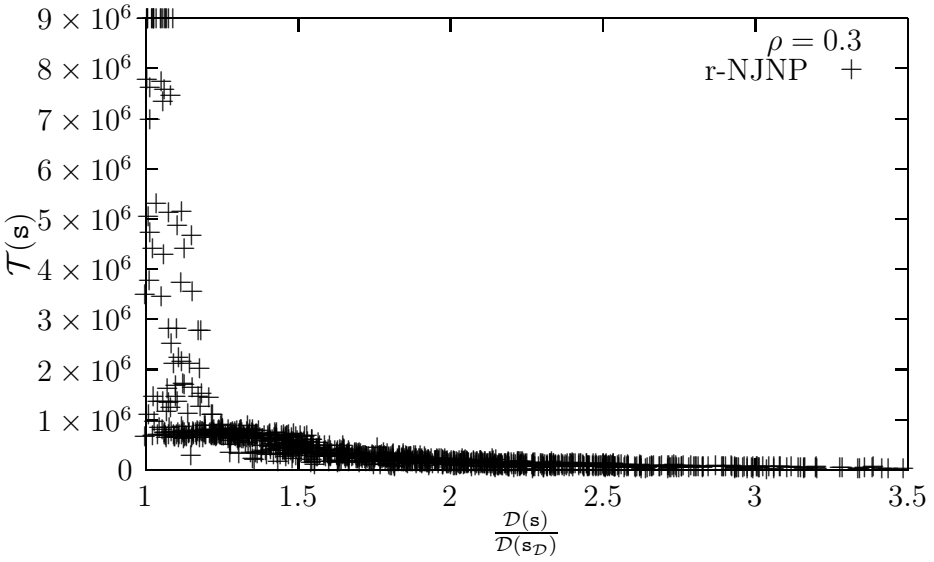

Figure E.24: *Termination time $\mathcal{T}(\mathtt{s})$ under the r-NJNP policy when each node assumes the role of the sink, as a function of the distance ratio $\frac{\mathcal{D}(\mathtt{s})}{\mathcal{D}(\mathtt{s}_\mathcal{D})}$ for $\rho = 0.3$.*

of two recharging policies, both relying on local information. These policies are: (i) a simple recharging policy under which a request is sent to the sink node to initiate a recharging process if the battery level of a sensor node is below a fixed recharging threshold and (ii) a recharging policy which by enhancing the previous one, recharges all nodes en route to the node that has requested for a recharge, it recharges its battery and then moves in a hop-by-hop manner to those neighbor nodes of the lowest energy level.

As it is shown, the recharging distance, under the first recharging policy, corresponds to an 1-median problem. Simulation results validate the analytical findings and show that when the sink is located at the solution of the latter 1-median problem, then the distance covered by the mobile recharger is minimized. Simulations conducted investigate the effect of the recharging threshold and particularly, how it affects the energy level of the sensor nodes' batteries and the distance covered by the mobile recharger. It is also shown that the value of recharging threshold does not affect the optimal position of the sink, thus the minimum recharging distance remains constant as expected by the analysis. Furthermore, this simple policy is improved by allowing the recharging device to replenish the nodes' battery along the trajectory towards the particular node that initiated the recharging request in the first place. As it is expected, the results are further improved and in compliance with the analysis.

The second proposed policy is evaluated using simulation results against the NJNP policy and a variation of the latter that, similarly to the proposed recharging

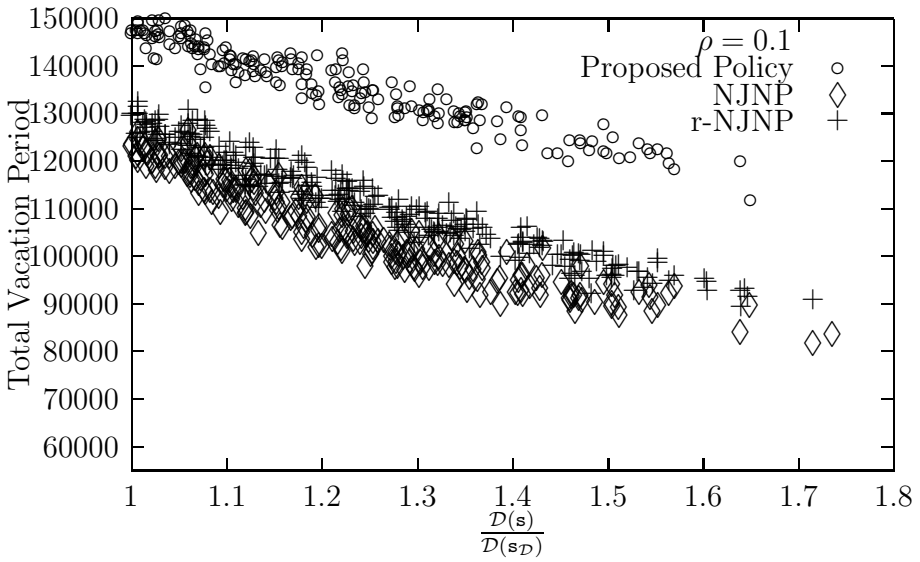

Figure E.25: *Total vacation period under the three considered policies when each node assumes the role of the sink, as a function of the distance ratio* $\frac{\mathcal{D}(\mathbf{s})}{\mathcal{D}(\mathbf{s}_\mathcal{D})}$ *for* $\rho = 0.1$ *and* $t = 2 \times 10^5$.

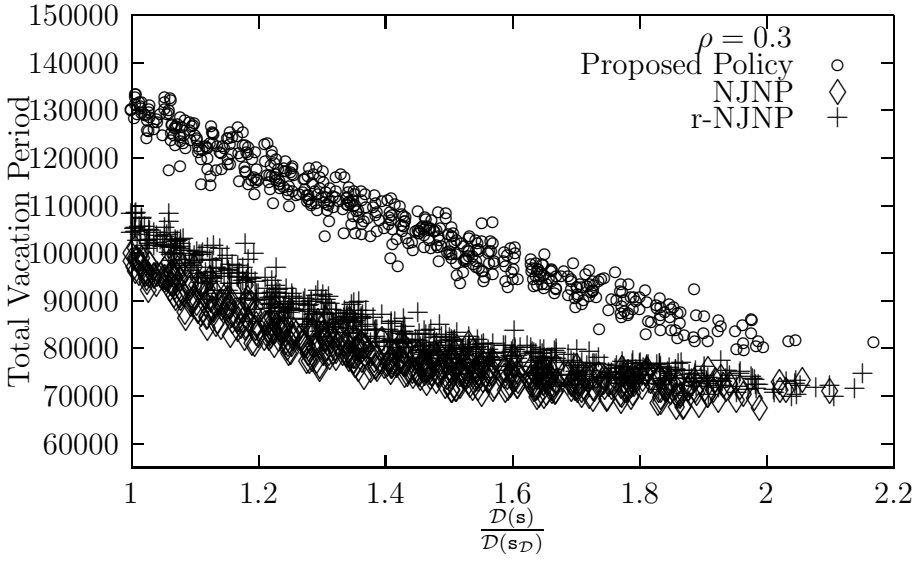

Figure E.26: *Total vacation period under the three considered policies when each node assumes the role of the sink, as a function of the distance ratio* $\frac{\mathcal{D}(\mathbf{s})}{\mathcal{D}(\mathbf{s}_\mathcal{D})}$ *for* $\rho = 0.3$ *and* $t = 2 \times 10^5$.

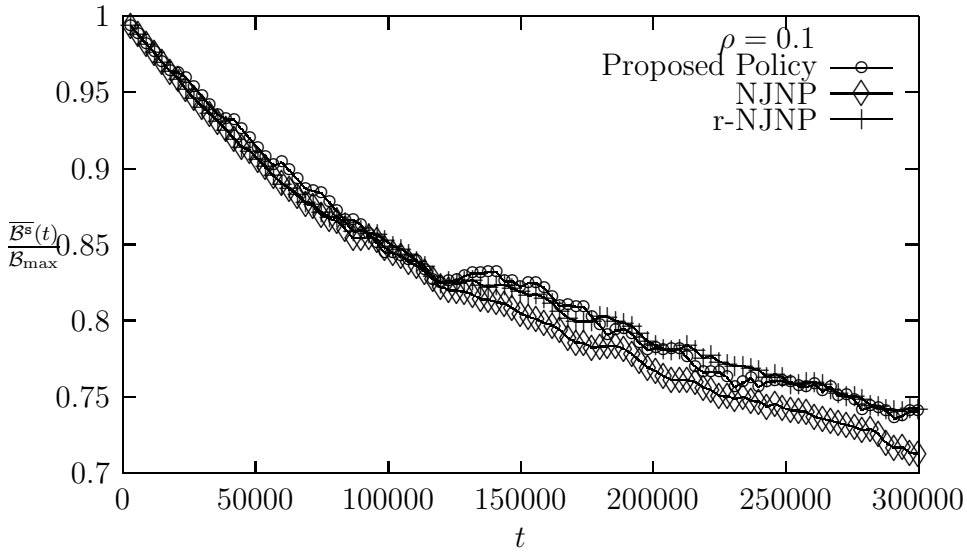

Figure E.27: *Average of the battery level ratio* $\frac{\overline{\mathcal{B}^s}(t)}{\mathcal{B}_{\max}}$ *as a function of time* t *under the three considered policies for* $\rho = 0.1$.

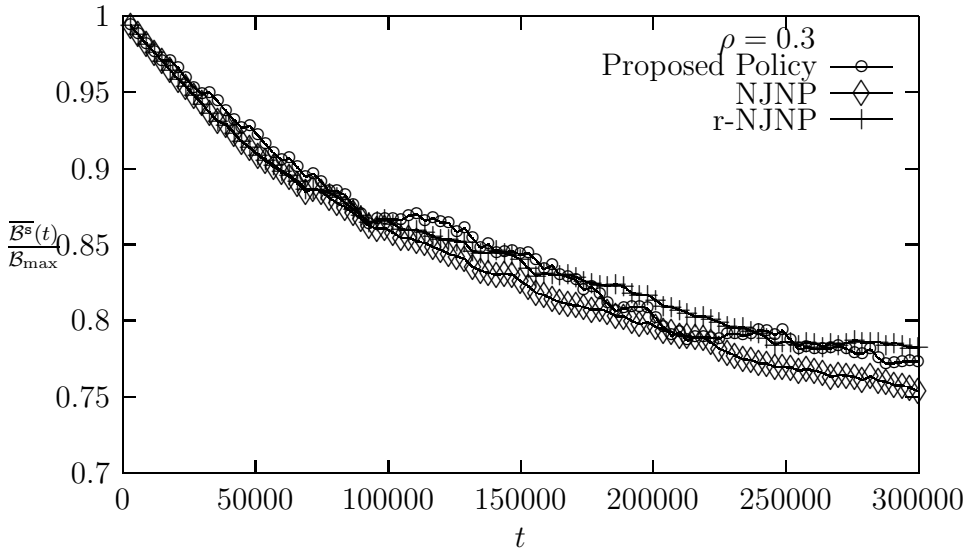

Figure E.28: *Average of the battery level ratio* $\frac{\overline{\mathcal{B}^s}(t)}{\mathcal{B}_{\max}}$ *as a function of time* t *under the three considered policies for* $\rho = 0.3$.

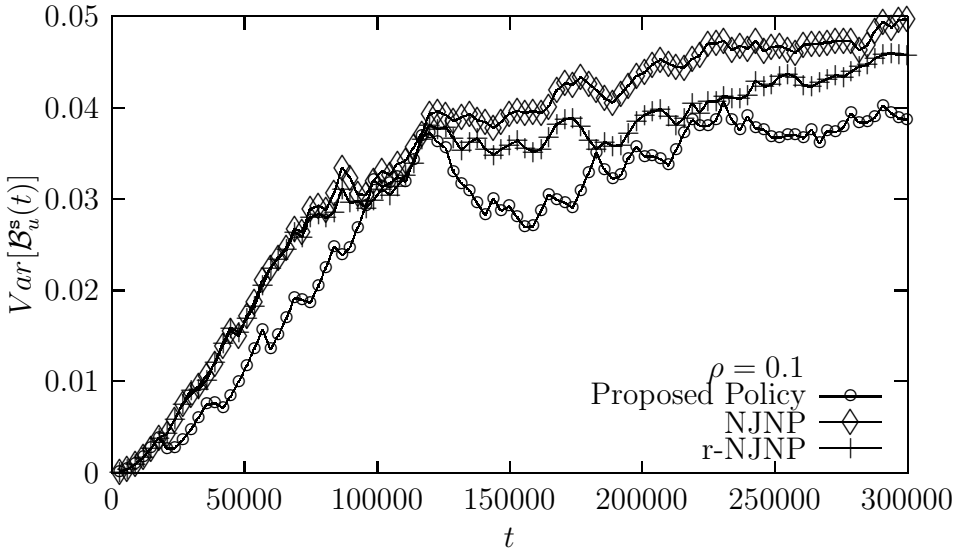

Figure E.29: *Variance of the nodes' remaining energy* $Var[\mathcal{B}_u^s(t)]$ *as a function of time* t *under the three considered policies for* $\rho = 0.1$.

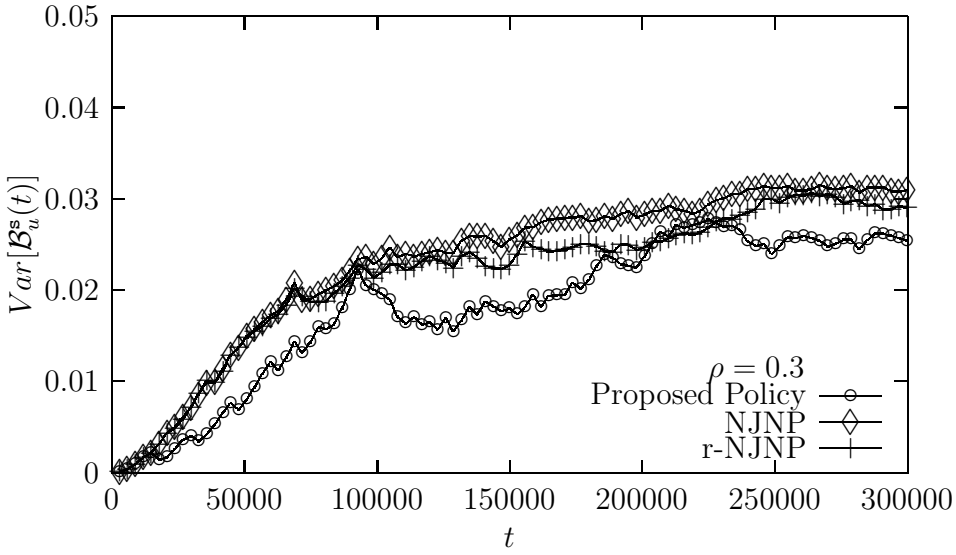

Figure E.30: *Variance of the nodes' remaining energy* $Var[\mathcal{B}_u^s(t)]$ *as a function of time* t *under the three considered policies for* $\rho = 0.3$.

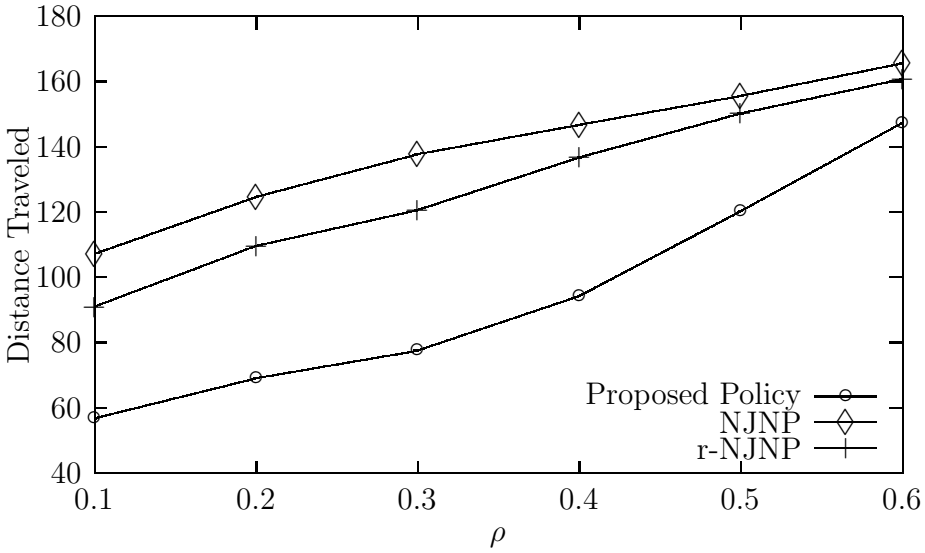

Figure E.31: *Distance covered by the mobile recharger under the three considered policies as a function of ρ at time instance $t = 3 \times 10^5$.*

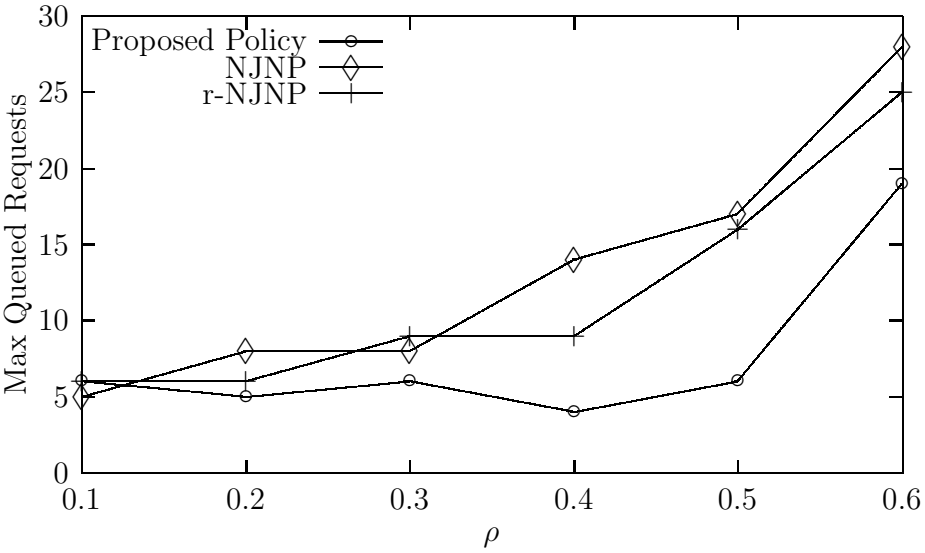

Figure E.32: *The number of pending recharging requests under the three considered policies as a function of ρ at time instance $t = 3 \times 10^5$.*

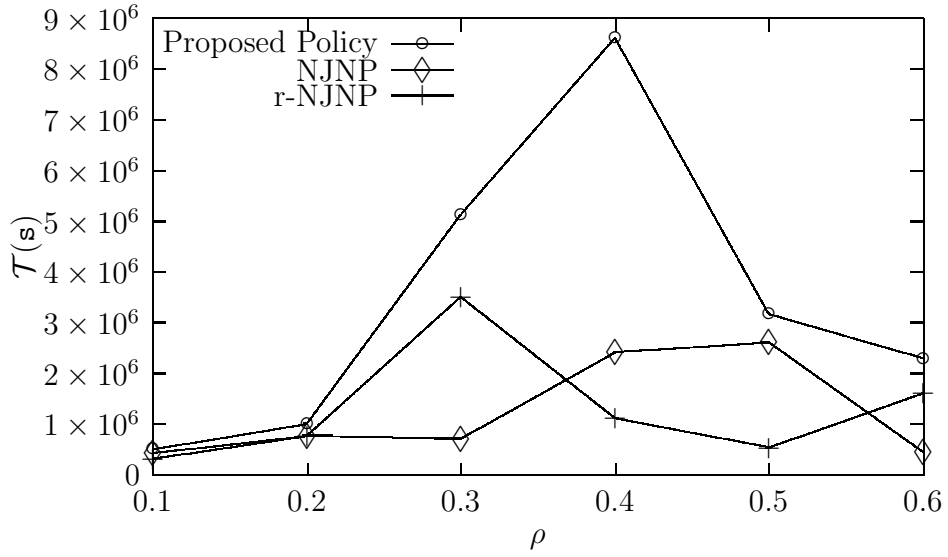

Figure E.33: *Termination time* $\mathcal{T}(\mathbf{s})$ *under the three considered policies as a function of* ρ.

policy, recharges all nodes en route. First, the median problem is also considered and it is demonstrated that, depending on the location of the sink, the performance of all three considered recharging policies changes; the best location being the solution of the median problem. This enhances the contribution derived by the first policy's approach, since it confirms the relation of the battery replenishment problems in wireless sensor networks to facility location problems. Second, the location of the sink for the simulation experiments is assumed the one that corresponds to the solution of the particular median problem. The simulation results also demonstrate the fact that the proposed policy, even if it bases its operation on local information, operates close to the NJNP and the r-NJNP policies and in some cases it outperforms them both, in terms of (mobile recharger's) covered distance, average and variance of the battery level in the network nodes, total (mobile recharger's) vacation period, pending of recharging requests and termination time.

Chapter F

Conclusions and Future Work

THIS thesis proposes two approaches that counter the energy hole problem's effects from two perspectives: (i) the minimization of the energy consumption by approaching the *sink placement problem* as a *k-median problem* and (ii) the prolongation of the network lifetime by recharging its sensor nodes. In this chapter the conclusions are given, along with possible future directions.

F.1 Summary and Conclusions

The network's lifetime prolongation is closely related to energy consumption and particularly the energy hole problem. In order to tackle the energy hole problem's effects, two approaches are studied in this thesis.

In the first approach, the energy consumption problem in wireless sensor networks is revisited by means of analytical investigation and formulation as a facility location problem. An analytical model is presented in his thesis and it is analytically demonstrated that when the sinks are placed according to the solution of the k-median problem, the overall energy consumption in the network is minimized, thus allowing for subsequent network lifetime prolongation. In addition, the presented simulation results validate the proposed analytical model, thus revealing a significant gain with respect to energy savings and network lifetime.

In the second approach proposed in this thesis, the problem of recharging the batteries of the nodes of a wireless sensor network is considered and two recharging policies are proposed, allowing a recharging vehicle stationed at the sink node to recharge other nodes' batteries when failing under a certain recharging threshold. As it is shown in the first recharging policy's (the simple recharging policy) study proposed here, the distance minimization problem can be formulated as an 1-median problem. The presented simulation results demonstrate the behavior of the proposed

policy and reveal a significant decrement with respect to the recharging distance when the analytical results are used. An enhanced version of this policy is also employed and simulation results are derived showing an improvement in performance. Eventually, as it is clearly demonstrated, if the sink is located at the particular node that is the solution of the formulated 1-median problem, then the covered distance under the proposed recharging policy is minimized. The second proposed policy (the enhanced recharging policy) considered here, is a novel on-demand recharging policy capable of moving a mobile recharger based on local information towards nodes of nearly exhausted battery level. As it is demonstrated using simulation results, this policy is capable of prolonging the network's lifetime by reducing the effects of the energy hole problem better than an existing on-demand recharging policy and a variation of it, both relying on global information. Furthermore, it is observed that the network's lifetime is maximized when the basis of the mobile recharger is located at the solution of the mentioned median problem for all studied policies.

Common case and basic contribution of the two proposed approaches is their establishing a relation between facility location problems and the problem each one is studied for. More specifically, the first approach formulates the sink placement problem as a k-median facility location problem, while the second establishes a relation between the k-median facility location problems and battery replenishment, along with proposing a new policy for recharging the network nodes.

F.2 Future Work Directions

Future work directions in this area are related to (i) enhancing the findings by the first approach here (i.e., the sink placement) and (ii) further studying the recharging policies in wireless sensor networks. More specifically, regarding the sink placement problem, a possible direction is to further evaluate the analytical findings by comparing them against results that will be taken from real wireless sensors networks. Nodes consisting these networks will be based on boards (e.g., Arduino) that use a variety of microprocessors and controllers.

As for the recharging policies, the approaches in the thesis are based on the on-demand category of them (where a request is created by a node when in need of a recharge). It appears that another interesting field correspond to the development of recharging policies based on predetermined routes (called *recharging cycles*) regarding the mobile rechargers' behavior. Future work directions here will consider further implementing new on-demand recharging policies, as well as studying the recharging policies', that are based on recharging cycles, behavior regarding the analytical findings of this thesis.

Additionally, the correlation between energy consumption and battery replenishment with facility location problems established in this thesis is expected to trigger future work in the area and reveal further aspects of the energy consumption issues and how lifetime may be prolonged in wireless sensor networks.

Appendices

Appendix A

Various Proofs

A.1 Proof of Lemma 2

For convenience, let $\Lambda_i = \Lambda^{\mathtt{s}}(u)$, if node u is at level i of an l-ary tree of m levels. It is easy to observe that $\Lambda_i = l\Lambda_{i+1} + \lambda$ and $\Lambda_{m-1} = \lambda$. Consequently, $\Lambda_{m-2} = \lambda\Lambda_{m-1} + \lambda = l\lambda + \lambda$. Accordingly, $\Lambda_{m-3} = \lambda\Lambda_{m-2} + \lambda = l^2\lambda + l\lambda + \lambda$, $\Lambda_{m-4} = l^3\lambda + l^2\lambda + l\lambda + \lambda$, $\ldots$, $\Lambda_i = l^{m-i-1}\lambda + l^{m-i-2}\lambda + \cdots + l\lambda + \lambda = \sum_{j=0}^{m-i-1} l^j\lambda$. Eventually, $\Lambda_i = \lambda\sum_{j=0}^{m-i-1} l^j$. Similarly, it can be shown that, $\sum_{j=0}^{m-i-1} l^j = \frac{l^{m-i}-1}{l-1}$. Consequently, $\Lambda_i = \frac{l^{m-i}-1}{l-1}\lambda$, for $i = 0, \ldots, m-1$.

A.2 Proof of Theorem 1

In an l-tree of m levels, l^i nodes belong to each level i, where $i = 0, \ldots, m-1$. Therefore, the corresponding number of nodes is $n = \sum_{i=0}^{m-1} l^i$. The latter expression can be written as $ln = \sum_{i=1}^{m} l^i$. Therefore, $n - ln = \sum_{i=0}^{m-1} l^i - \sum_{i=1}^{I} l^i = 1 - l^m$. Eventually, $n = \sum_{i=0}^{m-1} l^i = \frac{l^m-1}{l-1}$ and $l^m = n(l-1)+1$. Thus, $m = \log_l(n(l-1)+1)$. Note that without loss of generality, it is assumed that n is such that $n = \sum_{i=0}^{m-1} l^i$.

Given that, $\mathbb{E}[\Lambda^{\mathtt{s}}(u)] = \frac{1}{n}\sum_{u\in V(\mathbb{G})}\Lambda^{\mathtt{s}}(u)$, then, under the simplified notation of the proof of Lemma 2, Λ_i can be written as $\frac{1}{n}\sum_{i=0}^{m-1}\sum_{j=1}^{l^i}\Lambda_i$, or $\frac{1}{n}\sum_{i=0}^{m-1} l^i\Lambda_i$, or $\frac{1}{n}\sum_{i=0}^{m-1} l^i\frac{l^{m-i}-1}{l-1}\lambda$, or $\frac{1}{n}\sum_{i=0}^{m-1}\frac{l^m-l^i}{l-1}\lambda$, or $\frac{1}{n}\frac{ml^m-\sum_{i=0}^{m-1} l^i}{l-1}\lambda$, or $\mathbb{E}[\Lambda^{\mathtt{s}}(u)] = \frac{ml^m-n}{n(l-1)}\lambda$. Given these relationships, $m = \log_l(n(l-1)+1)$ and $l^m = n(l-1)+1$, and eventually, $\mathbb{E}[\Lambda^{\mathtt{s}}(u)] = \frac{(n(l-1)+1)\log_l(n(l-1)+1)-n}{n(l-1)}\lambda$.

Given that the sink node s belongs at the higher layer (i.e., layer 0), then $\Lambda^{\mathtt{s}}(s) = \Lambda_0 = \frac{l^m-1}{l-1}\lambda = \frac{n(l-1)+1-1}{l-1}\lambda = n\lambda$. Therefore, $\frac{\mathbb{E}[\Lambda^{\mathtt{s}}(u)]}{\Lambda^{\mathtt{s}}(s)} = \frac{(n(l-1)+1)\log_l(n(l-1)+1)-n}{n^2(l-1)\lambda}\lambda = \frac{(n(l-1)+1)\log_l(n(l-1)+1)-n}{n^2(l-1)}$.

A.3 Proof of Corollary 1

For the case of the 2-ary (i.e., binary) tree, it is sufficient to substitute $l = 2$ in the expression of Theorem 1, i.e., $\frac{\mathbb{E}[\Lambda^{\mathtt{s}}(u)]}{\Lambda^{\mathtt{s}}(s)} = \frac{(n+1)\log_2(n+1)-n}{n^2}$. The latter fraction can be written as $\frac{(n+1)\log_2(n+1)}{n^2} - \frac{n}{n^2} = \frac{(n+1)\log_2(n+1)}{n^2} - \frac{1}{n}$. Because for high values of n, $n+1 \approx n$, and $\frac{1}{n} \to 0$, the previous expression can be written as $\frac{(n+1)\log_2(n+1)}{n^2} - \frac{1}{n} \to \frac{n\log_2(n)}{n^2} = \frac{\log_2(n)}{n}$.

The complete graph corresponds to the case where all nodes are connected to each other. In such a graph, the sink node will have $n-1$ neighbor nodes over the corresponding shortest path routing tree. This case corresponds to a l-ary tree where $l = n-1$. By substituting this relationship into the expression of Theorem 1 then, $\frac{\mathbb{E}[\Lambda^{\mathtt{s}}(u)]}{\Lambda^{\mathtt{s}}(s)} = \frac{(n(n-1-1)+1)\log_{n-1}(n(n-1-1)+1)-n}{n^2(n-1-1)} = \frac{(n^2-2n+1)\log_{n-1}(n^2-2n+1)-n}{n^2(n-2)} = \frac{(n-1)^2\log_{n-1}(n-1)^2-n}{n^2(n-2)} = \frac{2(n-1)^2-n}{n^2(n-2)} = \frac{(n-2)(2n-1)}{n^2(n-2)} = \frac{2n-1}{n^2}$ for large values of n, $\frac{2n-1}{n^2} \to \frac{2}{n}$.

A.4 Proof of Lemma 3

The variance of the energy available at network nodes at some time t [84] can be expressed as $Var[\mathcal{B}^{\mathtt{s}}_u(t)] = \mathbb{E}[(\mathcal{B}^{\mathtt{s}}_u(t))^2] - \mathbb{E}^2[\mathcal{B}^{\mathtt{s}}_u(t)]$. Given that $\mathcal{B}^{\mathtt{s}}_u(t) = \mathcal{B}_{\max} - \Lambda^{\mathtt{s}}(u)t$, $\mathbb{E}[(\mathcal{B}^{\mathtt{s}}_u(t))^2] = \frac{1}{n}\sum_{u\in V(\mathbb{G})}(\mathcal{B}_{\max} - \Lambda^{\mathtt{s}}(u)t)^2$, and $\mathbb{E}^2[calB^{\mathtt{s}}_u(t)] = (\mathcal{B}_{\max} - \mathbb{E}[\Lambda^{\mathtt{s}}(u)]t)^2 = \mathbb{E}[(\mathcal{B}^{\mathtt{s}}_u(t))^2] = \frac{1}{n}\sum_{u\in V(\mathbb{G})}(\mathcal{B}^2_{\max} - 2\mathcal{B}_{\max}\Lambda^{\mathtt{s}}(u)t + (\Lambda^{\mathtt{s}}(u)t)^2) = \mathcal{B}^2_{\max} - 2\mathcal{B}_{\max}\frac{1}{n}\sum_{u\in V(\mathbb{G})}\Lambda^{\mathtt{s}}(u)t + \frac{1}{n}\sum_{u\in V(\mathbb{G})}(\Lambda^{\mathtt{s}}(u)t)^2$. Eventually, $\mathbb{E}[(\mathcal{B}^{\mathtt{s}}_u(t))^2] = \mathcal{B}^2_{\max} - 2\mathcal{B}_{\max}\mathbb{E}[\Lambda^{\mathtt{s}}(u)]t + \mathbb{E}[(\Lambda^{\mathtt{s}}(u))^2]t^2$. Similarly, $\mathbb{E}^2[\mathcal{B}^{\mathtt{s}}_u(t)]$ can be written as $\mathcal{B}^2_{\max} - 2\mathcal{B}_{\max}\mathbb{E}[\Lambda^{\mathtt{s}}(u)]t + \mathbb{E}^2[\Lambda^{\mathtt{s}}(u)]t^2$. Therefore, it follows that, $Var[\mathcal{B}^{\mathtt{s}}_u(t)] = (\mathbb{E}[(\Lambda^{\mathtt{s}}(u))^2] - \mathbb{E}^2[\Lambda^{\mathtt{s}}(u)])\,t^2$. Given that $\mathbb{E}[(\Lambda^{\mathtt{s}}(u))^2] - \mathbb{E}^2[\Lambda^{\mathtt{s}}(u)] = Var[\Lambda^{\mathtt{s}}(u)]$, then $Var[\mathcal{B}^{\mathtt{s}}_u(t)] = Var[\Lambda^{\mathtt{s}}(u)]t^2$. Using Equation (C.4), $Var[\mathcal{B}^{\mathtt{s}}_u(\mathcal{T}(\mathtt{s}))] = Var[\Lambda^{\mathtt{s}}(u)]\mathcal{T}(\mathtt{s})^2 = Var[\Lambda^{\mathtt{s}}(u)]\left(\frac{\mathcal{B}_{\max}}{\Lambda^{\mathtt{s}}(s)}\right)^2 = \mathcal{B}^2_{\max}\frac{Var[\Lambda^{\mathtt{s}}(u)]}{(\Lambda^{\mathtt{s}}(s))^2}$.

A.5 Proof of Theorem 2

In the proof of Theorem 1, it was shown that $\mathbb{E}[\Lambda^{\mathtt{s}}(u)] = \frac{ml^m-n}{n(l-1)}\lambda$.
$\mathbb{E}[(\Lambda^{\mathtt{s}}(u))^2] = \frac{1}{n}\sum_{u\in V(\mathbb{G})}\Lambda^{\mathtt{s}}(u)$ and, by changing the notation, the latter can be written as $\frac{1}{n}\sum_{i=0}^{m-1}\sum_{j=1}^{l^i}\Lambda_i^2$, or $\frac{1}{n}\sum_{i=0}^{m-1} l^i\Lambda_i^2$. As shown in the proof of Lemma 2, $\Lambda_i = \frac{l^{m-i}-1}{l-1}\lambda$. Consequently, $\mathbb{E}[(\Lambda^{\mathtt{s}}(u))^2] = \frac{1}{n}\sum_{i=0}^{m-1} l^i\frac{(l^{m-i}-1)^2}{(l-1)^2}\lambda^2 = \frac{1}{n}\sum_{i=0}^{m-1} l^i\frac{l^{2m-2i}-2l^{m-i}+1}{(l-1)^2}\lambda^2 = \frac{1}{n}\sum_{i=0}^{m-1}\frac{l^{2m-i}-2l^m+l^i}{(l-1)^2}\lambda^2 = \frac{\sum_{i=0}^{m-1} l^{2m-i}-2\sum_{i=0}^{m-1} l^m+\sum_{i=0}^{m-1} l^i}{n(l-1)^2}\lambda^2$.

Given that $n = \sum_{i=0}^{m-1} l^i$, $\mathbb{E}[(\Lambda^{\mathtt{s}}(u))^2] = \frac{l^m\sum_{i=0}^{m-1} l^{m-i}-2ml^m+n}{n(l-1)^2}\lambda^2$.
Note that $\sum_{i=0}^{m-1} l^{m-i} = l^m + l^{m-1} + \cdots + l^2 + l = \sum_{i=0}^{m-1} l^{i+1} = l\sum_{i=0}^{m-1} l^i = ln$. Therefore, $\mathbb{E}[(\Lambda^{\mathtt{s}}(u))^2] = \frac{nl^{m+1}-2ml^m+n}{n(l-1)^2}\lambda^2$. On the other hand, $Var[\Lambda^{\mathtt{s}}(u)] = \mathbb{E}[(\Lambda^{\mathtt{s}}(u))^2] -$

$\mathbb{E}^2[\Lambda^{\mathtt{s}}(u)] = \frac{nl^{m+1}-2ml^m+n}{n(l-1)^2}\lambda^2 - \left(\frac{ml^m-n}{n(l-1)}\lambda\right)^2 = \frac{n^2l^{m+1}-2nml^m+n^2-(ml^m-n)^2}{n^2(l-1)^2}\lambda^2 = \frac{n^2l^{m+1}-2nml^m+n^2-m^2l^{2m}+2nml^m-n^2}{n^2(l-1)^2}\lambda^2 = \frac{n^2l^{m+1}-m^2l^{2m}}{n^2(l-1)^2}\lambda^2$. It was shown in the proof of Theorem 1 that $m = \log_l(n(l-1)+1)$ and $l^m = n(l-1)+1$. Therefore, $Var[\Lambda^{\mathtt{s}}(u)] = (n(l-1)+1)\,\frac{n^2l-(n(l-1)+1)\log_l^2(n(l-1)+1)}{n^2(l-1)^2}\lambda^2$.

As also shown in the proof of Theorem 1, $\Lambda^{\mathtt{s}}(s) = n\lambda$ and substituting it in the previous expression yields $\frac{Var[\Lambda^{\mathtt{s}}(u)]}{(\Lambda^{\mathtt{s}}(s))^2} =$
$(n(l-1)+1)\,\frac{n^2l-(n(l-1)+1)\log_l^2(n(l-1)+1)}{n^4(l-1)^2}$.

A.6 Proof of Corollary 2

For the case of the 2-ary (i.e., binary) tree, it is sufficient to substitute $l = 2$ into the expression of Theorem 2, i.e., $\frac{Var[\Lambda^{\mathtt{s}}(u)]}{(\Lambda^{\mathtt{s}}(s))^2} = (n+1)\frac{2n^2-(n+1)\log_2^2(n+1)}{n^4}$. The latter expression can be written as $\frac{2(n+1)n^2}{n^4} - \frac{(n+1)^2\log_2^2(n+1)}{n^4}$. Given that for high values of n, $n+1 \approx n$, the previous expression is written as $\frac{2n^3}{n^4} - \frac{n^2\log_2^2(n)}{n^4} = \frac{2}{n} - \frac{\log_2^2(n)}{n^2}$. Thus, for high values of n, $\frac{2}{n} - \frac{\log_2^2(n)}{n^2} \to \frac{2}{n}$.

For the complete graph, as shown in the proof of Corollary 1, $l = n-1$ and substituting into Theorem 2, $\frac{Var[\Lambda^{\mathtt{s}}(u)]}{(\Lambda^{\mathtt{s}}(s))^2} =$
$(n(n-2)+1)\,\frac{n^2(n-1)-(n(n-2)+1)\log_{n-1}^2(n(n-2)+1)}{n^4(n-2)^2} =$
$(n-1)^2\frac{n^2(n-1)-(n-1)^2\log_{n-1}^2(n-1)^2}{n^4(n-2)^2} = (n-1)^2\frac{n^2(n-1)-4(n-1)^2}{n^4(n-2)^2} =$
$(n-1)^3\frac{n^2-4(n-1)}{n^4(n-2)^2} = (n-1)^3\frac{(n-2)^2}{n^4(n-2)^2} = \frac{(n-1)^3}{n^4}$. For high values of n, $n-1 \approx n$, and therefore, $\frac{(n-1)^3}{n^4} \approx \frac{n^3}{n^4} = \frac{1}{n}$.

A.7 Proof of Theorem 3

The starting point is $\mathcal{E}(\mathtt{s}_1) < \mathcal{E}(\mathtt{s}_2) \overset{\text{Equation (D.6)}}{\Leftrightarrow} \sum_{u\in V}\lambda_u\,(\mathtt{d}(\mathtt{s}_1(u),\mathtt{s}_1) -$
$\mathtt{d}(\mathtt{s}_1(u),\mathtt{s}_2)) < 0$. Three sets of nodes ($X$, Y, Φ) are defined such that $X = \{u : \mathtt{d}(u,\mathtt{s}_2(u)) = \mathtt{d}(u,\mathtt{s}_1(u)) + \mathtt{d}(\mathtt{s}_1(u),\mathtt{s}_2(u)\}$, $Y = \{u : \mathtt{d}(u,\mathtt{s}_1(u)) = \mathtt{d}(u,\mathtt{s}_2(u)) + \mathtt{d}(\mathtt{s}_1(u),\mathtt{s}_2(u)\}$, and $\Phi = \{u : \mathtt{d}(u,\mathtt{s}_1(u)) \le \mathtt{d}(u,\mathtt{s}_2(u)) + \mathtt{d}(\mathtt{s}_1(u),$
$\mathtt{s}_2(u)) \wedge \mathtt{d}(u,\mathtt{s}_2(u)) \le \mathtt{d}(u,\mathtt{s}_1(u)) + \mathtt{d}(\mathtt{s}_1(u),\mathtt{s}_2(u)\}$. Obviously, $X \cup Y \cup \Phi = V(\mathbb{G})$ and the three sets have no common elements. Note that $u \in X$, $\mathtt{d}(u,\mathtt{s}_1(u)) - \mathtt{d}(u,\mathtt{s}_2(u)) = -\mathtt{d}(\mathtt{s}_1(u),\mathtt{s}_2(u)$ and $u \in Y$, $\mathtt{d}(u,\mathtt{s}_1(u)) - \mathtt{d}(u,\mathtt{s}_2(u)) = \mathtt{d}(\mathtt{s}_1(u),\mathtt{s}_2(u)$. Therefore, it holds that $\sum_{u\in V}\lambda_u\,(\mathtt{d}(u,\mathtt{s}_1(u)) -$
$\mathtt{d}(u,\mathtt{s}_2(u))) = \sum_{u\in X} -\lambda_u\mathtt{d}(\mathtt{s}_1(u),\mathtt{s}_2(u)) + \sum_{u\in Y}\lambda_u\mathtt{d}(\mathtt{s}_1(u),\mathtt{s}_2(u) +$
$\sum_{u\in\Phi}\lambda_u\,(\mathtt{d}(u,\mathtt{s}_1(u)) - \mathtt{d}(u,\mathtt{s}_2(u)))$. Eventually, $\mathcal{E}(\mathtt{s}_1(u)) < \mathcal{E}(\mathtt{s}_2(u))$ is satisfied if,

$$\sum_{u\in Y}\lambda_u - \sum_{u\in X}\lambda_u < \frac{\sum_{u\in\Phi}\left(\mathtt{d}(u,\mathtt{s}_2(u)) - \mathtt{d}(u,\mathtt{s}_1(u))\right)\lambda_u}{\mathtt{d}(\mathtt{s}_1(u),\mathtt{s}_2(u))}. \tag{A.1}$$

$\mathbb{E}[\Lambda^{\mathtt{s}_1}(u)] < \mathbb{E}[\Lambda^{\mathtt{s}_2}(u)]$ is satisfied when $\sum_{u\in V(\mathbb{G})}\left(\Lambda^{\mathtt{s}_1}(u) - \Lambda^{\mathtt{s}_2}(u)\right) < 0$ is also satisfied. For any node $u \in X$, the corresponding data packets sent toward sink node $\mathtt{s}_2(u)$ have to travel an additional distance compared to $\mathtt{s}_1(u)$ (being the sink node), over path $Z_{\mathtt{s}_1(u)\to\mathtt{s}_2(u)} = \{\mathtt{s}_1(u), \ldots, \mathtt{s}_2(u)\}$, thus, forcing each node over this path to forward the additional (on average) λ_u data packets. Eventually, any node $u \in X$ is responsible for decreasing $\sum_{u\in V(\mathbb{G})}\left(\Lambda^{\mathtt{s}_1}(u) - \Lambda^{\mathtt{s}_2}(u)\right)$ by $|Z_{\mathtt{s}_1(u)\to\mathtt{s}_2(u)}|\lambda_u$. On the other hand, any node $u \in Y$ is responsible for increasing the previous difference by $|Z_{\mathtt{s}_1(u)\to\mathtt{s}_2(u)}|\lambda_u$. Also, any node $u \in \Phi$ increases $\sum_{u\in V(\mathbb{G})}\left(\Lambda^{\mathtt{s}_1}(u) - \Lambda^{\mathtt{s}_2}(u)\right)$ by $|\Phi_{u\to\mathtt{s}_1(u)}|\lambda_u$ and decreases it by $|\Phi_{u\to\mathtt{s}_2(u)}|\lambda_u$, where $|\Phi_{u\to\mathtt{s}_1(u)}|$ is the set of nodes over path $\{u, \ldots, \mathtt{s}_1(u)\}$, and $|\Phi_{u\to\mathtt{s}_2(u)}|$ is the set of nodes over path $\{u, \ldots, \mathtt{s}_2(u)\}$. Eventually, it holds that $\sum_{u\in V(\mathbb{G})}\left(\Lambda^{\mathtt{s}_1}(u) - \Lambda^{\mathtt{s}_2}(u)\right) =$
$-\sum_{u\in X}|Z_{\mathtt{s}_1(u)\to\mathtt{s}_2(u)}|\lambda_u + \sum_{u\in Y}|Z_{\mathtt{s}_1(u)\to\mathtt{s}_2(u)}|\lambda_u +$
$\sum_{u\in\Phi}\left(|\Phi_{u\to\mathtt{s}_1(u)}| - |\Phi_{u\to\mathtt{s}_2(u)}|\right)\lambda_u$.
Therefore, for $\mathbb{E}[\Lambda^{\mathtt{s}_1}(u)] < \mathbb{E}[\Lambda^{\mathtt{s}_2}(u)]$ to hold, it is sufficient to have

$$\sum_{u\in Y}\lambda_u - \sum_{u\in X}\lambda_u < \frac{\sum_{u\in\Phi}\left(|\Phi_{u\to\mathtt{s}_2(u)}| - |\Phi_{u\to\mathtt{s}_1(u)}|\right)\lambda_u}{|Z_{\mathtt{s}_1(u)\to\mathtt{s}_2(u)}|}. \tag{A.2}$$

Now, given that $\mathtt{d}(\mathtt{s}_1(u), \mathtt{s}_2(u)$ is the distance of a shortest path between sink node $\mathtt{s}_1(u)$ and sink node $\mathtt{s}_2(u)$, then $|Z_{\mathtt{s}_1(u)\to\mathtt{s}_2(u)}|$ is the number of nodes between sink node $\mathtt{s}_1(u)$ and sink node $\mathtt{s}_2(u)$ over the particular shortest path. Furthermore, $\mathtt{d}(u, \mathtt{s}_1(u))$ and $\mathtt{d}(u, \mathtt{s}_2(u))$ correspond to the distance between nodes u and $\mathtt{s}_1(u), \mathtt{s}_2(u)$ over the said shortest path, respectively. Finally, $|\Phi_{u\to\mathtt{s}_1(u)}|$ and $|\Phi_{u\to\mathtt{s}_2(u)}|$ correspond to the number of nodes over this shortest path. Given that link weights are equal (and normalized to unity), the right terms of both conditions of equations (A.1) and (A.2), are equivalent and the hypothesis is proved.

A.8 Proof of Lemma 5

Assuming that node u is the first node to exhaust its battery, then $\mathcal{B}_u^{\mathtt{s}}(\mathcal{T}(\mathtt{s})) = 0$. On average, $\mathbb{E}[\Lambda^{\mathtt{s}}(s)] = \mathbb{E}[\sum_{v\in V(\mathbb{G})}\lambda_v] = n\mathbb{E}[\lambda_u] = 1/2$. Given Equation (D.7), $0 = 1 - 6/5\frac{1}{2}r_c^3\mathcal{T}(\mathtt{s})$, then finally, $\mathcal{T}(\mathtt{s}) = \frac{5}{3r_c^3}$. Regarding the mean energy of $\mathcal{B}_u^{\mathtt{s}}(\mathcal{T}(\mathtt{s}))$, it is sufficient to derive the particular value of $\mathbb{E}[\Lambda^{\mathtt{s}}(u)]$. In the proof of Theorem 1, it was shown that $\mathbb{E}[\Lambda^{\mathtt{s}}(u)] = \frac{(n(l-1)+1)\log_l(n(l-1)+1)-n}{n(l-1)}\lambda$. Setting $\lambda = \mathbb{E}[\lambda_u] = \frac{1}{2n}$ and $l = 2$ (note that this topology corresponds to $r_c = 0.06$ which is a topology of reduced number of links and a large diameter and therefore a binary tree can be a good approximation as opposed to any other value of $l > 2$), $\mathbb{E}[\Lambda^{\mathtt{s}}(u)] = \frac{(n+1)\log_2(n+1)-n}{2n^2}$. Given Equation (D.7), then the mean energy is given by $\mathbb{E}[\mathcal{B}_u^{\mathtt{s}}(\mathcal{T}(\mathtt{s}))] = 1 - 6/5\frac{(n+1)\log_2(n+1)-n}{2n^2}r_c^3\mathcal{T}(\mathtt{s})$.

A.9 Proof of Corollary 4

Assume that $\mathtt{s}_{\mathcal{D}} \neq \mathtt{s}_{\mathcal{E}}$. For the first part, it is known by Theorem 4 that $\mathbb{E}[\Lambda^{\mathtt{s}_{\mathcal{D}}}(u)] < \mathbb{E}[\Lambda^{\mathtt{s}_{\mathcal{E}}}(u)]$. By the hypothesis, $\mathbb{E}[\Lambda^{\mathtt{s}_{\mathcal{E}}}(u)] = \mathbb{E}[\Lambda^{\mathtt{s}_{\mathcal{E}}}(u)]$ and therefore, $\mathbb{E}[\Lambda^{\mathtt{s}_{\mathcal{D}}}(u)] < \mathbb{E}[\Lambda^{\mathtt{s}_{\mathcal{E}}}(u)]$. By definition (see Eq. (E.7)), $\mathbb{E}[\Lambda^{\mathtt{s}}(u)] \geq \mathbb{E}[\Lambda^{\mathtt{s}}(u)]$, and consequently, $\mathbb{E}[\Lambda^{\mathtt{s}_{\mathcal{D}}}(u)] < \mathbb{E}[\Lambda^{\mathtt{s}_{\mathcal{E}}}(u)]$. However, the latter contradicts Theorem 3 and therefore, $\mathtt{s}_{\mathcal{E}} \equiv \mathtt{s}_{\mathcal{D}}$. For the second part and given that $\mathbb{E}[\Lambda^{\mathtt{s}}(u)] \geq \mathbb{E}[\Lambda^{\mathtt{s}}(u)]$, it is derived that $\mathbb{E}[\Lambda^{\mathtt{s}_{\mathcal{E}}}(u)] \leq \mathbb{E}[\Lambda^{\mathtt{s}_{\mathcal{D}}}(u)]$, which contradicts Theorem 4.

Appendix B

Simulation Details

In all simulation parts of this thesis, the considered scenarios were implemented in OMNeT++ (Objective Modular Network Testbed in C++) simulator; thus it is necessary to make a special mention to its main features. OMNeT++ simulator is a modular, component-based C/C++ simulation library and framework, primarily for building network simulators. It has been developed by András Varga at the Technical University of Budapest, Department of Telecommunications (BME-HIT), his first related work being published in 1999 in his paper called 'Using the OMNeT++ discrete event simulation system in education' [165]. OMNeT++, being a discrete event simulation platform, bases its operation on a discrete sequence of events in time. Moving from one event to another depends on the messages exchanged between the modules consisting it, while no changes in the system are assumed between consecutive events.

A model (e.g., a wireless network model) created in OMNeT++ consists of modules that communicate with each other by exchanging messages. Modules can be either simple, that is one module representing a model's component, or compound where a component consists of many nested simple modules. For example, a compound module can represent a node that consists of nested simple modules each one adding functionality to the node based on the protocol stack layer presented in Section A.1 (e.g., application layer, network layer, etc.).

The model structure in OMNeT++ is defined in *NED* (NEtwork Description) programming language. The latter's features [166] include: (i) hierarchical, typed module structure (e.g., compound module type can be written once, and then several instances of it can be created); (ii) flexible topology description (e.g., NED's parameters can define: the number of submodules, the submodule types and the interconnection structure); (iii) parameters features (e.g., parameters may contain random variables, thus making them available for use as a source of random numbers generation) and (iv) partitioning of the model for parallel execution. After complet-

ing the model designing procedure under the NED language, the simple modules consisting the model (either if they represent a component themselves or they are part of a compound module) described there can be programmed in C++, using the simulation kernel and class library, in order to acquire the desired functionality.

In addition, the OMNeT++ configuration and parameters of the designed model are held by the configuration file, usually called 'omnetpp.ini'. This file is an ASCII text file (non-ASCII characters are permitted in comments and string literals) and it can describe several simulation runs with different parameters.

For this thesis, three projects were implemented in OMNeT++ for simulation purposes, one project for simulating the scenarios related to the energy efficient sink placement approach and two projects for simulating the scenarios regarding the proposed recharging policies. Nodes and mobile rechargers, along with the networks containing them, implemented in OMNeT++, consist of all the characteristics described in the thesis, in the specific sections (see Section D.3 and Section E.3). Note that for the implementation of some of the projects (i.e., the projects for simulating scenarios related to (i) the energy efficient sink placement and (ii) the second proposed policy), an additional framework was used alongside OMNeT++ libraries, the so-called INET [163] framework. Most implemented features in INET have been largely used by the scientific community, so applying them to this thesis simulation, allows for 'safer' results and easier future implementation by interested researchers. The most significant INET's implemented modules used here are (i) CSMA/CA module that was added to nodes (nodes were designed in a compound module nature), thus implementing CSMA/CA MAC protocol with acknowledgments and this specific MAC's retry mechanism and (ii) mobility module that was added to the mobile rechargers so as to measure the results regarding their mobility aspects (e.g., distance traveled) and add essential characteristics to them (e.g., velocity).

Bibliography

[1] I.F. Akyildiz, W. Su, Y. Sankarasubramaniam, and E. Cayirci, "Wireless sensor networks: a survey", *Computer networks*, vol. 38, no. 4, pp. 393–422, 2002.

[2] I.F. Akyildiz, T. Melodia, and K.R. Chowdhury, "A survey on wireless multimedia sensor networks", *Computer networks*, vol. 51, no. 4, pp. 921–960, 2007.

[3] Constantinos Marios Angelopoulos, Sotiris Nikoletseas, and Theofanis P. Raptis, "Wireless energy transfer in sensor networks with adaptive, limited knowledge protocols", *Computer Networks*, vol. 70, pp. 113–141, 2014.

[4] Guangjie Han, Aihua Qian, Jinfang Jiang, Ning Sun, and Li Liu, "A grid-based joint routing and charging algorithm for industrial wireless rechargeable sensor networks", *Computer Networks*, vol. 101, pp. 19–28, 2016, Industrial Technologies and Applications for the Internet of Things.

[5] Liang He, Yu Gu, Jianping Pan, and Ting Zhu, "On-demand Charging in Wireless Sensor Networks: Theories and Applications", in *Proceedings of the 2013 IEEE 10th International Conference on Mobile Ad-Hoc and Sensor Systems*, ser. MASS '13, Washington, DC, USA: IEEE Computer Society, 2013, pp. 28–36.

[6] André Kurs, Aristeidis Karalis, Robert Moffatt, J. D. Joannopoulos, Peter Fisher, and Marin Soljacic, "Wireless Power Transfer via Strongly Coupled Magnetic Resonances", *Science*, vol. 317, no. 5834, pp. 83–86, Jul. 2007.

[7] O. Jonah and S.V. Georgakopoulos, "Wireless Power Transfer in Concrete via Strongly Coupled Magnetic Resonance", *IEEE Transactions on Antennas and Propagation*, vol. 61, no. 3, pp. 1378–1384, Mar. 2013.

[8] Luís ML Oliveira and Joel JPC Rodrigues, "Wireless Sensor Networks: A Survey on Environmental Monitoring.", *JCM*, vol. 6, no. 2, pp. 143–151, 2011.

[9] Peter Corke, Tim Wark, Raja Jurdak, Wen Hu, Philip Valencia, and Darren Moore, "Environmental wireless sensor networks", *Proceedings of the IEEE*, vol. 98, no. 11, pp. 1903–1917, 2010.

[10] Kay Soon Low, Win Nu Nu Win, and Meng Joo Er, "Wireless sensor networks for industrial environments", in *null*, IEEE, 2005, pp. 271–276.

[11] Gang Zhao, "Wireless sensor networks for industrial process monitoring and control: A survey", *Network Protocols and Algorithms*, vol. 3, no. 1, pp. 46–63, 2011.

[12] Levente Buttyán, Dennis Gessner, Alban Hessler, and Peter Langendoerfer, "Application of wireless sensor networks in critical infrastructure protection: challenges and design options [Security and Privacy in Emerging Wireless Networks]", *IEEE Wireless Communications*, vol. 17, no. 5, 2010.

[13] Cristina Alcaraz and Sherali Zeadally, "Critical infrastructure protection: Requirements and challenges for the 21st century", *International journal of critical infrastructure protection*, vol. 8, pp. 53–66, 2015.

[14] Guan Hua, Yan-Xiao Li, and Xiao-Mei Yan, "Research on the wireless sensor networks applied in the battlefield situation awareness system", in *Advanced research on electronic commerce, web application, and communication*, Springer, 2011, pp. 443–449.

[15] Tatiana Bokareva, Wen Hu, Salil Kanhere, Branko Ristic, Neil Gordon, Travis Bessell, Mark Rutten, and Sanjay Jha, "Wireless sensor networks for battlefield surveillance", in *Proceedings of the land warfare conference*, 2006, pp. 1–8.

[16] Anthony D Wood, John A Stankovic, Gilles Virone, *et al.*, "Context-aware wireless sensor networks for assisted living and residential monitoring", *IEEE network*, vol. 22, no. 4, 2008.

[17] Nagender Kumar Suryadevara, Subhas Chandra Mukhopadhyay, Sean Dieter Tebje Kelly, and Satinder Pal Singh Gill, "WSN-based smart sensors and actuator for power management in intelligent buildings", *IEEE/ASME transactions on mechatronics*, vol. 20, no. 2, pp. 564–571, 2015.

[18] Tifenn Rault, Abdelmadjid Bouabdallah, and Yacine Challal, "Energy efficiency in wireless sensor networks: A top-down survey", *Computer Networks*, vol. 67, pp. 104–122, 2014.

[19] http://www.zigbee.org/, *ZigBee Alliance*, [Online; accessed 30-June-2018], 2018.

[20] https://fieldcommgroup.org/technologies/hart/hart-technology, *WirelessHART - How it works*, [Online; accessed 30-June-2018], 2018.

[21] https://www.isa.org/, *Wireless Systems for Automation*, [Online; accessed 30-June-2018], 2018.

[22] Carles Gomez, Joaquim Oller, and Josep Paradells, "Overview and evaluation of bluetooth low energy: An emerging low-power wireless technology", *Sensors*, vol. 12, no. 9, pp. 11 734–11 753, 2012.

[23] http://www.ieee802.org/15/pub/TG6.html, *IEEE 802.15 Task Group 6*, [Online; accessed 30-June-2018], 2018.

[24] https://datatracker.ietf.org/wg/6lowpan/charter/, *IPv6 over Low power WPAN (6lowpan)*, [Online; accessed 30-June-2018], 2018.

[25] https://datatracker.ietf.org/wg/roll/charter/, *Routing Over Low power and Lossy networks (roll)*, [Online; accessed 30-June-2018], 2018.

[26] Priyanka Rawat, Kamal Deep Singh, Hakima Chaouchi, and Jean Marie Bonnin, "Wireless sensor networks: a survey on recent developments and potential synergies", *The Journal of supercomputing*, vol. 68, no. 1, pp. 1–48, 2014.

[27] Chiara Buratti, Andrea Conti, Davide Dardari, and Roberto Verdone, "An overview on wireless sensor networks technology and evolution", *Sensors*, vol. 9, no. 9, pp. 6869–6896, 2009.

[28] Eirini Karapistoli, Fotini-Niovi Pavlidou, Ioannis Gragopoulos, and Ioannis Tsetsinas, "An overview of the IEEE 802.15. 4a standard", *IEEE Communications Magazine*, vol. 48, no. 1, 2010.

[29] Khalid El Gholami, Kun-mean Hou, and Najib Elkamoun, "Enhanced superframe structure of the IEEE802. 15.4 standard for real-time data transmission in star network", *International Journal of Computer Applications*, vol. 51, no. 15, pp. 26–32, 2012.

[30] https://wsnet.files.wordpress.com/2006/08/zigbee-faq.pdf, *ZigBee FAQ*, [Online; accessed 04-July-2018], 2018.

[31] Jianping Song, Song Han, Al Mok, Deji Chen, Mike Lucas, Mark Nixon, and Wally Pratt, "WirelessHART: Applying wireless technology in real-time industrial process control", in *IEEE real-time and embedded technology and applications symposium*, IEEE, 2008, pp. 377–386.

[32] Hisanori Hayashi, Toshi Hasegawa, and Koji Demachi, "Wireless technology for process automation", in *ICCAS-SICE, 2009*, IEEE, 2009, pp. 4591–4594.

[33] Hend Fourati, Sabri Khssibi, Thierry Val, Hanen Idoudi, Adrien Van Den Bossche, and Leila Azzouz Saidane, "Comparative study of IEEE 802.15. 4 and IEEE 802.15. 6 for WBAN-based CANet", in *4th Performance Evaluation and Modeling in Wireless Networks (PEMWN 2015)*, 2015, pp–1.

[34] https://www.lsr.com/white-papers/zigbee-vs-6lowpan-for-sensor-networks, *ZigBee VS 6LoWPAN for Sensor Networks*, [Online; accessed 03-July-2018], 2018.

[35] David Waitzman, Craig Partridge, and Stephen E Deering, "Distance vector multicast routing protocol", Tech. Rep., 1988.

[36] Finn V Jensen, *An introduction to Bayesian networks*. UCL press London, 1996, vol. 210.

[37] G. Anastasi, M. Conti, M. Di Francesco, and A. Passarella, "Energy conservation in wireless sensor networks: A survey", *Ad Hoc Networks*, vol. 7, no. 3, pp. 537–568, 2009.

[38] Nikolaos A Pantazis, Stefanos A Nikolidakis, and Dimitrios D Vergados, "Energy-efficient routing protocols in wireless sensor networks: A survey", *IEEE Communications surveys & tutorials*, vol. 15, no. 2, pp. 551–591, 2013.

[39] Ilker Demirkol, Cem Ersoy, Fatih Alagoz, *et al.*, "MAC protocols for wireless sensor networks: a survey", *IEEE Communications Magazine*, vol. 44, no. 4, pp. 115–121, 2006.

[40] Tifenn Rault, Abdelmadjid Bouabdallah, and Yacine Challal, "Energy efficiency in wireless sensor networks: A top-down survey", *Computer Networks*, vol. 67, pp. 104–122, 2014.

[41] Nojeong Heo and Pramod K Varshney, "Energy-efficient deployment of intelligent mobile sensor networks", *IEEE Transactions on Systems, Man, and Cybernetics-Part A: Systems and Humans*, vol. 35, no. 1, pp. 78–92, 2005.

[42] Ines Khoufi, Pascale Minet, Anis Laouiti, and Saoucene Mahfoudh, "Survey of deployment algorithms in wireless sensor networks: coverage and connectivity issues and challenges", *International Journal of Autonomous and Adaptive Communications Systems*, vol. 10, no. 4, pp. 341–390, 2017.

[43] Davood Izadi, Jemal Abawajy, and Sara Ghanavati, "An alternative node deployment scheme for WSNs", *IEEE Sensors Journal*, vol. 15, no. 2, pp. 667–675, 2015.

[44] Sudip Misra, Manikonda Pavan Kumar, and Mohammad S Obaidat, "Connectivity preserving localized coverage algorithm for area monitoring using wireless sensor networks", *Computer communications*, vol. 34, no. 12, pp. 1484–1496, 2011.

[45] Abdelmalik Bachir, Walid Bechkit, Yacine Challal, and Abdelmadjid Bouabdallah, "Temperature-aware density optimization for low power wireless sensor networks", *IEEE Communications Letters*, vol. 17, no. 2, pp. 325–328, 2013.

[46] Ossama Younis, Marwan Krunz, and Srinivasan Ramasubramanian, "Node clustering in wireless sensor networks: recent developments and deployment challenges", *IEEE network*, vol. 20, no. 3, pp. 20–25, 2006.

[47] Wendi Rabiner Heinzelman, Anantha Chandrakasan, and Hari Balakrishnan, "Energy-efficient communication protocol for wireless microsensor networks", in *System sciences, 2000. Proceedings of the 33rd annual Hawaii international conference on*, IEEE, 2000, 10–pp.

[48] Xu Xu and Weifa Liang, "Placing optimal number of sinks in sensor networks for network lifetime maximization", in *Communications (ICC), 2011 IEEE International Conference on*, IEEE, 2011, pp. 1–6.

[49] Mianxiong Dong, Kaoru Ota, and Anfeng Liu, "RMER: Reliable and energy-efficient data collection for large-scale wireless sensor networks", *IEEE Internet of Things Journal*, vol. 3, no. 4, pp. 511–519, 2016.

[50] Xiao-Yang Liu, Yanmin Zhu, Linghe Kong, Cong Liu, Yu Gu, Athanasios V Vasilakos, and Min-You Wu, "CDC: Compressive data collection for wireless sensor networks", *IEEE Transactions on Parallel & Distributed Systems*, no. 1, pp. 1–1, 2015.

[51] Mario Di Francesco, Sajal K Das, and Giuseppe Anastasi, "Data collection in wireless sensor networks with mobile elements: A survey", *ACM Transactions on Sensor Networks (TOSN)*, vol. 8, no. 1, p. 7, 2011.

[52] Jian Zhang, Jian Tang, Tianbao Wang, and Fei Chen, "Energy-efficient data-gathering rendezvous algorithms with mobile sinks for wireless sensor networks", *International Journal of Sensor Networks*, vol. 23, no. 4, pp. 248–257, 2017.

[53] Halil Yetgin, Kent Tsz Kan Cheung, Mohammed El-Hajjar, and Lajos Hanzo Hanzo, "A survey of network lifetime maximization techniques in wireless sensor networks", *IEEE Communications Surveys & Tutorials*, vol. 19, no. 2, pp. 828–854, 2017.

[54] Wei Ye, John Heidemann, and Deborah Estrin, "Medium access control with coordinated adaptive sleeping for wireless sensor networks", *IEEE/ACM Transactions on Networking (ToN)*, vol. 12, no. 3, pp. 493–506, 2004.

[55] Sujesha Sudevalayam and Purushottam Kulkarni, "Energy harvesting sensor nodes: Survey and implications", *IEEE Communications Surveys & Tutorials*, vol. 13, no. 3, pp. 443–461, 2011.

[56] Faisal Karim Shaikh and Sherali Zeadally, "Energy harvesting in wireless sensor networks: A comprehensive review", *Renewable and Sustainable Energy Reviews*, vol. 55, pp. 1041–1054, 2016.

[57] Jian Li and Prasant Mohapatra, "Analytical Modeling and Mitigation Techniques for the Energy Hole Problem in Sensor Networks", *Pervasive Mob. Comput.*, vol. 3, no. 3, pp. 233–254, Jun. 2007.

[58] An-Feng Liu, Peng-Hui Zhang, and Zhi-Gang Chen, "Theoretical analysis of the lifetime and energy hole in cluster based wireless sensor networks", *Journal of Parallel and Distributed Computing*, vol. 71, no. 10, pp. 1327–1355, 2011.

[59] Cian Mathuna, Terence O'Donnell, Rafael V. Martinez-Catala, James Rohan, and Brendan O'Flynn, "Energy scavenging for long-term deployable wireless sensor networks", *Talanta*, vol. 75, no. 3, pp. 613–623, 2008, Special Section: Remote Sensing.

[60] Mohamed Younis and Kemal Akkaya, "Strategies and techniques for node placement in wireless sensor networks: A survey", *Ad Hoc Networks*, vol. 6, no. 4, pp. 621–655, 2008.

[61] E.L. Lloyd and Guoliang Xue, "Relay Node Placement in Wireless Sensor Networks", *IEEE Transactions on Computers*, vol. 56, no. 1, pp. 134–138, Jan. 2007.

[62] Y.T. Hou, Yi Shi, H.D. Sherali, and S.F. Midkiff, "On energy provisioning and relay node placement for wireless sensor networks", *IEEE Transactions on Wireless Communications*, vol. 4, no. 5, pp. 2579–2590, Sep. 2005.

[63] Subir Halder and Sipra Das Bit, "Enhancement of wireless sensor network lifetime by deploying heterogeneous nodes", *Journal of Network and Computer Applications*, vol. 38, no. 0, pp. 106–124, 2014.

[64] Yuanzhu Chen, AL. Liestman, and Jiangchuan Liu, "A hierarchical energy-efficient framework for data aggregation in wireless sensor networks", *IEEE Transactions on Vehicular Technology*, vol. 55, no. 3, pp. 789–796, May 2006.

[65] Hashim A Hashim, Babajide Odunitan Ayinde, and Mohamed A Abido, "Optimal placement of relay nodes in wireless sensor network using artificial bee colony algorithm", *Journal of Network and Computer Applications*, vol. 64, pp. 239–248, 2016.

[66] Rizwan Akhtar, Supeng Leng, Imran Memon, Mushtaq Ali, and Liren Zhang, "Architecture of hybrid mobile social networks for efficient content delivery", *Wireless Personal Communications*, vol. 80, no. 1, pp. 85–96, 2015.

[67] A Efrat, S. Har-Peled, and J.S.B. Mitchell, "Approximation algorithms for two optimal location problems in sensor networks", in *2nd International Conference on Broadband Networks, BroadNets 2005*, Oct. 2005, 714–723 Vol. 1.

[68] A Bogdanov, E. Maneva, and S. Riesenfeld, "Power-aware base station positioning for sensor networks", in *IEEE INFOCOM*, vol. 1, Mar. 2004, pp. 574–585.

[69] E.I Oyman and C. Ersoy, "Multiple sink network design problem in large scale wireless sensor networks", in *IEEE International Conference on Communications*, vol. 6, Jun. 2004, pp. 3663–3667.

[70] Wenzhong Li, E. Chan, M. Hamdi, Sanglu Lu, and Daoxu Chen, "Communication Cost Minimization in Wireless Sensor and Actor Networks for Road Surveillance", *IEEE Transactions on Vehicular Technology*, vol. 60, no. 2, pp. 618–631, Feb. 2011.

[71] M. Emre Keskin, I. Kuban Altinel, Necati Aras, and Cem Ersoy, "Wireless sensor network lifetime maximization by optimal sensor deployment, activity scheduling, data routing and sink mobility", *Ad Hoc Networks*, vol. 17, pp. 18–36, 2014.

[72] Zoltan Vincze, Rolland Vida, and Attila Vidacs, "Deploying Multiple Sinks in Multi-hop Wireless Sensor Networks", in *IEEE International Conference on Pervasive Services*, Jul. 2007, pp. 55–63.

[73] Stefano Basagni, Alessio Carosi, Emanuel Melachrinoudis, Chiara Petrioli, and Z. Maria Wang, "Controlled Sink Mobility for Prolonging Wireless Sensor Networks Lifetime", *Wirel. Netw.*, vol. 14, no. 6, pp. 831–858, Dec. 2008.

[74] Jun Luo and J-P Hubaux, "Joint mobility and routing for lifetime elongation in wireless sensor networks", in *IEEE INFOCOM*, vol. 3, Mar. 2005, 1735–1746 vol. 3.

[75] Guojun Wang, Tian Wang, Weijia Jia, Minyi Guo, and Jie Li, "Adaptive location updates for mobile sinks in wireless sensor networks", English, *The Journal of Supercomputing*, vol. 47, no. 2, pp. 127–145, 2009.

[76] Yi Shi and Y. Thomas Hou, "Some Fundamental Results on Base Station Movement Problem for Wireless Sensor Networks", *IEEE/ACM Trans. Netw.*, vol. 20, no. 4, pp. 1054–1067, Aug. 2012.

[77] I. Papadimitriou and L. L. Georgiadis, "Energy-aware Routing to Maximize Lifetime in Wireless Sensor Networks with Mobile Sink", *IEEE JCOMSS - Special Issue on Future Wireless Systems*, vol. 2, no. 2, pp. 141–151, Jun. 2006.

[78] Jun Luo, Jacques Panchard, Michał Piórkowski, Matthias Grossglauser, and Jean-Pierre Hubaux, "Mobiroute: Routing towards a mobile sink for improving lifetime in sensor networks", in *Sensor Networks in the 2nd IEEE/ACM DCOSS*, Springer Verlag, 2006, pp. 480–497.

[79] Jun Luo and Jean-Pierre Hubaux, "Joint Sink Mobility and Routing to Maximize the Lifetime of Wireless Sensor Networks: The Case of Constrained Mobility", *IEEE/ACM Trans. Netw.*, vol. 18, no. 3, pp. 871–884, Jun. 2010.

[80] Juan Luo, Jinyu Hu, Di Wu, and Renfa Li, "Opportunistic routing algorithm for relay node selection in wireless sensor networks", *IEEE Transactions on Industrial Informatics*, vol. 11, no. 1, pp. 112–121, 2015.

[81] P.B. Mirchandani and R.L. Francis, *Discrete location theory*. John Wiley & Sons, 1990.

[82] G. Smaragdakis, N. Laoutaris, K. Oikonomou, I Stavrakakis, and A Bestavros, "Distributed Server Migration for Scalable Internet Service Deployment", *IEEE/ACM Transactions on Networking*, vol. 22, no. 3, pp. 917–930, Jun. 2014.

[83] Denis Krivitski, Assaf Schuster, and Ran Wolff, "A local facility location algorithm for sensor networks", in *DCOSS '05*, 2005, pp. 368–375.

[84] K. Oikonomou and S. Aïssa, "Dynamic sink assignment for efficient energy consumption in wireless sensor networks", in *IEEE Wireless Communications and Networking Conference (WCNC)*, Apr. 2012, pp. 1876–1881.

[85] Marios Gatzianas, L. Georgiadis, and L. Tassiulas, "Control of wireless networks with rechargeable batteries", *IEEE Transactions on Wireless Communications*, vol. 9, no. 2, pp. 581–593, Feb. 2010.

[86] Weijian Tu, Xianghua Xu, Tingcong Ye, and Zongmao Cheng, "A Study on Wireless Charging for Prolonging the Lifetime of Wireless Sensor Networks", *Sensors*, vol. 17, no. 7, p. 1560, 2017.

[87] Yang Peng, Zi Li, Wensheng Zhang, and Daji Qiao, "Prolonging sensor network lifetime through wireless charging", in *Real-time systems symposium (RTSS), 2010 IEEE 31st*, IEEE, 2010, pp. 129–139.

[88] Cong Wang, Ji Li, Fan Ye, and Yuanyuan Yang, "Netwrap: An ndn based real-timewireless recharging framework for wireless sensor networks", *IEEE Transactions on Mobile Computing*, vol. 13, no. 6, pp. 1283–1297, 2014.

[89] Yi Shi, Liguang Xie, Y Thomas Hou, and Hanif D Sherali, "On renewable sensor networks with wireless energy transfer", in *INFOCOM, 2011 Proceedings IEEE*, IEEE, 2011, pp. 1350–1358.

[90] Zhenquan Qin, Chunting Zhou, Yu Yue, Lei Wang, Liang Sun, and Yuanyuan Zhang, "A practical solution to wireless energy transfer in WSNs", in *ICT Convergence (ICTC), 2013 International Conference on*, IEEE, 2013, pp. 660–665.

[91] Liguang Xie, Yi Shi, Y Thomas Hou, Wenjing Lou, Hanif D Sherali, and Scott F Midkiff, "On renewable sensor networks with wireless energy transfer: The multi-node case", in *Sensor, mesh and ad hoc communications and networks (SECON), 2012 9th annual IEEE communications society conference on*, IEEE, 2012, pp. 10–18.

[92] Miao Zhao, Ji Li, and Yuanyuan Yang, "A framework of joint mobile energy replenishment and data gathering in wireless rechargeable sensor networks", *IEEE Transactions on Mobile Computing*, vol. 13, no. 12, pp. 2689–2705, 2014.

[93] Lingkun Fu, Peng Cheng, Yu Gu, Jiming Chen, and Tian He, "Optimal charging in wireless rechargeable sensor networks", *IEEE Transactions on Vehicular Technology*, vol. 65, no. 1, pp. 278–291, 2016.

[94] Mario Di Francesco, Sajal K Das, and Giuseppe Anastasi, "Data collection in wireless sensor networks with mobile elements: A survey", *ACM Transactions on Sensor Networks (TOSN)*, vol. 8, no. 1, p. 7, 2011.

[95] Liguang Xie, Yi Shi, Y Thomas Hou, Wenjing Lou, Hanif D Sherali, Huaibei Zhou, and Scott F Midkiff, "A mobile platform for wireless charging and data collection in sensor networks", *IEEE Journal on Selected Areas in Communications*, vol. 33, no. 8, pp. 1521–1533, 2015.

[96] Liguang Xie, Yi Shi, Y Thomas Hou, Wenjing Lou, Hanif D Sherali, and Scott F Midkiff, "Bundling mobile base station and wireless energy transfer: Modeling and optimization", in *INFOCOM, 2013 Proceedings IEEE*, IEEE, 2013, pp. 1636–1644.

[97] Zi Li, Yang Peng, Wensheng Zhang, and Daji Qiao, "J-RoC: A joint routing and charging scheme to prolong sensor network lifetime", in *Network Protocols (ICNP), 2011 19th IEEE International Conference on*, IEEE, 2011, pp. 373–382.

[98] Xiao Lu, Ping Wang, Dusit Niyato, Dong In Kim, and Zhu Han, "Wireless charging technologies: Fundamentals, standards, and network applications", *IEEE Communications Surveys & Tutorials*, vol. 18, no. 2, pp. 1413–1452, 2016.

[99] Liguang Xie, Yi Shi, Y Thomas Hou, and Hanif D Sherali, "Making sensor networks immortal: An energy-renewal approach with wireless power transfer", *IEEE/ACM Transactions on networking*, vol. 20, no. 6, pp. 1748–1761, 2012.

[100] Lei Shi, Jianghong Han, Dong Han, Xu Ding, and Zhenchun Wei, "The dynamic routing algorithm for renewable wireless sensor networks with wireless power transfer", *Computer Networks*, vol. 74, pp. 34–52, 2014.

[101] Liguang Xie, Yi Shi, Y Thomas Hou, Wenjing Lou, Hanif D Sherali, and Scott F Midkiff, "Multi-node wireless energy charging in sensor networks", *IEEE/ACM Transactions on Networking (ToN)*, vol. 23, no. 2, pp. 437–450, 2015.

[102] Xiaojiang Ren, Weifa Liang, and Wenzheng Xu, "Maximizing charging throughput in rechargeable sensor networks", in *Computer Communication and Networks (ICCCN), 2014 23rd International Conference on*, IEEE, 2014, pp. 1–8.

[103] Liang He, Lingkun Fu, Likun Zheng, Yu Gu, Peng Cheng, Jiming Chen, and Jianping Pan, "Esync: An energy synchronized charging protocol for rechargeable wireless sensor networks", in *Proceedings of the 15th ACM international symposium on Mobile ad hoc networking and computing*, ACM, 2014, pp. 247–256.

[104] Constantinos Marios Angelopoulos, Sotiris Nikoletseas, and Theofanis P Raptis, "Wireless energy transfer in sensor networks with adaptive, limited knowledge protocols", *Computer Networks*, vol. 70, pp. 113–141, 2014.

[105] Lintong Jiang, Xiaobing Wu, Guihai Chen, and Yuling Li, "Effective on-demand mobile charger scheduling for maximizing coverage in wireless rechargeable sensor networks", *Mobile Networks and Applications*, vol. 19, no. 4, pp. 543–551, 2014.

[106] Liang He, Linghe Kong, Yu Gu, Jianping Pan, and Ting Zhu, "Evaluating the on-demand mobile charging in wireless sensor networks", *IEEE Transactions on Mobile Computing*, vol. 14, no. 9, pp. 1861–1875, 2015.

[107] Hongli Yu, Guilin Chen, Shenghui Zhao, Chih-Yung Chang, and Yu-Ting Chin, "An Efficient Wireless Recharging Mechanism for Achieving Perpetual Lifetime of Wireless Sensor Networks", *Sensors*, vol. 17, no. 1, p. 13, 2016.

[108] Sheng Zhang, Jie Wu, and Sanglu Lu, "Collaborative mobile charging for sensor networks", in *Mobile Adhoc and Sensor Systems (MASS), 2012 IEEE 9th International Conference on*, IEEE, 2012, pp. 84–92.

[109] Sheng Zhang and Jie Wu, "Collaborative mobile charging", in *Wireless Power Transfer Algorithms, Technologies and Applications in Ad Hoc Communication Networks*, Springer, 2016, pp. 505–531.

[110] Haipeng Dai, Xiaobing Wu, Guihai Chen, Lijie Xu, and Shan Lin, "Minimizing the number of mobile chargers for large-scale wireless rechargeable sensor networks", *Computer Communications*, vol. 46, pp. 54–65, 2014.

[111] Yawei Pang, Zaixin Lu, Miao Pan, and W.W. Li, "Charging coverage for energy replenishment in wireless sensor networks", in *11th IEEE International Conference on Networking, Sensing and Control (ICNSC)*, Apr. 2014, pp. 251–254.

[112] Jian Wang, Xiumei Wu, Xiaolin Xu, Yinchun Yang, and Xiaoming Hu, "Programming wireless recharging for target-oriented rechargeable sensor networks", in *11th IEEE International Conference on Networking, Sensing and Control (ICNSC)*, Apr. 2014, pp. 367–371.

[113] Guangjie Han, Aihua Qian, Li Liu, Jinfang Jiang, and Chuan Zhu, "Impacts of traveling paths on energy provisioning for industrial wireless rechargeable sensor networks", *Microprocessors and Microsystems*, vol. 39, no. 8, pp. 1271–1278, 2015.

[114] Zi Li, Yang Peng, Wensheng Zhang, and Daji Qiao, "Study of Joint Routing and Wireless Charging Strategies in Sensor Networks", in *Proceedings of the 5th International Conference on Wireless Algorithms, Systems, and Applications*, ser. WASA'10, Beijing, China: Springer-Verlag, 2010, pp. 125–135.

[115] Zhao Cheng, Mark Perillo, and Wendi B Heinzelman, "General network lifetime and cost models for evaluating sensor network deployment strategies", *IEEE Transactions on mobile computing*, vol. 7, no. 4, pp. 484–497, 2008.

[116] W.K.-G. Seah, Zhi Ang Eu, and H. Tan, "Wireless sensor networks powered by ambient energy harvesting (WSN-HEAP) - Survey and challenges", in *1st Int. Conference on Wireless VITAE*, May 2009, pp. 1–5.

[117] S. Sudevalayam and P. Kulkarni, "Energy Harvesting Sensor Nodes: Survey and Implications", *IEEE Communications Surveys & Tutorials*, vol. 13, no. 3, pp. 443–461, Third 2011.

[118] Faisal Karim Shaikh and Sherali Zeadally, "Energy harvesting in wireless sensor networks: A comprehensive review", *Renewable and Sustainable Energy Reviews*, vol. 55, pp. 1041–1054, 2016.

[119] Georgios Tsoumanis, Konstantinos Oikonomou, Sonia Aïssa, and Ioannis Stavrakakis, "Recharging Vehicle Distance Minimization in Wireless Sensor Networks", in *BalkanCom 2017, First International Balkan Conference on Communications and Networking, Tirana, Albania*, (Tirana, Albania), Jun. 2017.

[120] San Murugesan, "Harnessing green IT: Principles and practices", *IT professional*, vol. 10, no. 1, 2008.

[121] Mathew Penrose, *Random geometric graphs*. Oxford University Press, 2003.

[122] www.eol.ucar.edu, *MICA2 - WIRELESS MEASUREMENT SYSTEM*, [Online; accessed 27-November-2017], 2017.

[123] Mark S Daskin, Lawrence V Snyder, and Rosemary T Berger, "Facility location in supply chain design", in *Logistics systems: Design and optimization*, Springer, 2005, pp. 39–65.

[124] Alan S Manne, "Plant location under economies-of-scale-decentralization and computation", *Management Science*, vol. 11, no. 2, pp. 213–235, 1964.

[125] Delbert Dueck, Brendan J Frey, Nebojsa Jojic, Vladimir Jojic, Guri Giaever, Andrew Emili, Gabe Musso, and Robert Hegele, "Constructing treatment portfolios using affinity propagation", in *Annual International Conference on Research in Computational Molecular Biology*, Springer, 2008, pp. 360–371.

[126] Hongdong Li, "Two-view motion segmentation from linear programming relaxation", in *Computer Vision and Pattern Recognition, 2007. CVPR'07. IEEE Conference on*, IEEE, 2007, pp. 1–8.

[127] Nevena Lazic, Inmar Givoni, Brendan Frey, and Parham Aarabi, "Floss: Facility location for subspace segmentation", in *Computer Vision, 2009 IEEE 12th International Conference on*, IEEE, 2009, pp. 825–832.

[128] Denis Krivitski, Assaf Schuster, and Ran Wolff, "A local facility location algorithm for large-scale distributed systems", *Journal of Grid Computing*, vol. 5, no. 4, pp. 361–378, 2007.

[129] Sudipto Guha, Adam Meyerson, and Kamesh Munagala, "Hierarchical placement and network design problems", in *Foundations of Computer Science, 2000. Proceedings. 41st Annual Symposium on*, IEEE, 2000, pp. 603–612.

[130] http://people.bath.ac.uk/ge277/index.php/flp-spreadsheet-solver, *FLP Spreadsheet Solver*, [Online; accessed 27-May-2018], 2018.

[131] Fred Glover, "Tabu search - part I", *ORSA Journal on computing*, vol. 1, no. 3, pp. 190–206, 1989.

[132] Gérard Cornuéjols, George L Nemhauser, and Lairemce A Wolsey, "The uncapacitated facility location problem", Carnegie-mellon univ pittsburgh pa management sciences research group, Tech. Rep., 1983.

[133] Christian Frank and Kay Römer, "Distributed facility location algorithms for flexible configuration of wireless sensor networks", in *International Conference on Distributed Computing in Sensor Systems*, Springer, 2007, pp. 124–141.

[134] Jakob Krarup and Peter Mark Pruzan, "The simple plant location problem: survey and synthesis", *European journal of operational research*, vol. 12, no. 1, pp. 36–81, 1983.

[135] Horst A Eiselt and Vladimir Marianov, *Foundations of location analysis*. Springer Science & Business Media, 2011, vol. 155.

[136] Harry R Lewis, *Computers and Intractability. A Guide to the Theory of NP-Completeness*, 1983.

[137] Jan Karel Lenstra and Alexander Hendrik George Rinnooy Kan, *Complexity of packing, covering and partitioning problems*. Econometric Institute, 1979.

[138] Sudipto Guha and Samir Khuller, "Greedy strikes back: Improved facility location algorithms", *Journal of algorithms*, vol. 31, no. 1, pp. 228–248, 1999.

[139] Kamal Jain, Mohammad Mahdian, and Amin Saberi, "A new greedy approach for facility location problems", in *Proceedings of the thiry-fourth annual ACM symposium on Theory of computing*, ACM, 2002, pp. 731–740.

[140] Dorit S Hochbaum, "Heuristics for the fixed cost median problem", *Mathematical programming*, vol. 22, no. 1, pp. 148–162, 1982.

[141] David B Shmoys, Éva Tardos, and Karen Aardal, "Approximation algorithms for facility location problems", in *Proceedings of the twenty-ninth annual ACM symposium on Theory of computing*, ACM, 1997, pp. 265–274.

[142] Jyh-Han Lin and Jeffrey Scott Vitter, "Approximation algorithms for geometric median problems", *Information Processing Letters*, vol. 44, no. 5, pp. 245–249, 1992.

[143] Kamal Jain and Vijay V Vazirani, "Approximation algorithms for metric facility location and k-median problems using the primal-dual schema and Lagrangian relaxation", *Journal of the ACM (JACM)*, vol. 48, no. 2, pp. 274–296, 2001.

[144] Kamal Jain, Mohammad Mahdian, Evangelos Markakis, Amin Saberi, and Vijay V Vazirani, "Greedy facility location algorithms analyzed using dual fitting with factor-revealing LP", *Journal of the ACM (JACM)*, vol. 50, no. 6, pp. 795–824, 2003.

[145] Jaroslaw Byrka, "An optimal bifactor approximation algorithm for the metric uncapacitated facility location problem", in *Approximation, Randomization, and Combinatorial Optimization. Algorithms and Techniques*, Springer, 2007, pp. 29–43.

[146] Jaroslaw Byrka and Karen Aardal, "An optimal bifactor approximation algorithm for the metric uncapacitated facility location problem", *SIAM Journal on Computing*, vol. 39, no. 6, pp. 2212–2231, 2010.

[147] Fabián A Chudak and David B Shmoys, "Improved approximation algorithms for the uncapacitated facility location problem", *SIAM Journal on Computing*, vol. 33, no. 1, pp. 1–25, 2003.

[148] Mohammad Mahdian, Yinyu Ye, and Jiawei Zhang, "Improved approximation algorithms for metric facility location problems", in *International Workshop on Approximation Algorithms for Combinatorial Optimization*, Springer, 2002, pp. 229–242.

[149] ——, "Approximation algorithms for metric facility location problems", *SIAM Journal on Computing*, vol. 36, no. 2, pp. 411–432, 2006.

[150] Shi Li, "A 1.488 approximation algorithm for the uncapacitated facility location problem", *Information and Computation*, vol. 222, pp. 45–58, 2013.

[151] Maxim Sviridenko, "An improved approximation algorithm for the metric uncapacitated facility location problem", in *International Conference on Integer Programming and Combinatorial Optimization*, Springer, 2002, pp. 240–257.

[152] Moses Charikar and Sudipto Guha, "Improved combinatorial algorithms for the facility location and k-median problems", in *Foundations of Computer Science, 1999. 40th Annual Symposium on*, IEEE, 1999, pp. 378–388.

[153] V. Rodoplu and T.H. Meng, "Minimum energy mobile wireless networks", *IEEE Journal on Selected Areas in Communications*, vol. 17, no. 8, pp. 1333–1344, 1999.

[154] V. Mhatre and C. Rosenberg, "Design guidelines for wireless sensor networks: communication, clustering and aggregation", *Ad Hoc Networks*, vol. 2, no. 1, pp. 45–63, 2004.

[155] Pei Huang, Li Xiao, S. Soltani, M.W. Mutka, and Ning Xi, "The Evolution of MAC Protocols in Wireless Sensor Networks: A Survey", *IEEE Communications Surveys & Tutorials*, vol. 15, no. 1, pp. 101–120, First 2013.

[156] J.N. Al-Karaki and AE. Kamal, "Routing techniques in wireless sensor networks: a survey", *IEEE Wireless Communications*, vol. 11, no. 6, pp. 6–28, Dec. 2004.

[157] Kemal Akkaya and Mohamed Younis, "A survey on routing protocols for wireless sensor networks", *Ad Hoc Networks*, vol. 3, no. 3, pp. 325–349, 2005.

[158] N.A Pantazis, S.A Nikolidakis, and D.D. Vergados, "Energy-Efficient Routing Protocols in Wireless Sensor Networks: A Survey", *Communications Surveys & Tutorials, IEEE*, vol. 15, no. 2, pp. 551–591, Second 2013.

[159] Rizwan Akhtar, Noor Ul Amin, Imran Memon, and Mohsin Shah, "Implementation of secure AODV in MANET", in *International Conference on Graphic and Image Processing (ICGIP 2012)*, International Society for Optics and Photonics, vol. 8768, 2013, p. 876 803.

[160] Dimitri Bertsekas and Robert Gallager, *Data Networks (2Nd Ed.)* Upper Saddle River, NJ, USA: Prentice-Hall, Inc., 1992.

[161] K. Oikonomou and I Stavrakakis, "Scalable service migration in autonomic network environments", *Selected Areas in Communications, IEEE Journal on*, vol. 28, no. 1, pp. 84–94, Jan. 2010.

[162] (2017). OMNeT++ Simulation Program, [Online]. Available: `http://www.omnetpp.org`.

[163] (2018). INET Framework, [Online]. Available: `https://inet.omnetpp.org/`.

[164] M. Haenggi, J.G. Andrews, F. Baccelli, O. Dousse, and M. Franceschetti, "Stochastic geometry and random graphs for the analysis and design of wireless networks", *IEEE Journal on Selected Areas in Communications*, vol. 27, no. 7, pp. 1029–1046, Sep. 2009.

[165] András Varga, "Using the OMNeT++ discrete event simulation system in education", *IEEE Transactions on Education*, vol. 42, no. 4, 11–pp, 1999.

[166] http://www.ewh.ieee.org/soc/es/Nov1999/18/ned.htm, *OMNeT++ Discrete Event Simulation System - NED language overview*, [Online; accessed 25-July-2018], 2018.

[167] Georgios Tsoumanis, Konstantinos Oikonomou, George Koufoudakis, and Sonia Aïssa, "Energy-Efficient Sink Placement in Wireless Sensor Networks", *Computer Networks*, vol. 141, pp. 166–178, 2018.

[168] Georgios Tsoumanis, Konstantinos Oikonomou, Sonia Aïssa, and Ioannis Stavrakakis, "A Recharging Distance Analysis for Wireless Sensor Networks", *Ad Hoc Networks*, vol. 75-76, pp. 80–86, 2018.

[169] George Koufoudakis, Konstantinos Oikonomou, and Georgios Tsoumanis, "Adapting Probabilistic Flooding in Energy Harvesting Wireless Sensor Networks", *Journal of Sensor and Actuator Networks*, vol. 7, no. 3, p. 39, 2018.

[170] Vasileios Komianos, Georgios Tsoumanis, Eleni Kavvadia, and Konstantinos Oikonomou, "A Framework for Cultural Heritage Content Organisation, Dissemination and Communication in Large-Scale Virtual Environments", *International Journal of Computational Intelligence Studies*, vol. 5, no. 1, pp. 71–93, 2016.

[171] Georgios Tsoumanis, Eleni Kavvadia, and Konstantinos Oikonomou, "A v(irtual)-City Implementation for Promoting Cultural Heritage", *International Journal of Computational Intelligence Studies*, vol. 4, no. 2, pp. 173–191, 2015.

[172] Georgios Tsoumanis, Konstantinos Oikonomou, Sonia Aïssa, and Ioannis Stavrakakis, "Performance Evaluation of a Proposed On-Demand Recharging Policy in Wireless Sensor Networks", in *2018 IEEE 19th International Symposium on "A World of Wireless, Mobile and Multimedia Networks" (WoWMoM) (IEEE WoWMoM 2018)*, Chania, Crete, Greece, Jun. 2018.

[173] Georgios Tsoumanis, George Koufoudakis, Konstantnos Oikonomou, Markos Avlonits, and Nikos Varotsis, "A Low-Cost Surface Wireless Sensor Network for Pollution Monitoring in the Ionian Sea", in *12th Panhellenic Symposium of Oceanography & Fisheries*, (Corfu, Greece), Abstract, May 2018.

[174] Georgios Tsoumanis, Eleni Kavvadia, and Konstantinos Oikonomou, "Changing the Look of a City: The v-Corfu Case", in *IISA 2014, The 5th International Conference on Information, Intelligence, Systems and Applications*, (Chania, Greece), Jul. 2014, pp. 419–424.

Publication Table

Refereed Journals

- Georgios Tsoumanis, Konstantinos Oikonomou, George Koufoudakis, and Sonia Aïssa, "Energy-Efficient Sink Placement in Wireless Sensor Networks", *Computer Networks*, vol. 141, pp. 166–178, 2018
- Georgios Tsoumanis, Konstantinos Oikonomou, Sonia Aïssa, and Ioannis Stavrakakis, "A Recharging Distance Analysis for Wireless Sensor Networks", *Ad Hoc Networks*, vol. 75-76, pp. 80–86, 2018
- George Koufoudakis, Konstantinos Oikonomou, and Georgios Tsoumanis, "Adapting Probabilistic Flooding in Energy Harvesting Wireless Sensor Networks", *Journal of Sensor and Actuator Networks*, vol. 7, no. 3, p. 39, 2018
- Vasileios Komianos, Georgios Tsoumanis, Eleni Kavvadia, and Konstantinos Oikonomou, "A Framework for Cultural Heritage Content Organisation, Dissemination and Communication in Large-Scale Virtual Environments", *International Journal of Computational Intelligence Studies*, vol. 5, no. 1, pp. 71–93, 2016
- Georgios Tsoumanis, Eleni Kavvadia, and Konstantinos Oikonomou, "A v(irtual)-City Implementation for Promoting Cultural Heritage", *International Journal of Computational Intelligence Studies*, vol. 4, no. 2, pp. 173–191, 2015

Refereed Conferences

- Georgios Tsoumanis, Konstantinos Oikonomou, Sonia Aïssa, and Ioannis Stavrakakis, "Performance Evaluation of a Proposed On-Demand Recharging Policy in Wireless Sensor Networks", in *2018 IEEE 19th International Symposium on "A World of Wireless, Mobile and Multimedia Networks" (WoWMoM) (IEEE WoWMoM 2018)*, Chania, Crete, Greece, Jun. 2018

- Georgios Tsoumanis, George Koufoudakis, Konstantnos Oikonomou, Markos Avlonits, and Nikos Varotsis, "A Low-Cost Surface Wireless Sensor Network for Pollution Monitoring in the Ionian Sea", in *12th Panhellenic Symposium of Oceanography & Fisheries*, (Corfu, Greece), Abstract, May 2018
- Georgios Tsoumanis, Konstantinos Oikonomou, Sonia Aïssa, and Ioannis Stavrakakis, "Recharging Vehicle Distance Minimization in Wireless Sensor Networks", in *BalkanCom 2017, First International Balkan Conference on Communications and Networking, Tirana, Albania*, (Tirana, Albania), Jun. 2017
- Georgios Tsoumanis, Eleni Kavvadia, and Konstantinos Oikonomou, "Changing the Look of a City: The v-Corfu Case", in *IISA 2014, The 5th International Conference on Information, Intelligence, Systems and Applications*, (Chania, Greece), Jul. 2014, pp. 419–424

Glossary

Aggregate traffic load of a node u	The sum of the traffic loads of all nodes consisting a routing tree which root is u.
l-ary tree	A rooted tree in which each node has no more than l children.
Capacitated facility location problems	Facility location problems in which each potential facility may serve a finite number of demands, i.e., facilities have a fixed capacity.
Connectivity radius	The maximum distance between two nodes that are able to communicate.
Energy hole problem	The problem in wireless networks, such as wireless sensor networks, where nodes that are closer to the sink node, tend to run out of energy faster.
Euclidean distance	The straight-line distance between two points in Euclidean space.
Local information	Information that is gained by nodes consisting a network.
k-median problems	Facility location problems in which each potential facility may serve an infinite number of demands and the number of facilities is fixed.
Mobile recharger	The vehicle that is implemented by the recharging policies in order to recharge the nodes' batteries.
Neighbors	Nodes that are able to communicate with each other.
Network consumed energy	The energy consumed by all nodes consisting a network.

`Network lifetime`	Time until one node of the network stops operating.
`Optimal energy sink placement`	The placement of a sink that optimizes the network consumed energy.
`Optimal distance sink node`	The node that when it holds the sink, then the mobile recharger covered distance is optimized.
`Packet loss`	The failure of data to reach their destination.
`Processing cost`	The energy spent by the node for processing issues.
`Recharger distance`	The distance the mobile recharger has traveled.
`Recharger moving consumption`	The energy the mobile recharger spents for traveling.
`Recharger vacation period`	The period during which a mobile recharger is placed on its initial location.
`Recharging period`	Time elepsed between a recharging operation on a node and the same node's need for its next recharge.
`Recharging policy`	The policy under which the mobile recharger operates.
`Recharging process`	The process of recharging a node's battery.
`Recharging request`	The request sent by a node to the sink node, asking for a new replenishment for its battery.
`Recharging threshold`	The node's remaining energy value that when reached, a recharging request is sent.
`Routing tree`	A tree consisted of network nodes and after being constructed by a routing algorithm, specifies the path the data travel on to reach their destination.
`Sink`	The feature that when a node is enhanced with, it is turned into a sink node.

`Sink node`	The node of a wireless sensor network that accumulates all sensed data.
`Termination time`	The time instance one or more nodes stop operating.
`Time delay`	Time needed for a bit of data to travel from one node to another.
`Traffic load`	The probability that a data packet is generated at some node at any time unit.
`Tree topology`	Type of network in which many connected nodes are arranged like the branches of a tree.
`Triangle inequality`	Triangle inequality states that the sum of the lengths of any two sides of a triabgle must be greater than or equal to the length of the remaining side.
`Uncapacitated facility location problems`	Facility location problems in which each potential facility may serve an infinite number of demands, i.e., facilities do not have a fixed capacity.

Notations

V	Set of network nodes
$\mathcal{B}_u^{\mathtt{s}}(t)$	Remaining energy at node?u's battery at time t
$\mathcal{B}_{\max}$	Initial energy (at time $t = 0$) for all nodes
$\mathtt{d}(u, v)$	Energy distance for the pair of nodes u, v
$\mathcal{E}(\mathtt{s})$	Network consumed energy for sink placement $\mathtt{s}$
$\frac{\mathcal{E}(\mathtt{s})}{\mathcal{E}(\mathtt{s}_\mathcal{E})}$	Energy ratio
k	Number of sinks in the network
l	Number of descendant nodes per node in an l-ary tree
m	Number of levels of an l-ary tree
n	Number of nodes in the network
r_c	Connectivity radius
s	The sink node that first exhaust its battery
$\mathtt{s}$	Sink placement (set of sink nodes)
$\mathtt{s}(u)$	Sink placement (The sink node corresponding to node)
$\mathtt{s}_\mathcal{E}$	Optimal energy sink placement
$\mathcal{T}(\mathtt{s})$	Termination time
$w(u, v)$	Consumed transmission energy over link (u, v)
$\mathtt{x}(u, v)$	Summation of euclidean distances between nodes u and v over a shortest path
λ_u	Traffic load of node u
$\Lambda^{\mathtt{s}}(u)$	Aggregate traffic load of node u
$\mathtt{\Lambda}^{\mathtt{s}}(u)$	Twice aggregated traffic load of node u
Λ_i	Aggregate traffic load at level i of an l-ary tree
$\chi(u, v)$	Euclidean distance for neighbor nodes u and v
$\mathcal{D}(\mathtt{s})$	Recharging distance for sink node $\mathtt{s}$
$D^{\mathtt{s}}(t)$	Covered distance for sink node $\mathtt{s}$ at time t
$\frac{\mathcal{D}(\mathtt{s})}{\mathcal{D}(\mathtt{s}_\mathcal{D})}$	Distance ratio
$\mathtt{s}_\mathcal{D}$	Optimal distance sink node
$\tau^{\mathtt{s}}(u)$	Recharging period for node u

ρ	Recharging threshold
$\mathcal{C}$	Initial - max capacity of recharger's battery
m	Recharger's moving consumption per time unit
`v`	Recharger's speed
`e`	Consumed transmission energy per time unit
`r`	Consumed reception energy per time unit
`p`	Processing per time unit
ϕ	Recharger's recharging ratio
ψ	Node's recharging ratio

Abbreviations

BAN	Body Area Network
BLE	Bluetooth Low Energy
CSMA-CA	Carrier Sense Multiple Access with Collision Avoidance
HBC	Human Body Communications
IEEE	The Institute of Electrical and Electronics Engineers
ISA100.11a	International Society of Automation - 100.11a
6LoWPAN	IPv6 over Low power Wireless Personal Area Networks
MAC	Medium Access Control
NB	Narrowband
NED	NEtwork Description
OMNeT++	Objective Modular Network Testbed in C++
S-MAC	Sensor Media Access Control
SPAN	Smart Phone Ad hoc Networks
TDMA	Time Division Multiple Access
UWB	Ultra-WideBand

VANET	Vehicular Ad hoc NETwork
WirelessHART	Wireless Highway Addressable Remote Transducer Protocol

Index